Near-Field Communications for 6G: Fundamentals, Potentials, Challenges, and Future Directions

Linglong Dai, Haiyang Zhang, and Yonina C. Eldar

Tsinghua University

Nanjing University of Posts and Telecommunications

Weizmann Institute of Science

June 9, 2024

Outline of the Tutorial

- Background of Near-Field Communications
- Fundamentals of Near-Field Communications
- Opportunities of Near-Field Communications
- Challenges of Near-Field Communications
- Future directions

Part 1: Background of Near-Field Communications

清華大學 Tsinghua University
南京郵電大學 Nanjing University of Posts and Telecommunications
WEIZMANN INSTITUTE OF SCIENCE

Objectives of 6G Communications

- New applications (e.g., holographic video) drive the upgrade from 5G to 6G
- Extended from 3 to 6 scenarios of IMT-2030 (6G): Compared with 5G, 3 new scenarios are ubiquitous connectivity, AI and communication, ISAC

Holographic Video

Digital Replica

Extended Reality

Autonomous driving

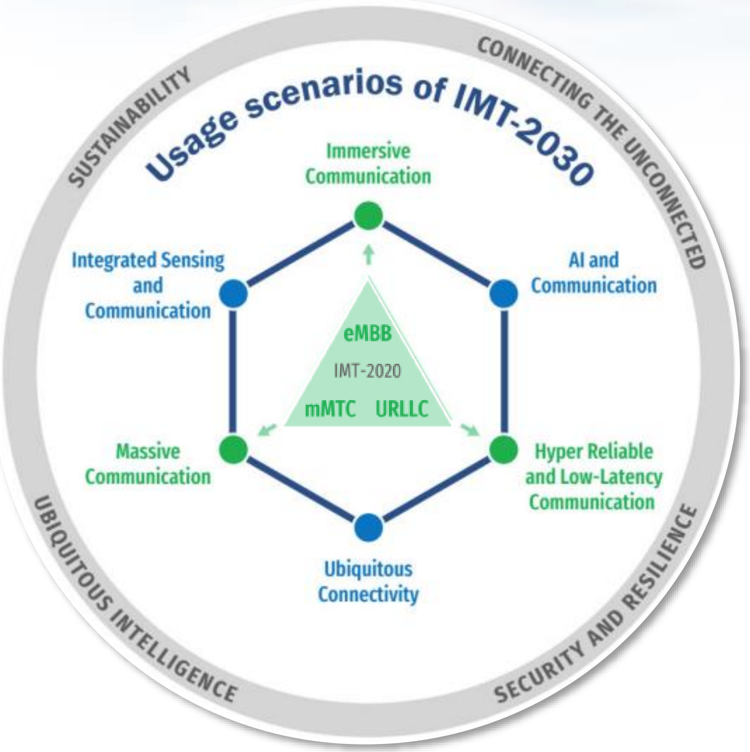

ITU-R WP 5D, "Framework and overall objectives of the future development of IMT for 2030 and beyond," Dec. 2023.

Key Performance Indicators (KPIs) of 6G

- KPIs of 6G should be orders of magnitude higher than those of 5G, e.g., 10x data rate
- New capabilities should be considered, e.g., coverage, sensing/AI-related capabilities, …

Coverage: 90%

Peak data rate: 1 Tbps

Low latency: 500 µs

Spectral efficiency: Kbps/Hz

Access density: 100 users/m^2

ITU-R WP 5D, "Framework and overall objectives of the future development of IMT for 2030 and beyond," Dec. 2023.

KPI 1: Spectral Efficiency

- 6G is expected to achieve **10 times higher spectral efficiency** compared with 5G
- The higher spectral efficiency can be achieved exploiting **spatial multiplexing**, which requires significantly increased number of antennas
  - 4G: 2-8 antennas → 5G: 64-256 antennas
  - 6G: 1024+ antennas with **ultra-massive MIMO (UM-MIMO)** and **cell-free massive MIMO (CF-MIMO)**

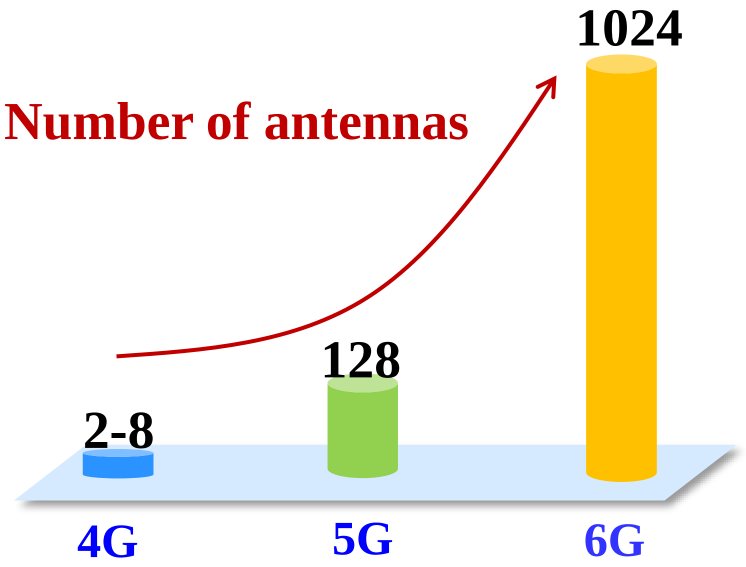

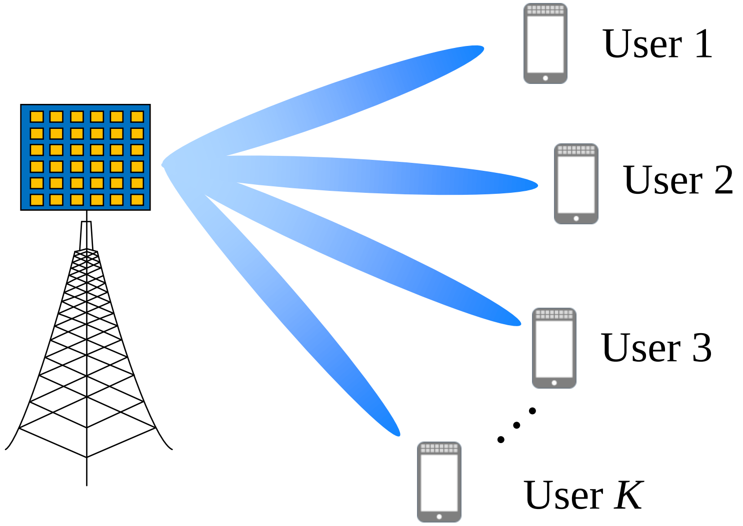

UM-MIMO

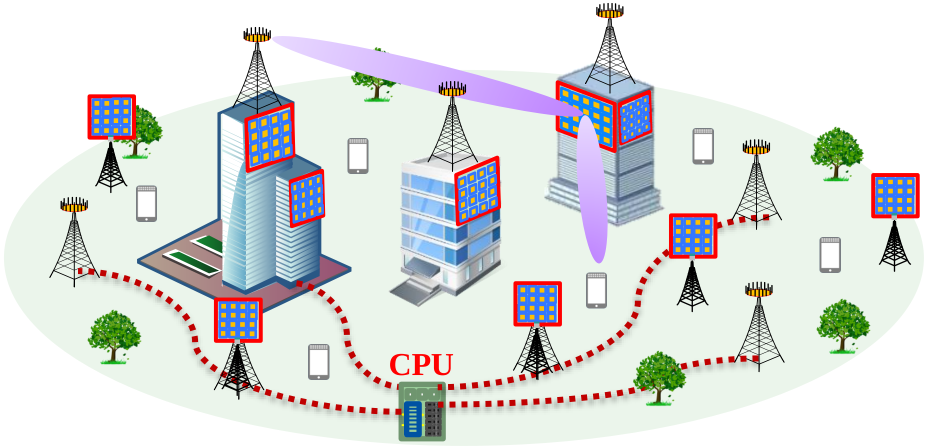

CF-MIMO

W. Jiang, B. Han, M. A. Habibi and H. D. Schotten, "The Road Towards 6G: A Comprehensive Survey," *IEEE Open J. Commun. Soc.*, vol. 2, pp. 334-366, Feb. 2021.

KPI 2: Peak Data Rate

- **100× peak data rate improvement for 6G**
  - ➢ **Using mmWave and THz can achieve this improvement with the abundant spectral resources**
  - ➢ **Very large antenna array is required to counteract the serious path loss in high-frequency band**

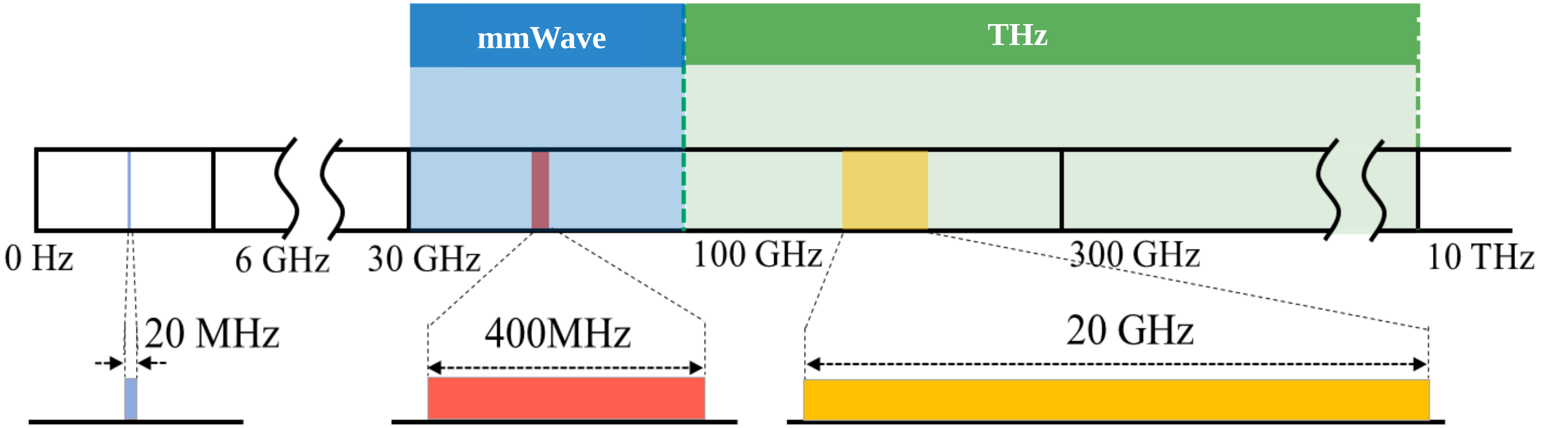

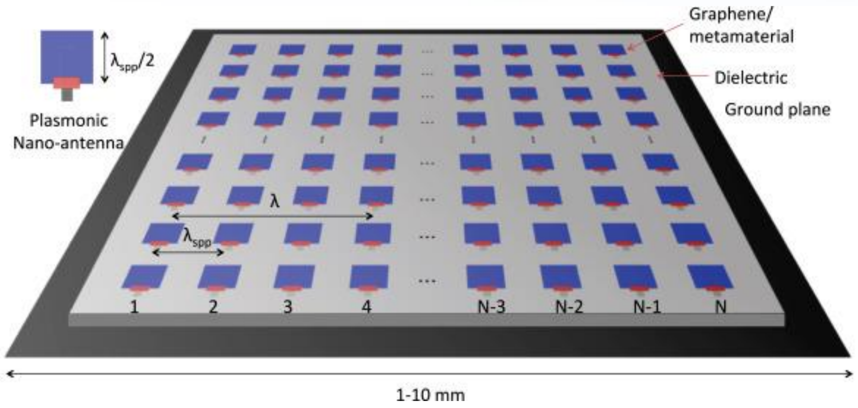

1024 ×1024 elements for THz band (0.06-10THz) [1]

I. F. Akyildiz, and J. M. Jornet, "Realizing ultra-massive MIMO (1024 ×1024) communication in the (0.06–10) terahertz band," *Nano Commun. Netw.*, vol. 8, pp. 46-54, Jun. 2016.

KPI 3: Coverage

- **By dynamically manipulating the transmission environment, reconfigurable intelligent surface (RIS) brings new possibilities for capacity and coverage enhancement**
- **Thousands of antennas are usually employed to overcome the "multiplicative fading" effect of RIS**

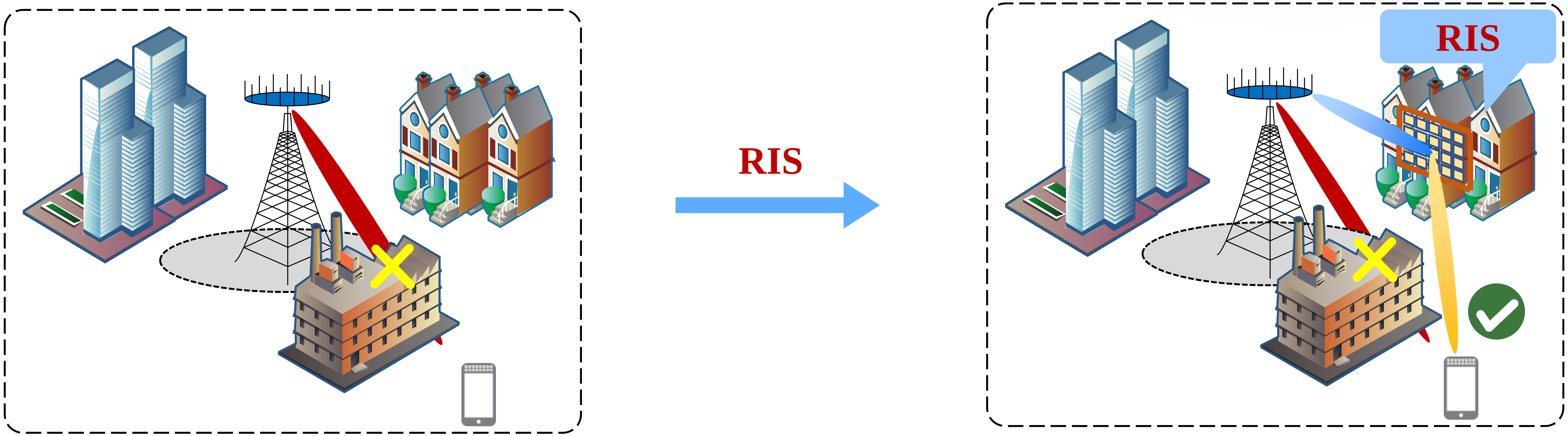

C. Huang, A. Zappone, G. C. Alexandropoulos, M. Debbah and C. Yuen, "Reconfigurable Intelligent Surfaces for Energy Efficiency in Wireless Communication," *IEEE Trans. Wireless Commun.*, vol. 18, no. 8, pp. 4157-4170, Aug. 2019.

Extremely Large Antenna Arrays (ELAA)

- **ELAA is the common feature for the above technologies**

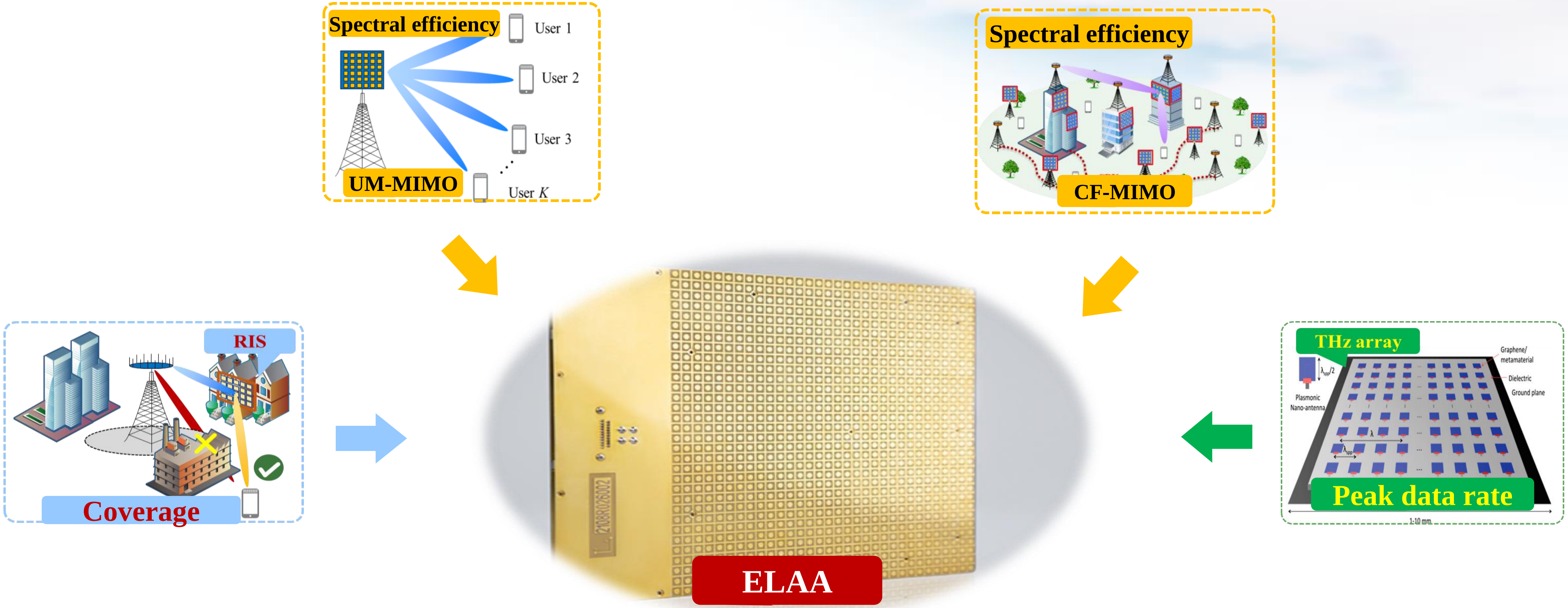

Massive MIMO vs. ELAA

	Massive MIMO	ELAA
Architecture	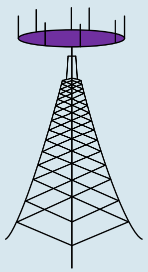	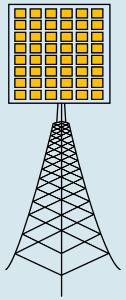
Number of antennas	64 ~ 256	1000+
Array aperture	Big	Bigger
Beam gain	High	Higher
Precoding complexity	High	Higher
Beam management	Difficult	Very difficult
Power consumption	High	Higher

Is there any fundamental change between the massive MIMO and ELAA

Electromagnetic Propagation: Near-Field vs. Far-Field

- **Electromagnetic (EM) propagation can be divided into far-field and near-field regions**
  - **Boundary of these regions is the Rayleigh distance**
  - **In far-field, EM propagation can be approximately modeled by the planar wave**
  - **In near-field, EM propagation has to be accurately modeled by the spherical wave**

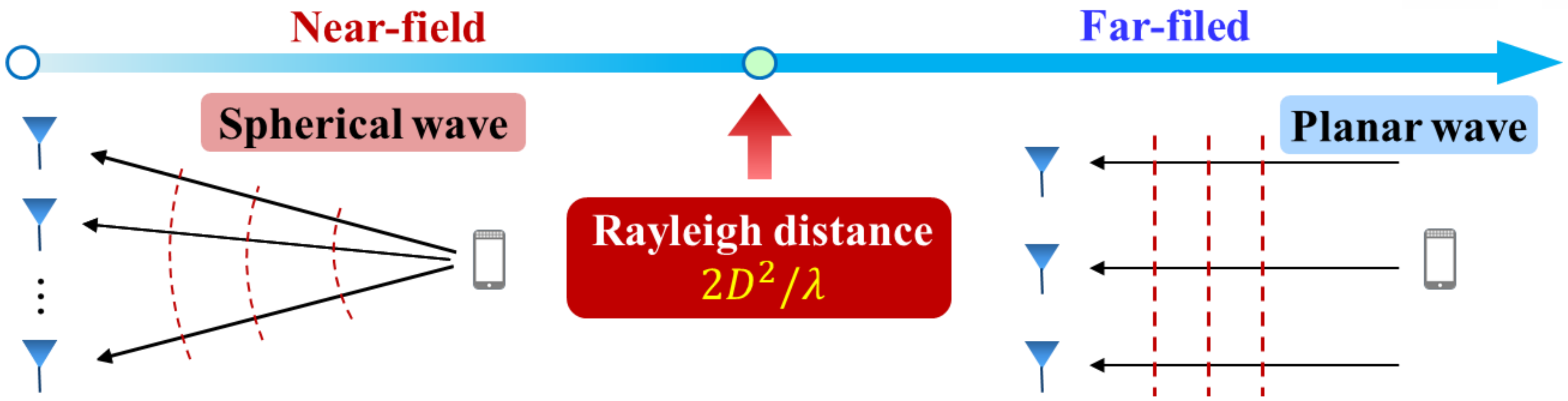

It has a critical difference of the EM characteristics between the near-field and far-field

M. Cui, Z. Wu, Y. Lu, X. Wei, and L. Dai, "Near-field MIMO communications for 6G: Fundamentals, challenges, potentials, and future directions," *IEEE Commun. Mag.*, vol. 61, no. 1, pp. 40-46, Jan. 2023.

Near-Field for ELAA

- **5G with massive MIMO: Users are located in the far-field region**
- **6G with ELAA: Users are more likely located in the near-field region**

Table I. Rayleigh distance [m] (Typical 5G cell radius: 150-250 m)

D \ f	3 GHz	7 GHz	28 GHz	142 GHz
0.5 m	5 m	12 m	47 m	237 m
1.6 m	51 m	119 m	476 m	/
3.0 m	180 m	420 m	/	/

Evolution from massive MIMO to ELAA results in fundamental change of spherical propagation model

M. Cui, Z. Wu, Y. Lu, X. Wei, and L. Dai, "Near-field MIMO communications for 6G: Fundamentals, challenges, potentials, and future directions," *IEEE Commun. Mag.*, vol. 61, no. 1, pp. 40-46, Jan. 2023.

Prototypes of ELAA for Near-Field Communications

- **MIT: 3200-element ELAA@2.4 GHz, Rayleigh distance 600 m**
- **Tsinghua: 2304-element ELAA@28 GHz, Rayleigh distance 25 m**
- **Qualcomm: 4096-element ELAA@13 GHz, Rayleigh distance 95 m**

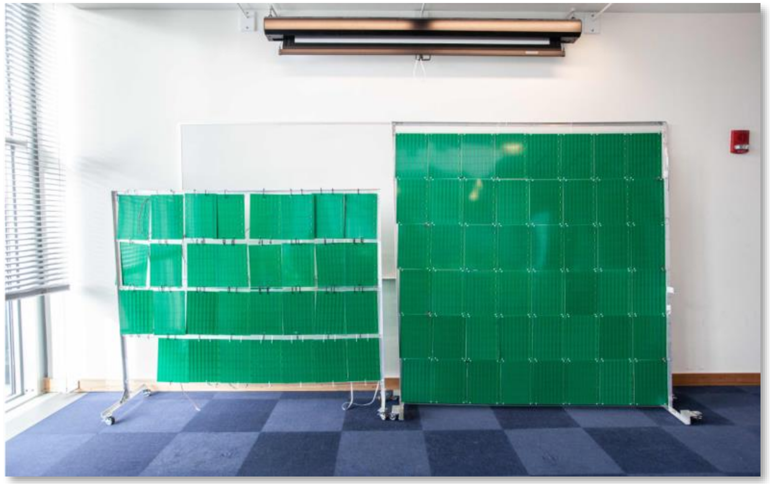

MIT: 3200-element ELAA

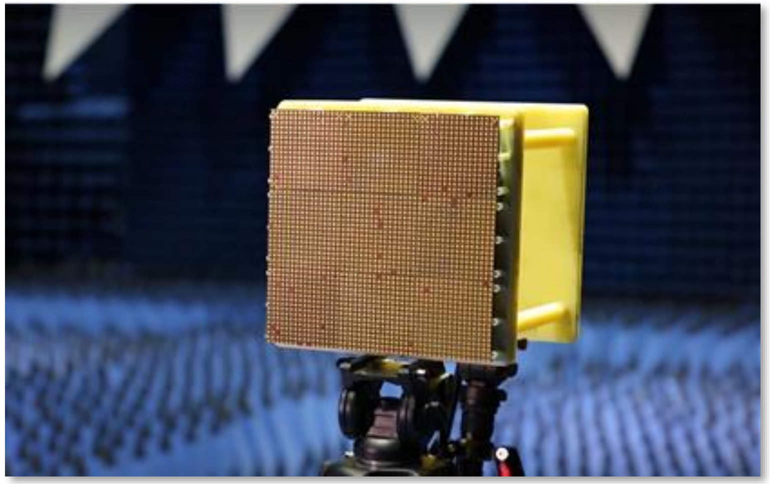

Tsinghua: 2304-element ELAA

Qualcomm: 4096-element ELAA

[1] M. Uusitalo, P. Rugeland, M. Boldi, E. C. Strinati, and Y. Zou, "RFocus: Beamforming using thousands of passive antennas," in *Proc. 17th USENIX Symposium on Networked Systems Design and Implementation (NSDI'20)*, Feb. 2020.
[2] M. Cui, Z. Wu, Y. Chen, S. Xu, F. Yang, and L. Dai, "Demo: Low-power communications based on RIS and AI for 6G," in *Proc. IEEE ICC*, May 2022. (**IEEE ICC 2022 Outstanding Demo Award**)
[3] Qualcomm, "MWC 2024: Wireless innovations enabling intelligent computing everywhere," Qualcomm, Feb. 2024. [Online]. Available: https://www.qualcomm.com/news/onq/2024/02/mwc-2024-wireless-innovations-enabling-intelligent-computing-everywhere.

Applications of Near-Field Communications

- **Near-field spherical waves enables near-field beamfocusing**

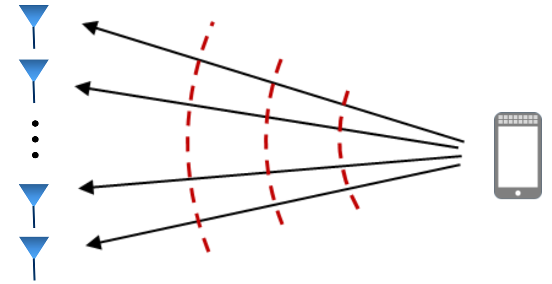

Near-Field Beamfocusing

Communications

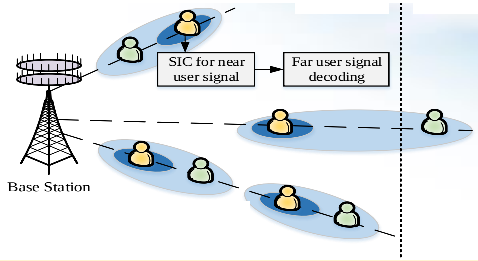

Sensing and Localization

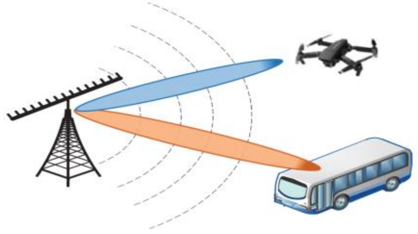

Wireless Power Transfer

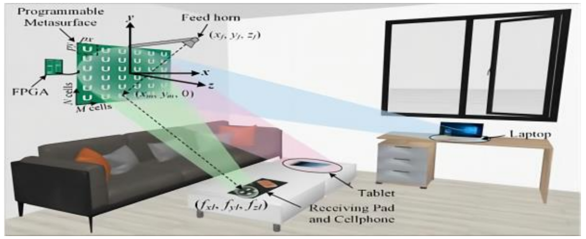

Increased capacity through signal focusing

Higher accuracy through distance sensing

Improved efficiency through energy focusing

3GPP Proposals for Near-Field Communications

- In Dec. 2023 and Apr. 2024, 3GPP has approved the 7-24 GHz channel modeling proposals, where near-field propagation is an important research topic

3GPP TSG RAN Meeting #102 RP-234018
Edinburgh, UK, 11th – 15th December, 2023

Source:	Nokia, Nokia Shanghai Bell
Title:	New SID: Study on channel modelling enhancements for 7-24GHz for NR
Document for:	Approval
Agenda Item:	9.1.1.8

Proposal at 3GPP TSG RAN Meeting in Dec. 2023

3GPP RAN1 Meeting #116-bis R1-2403261
Changsha, China, 15 April – 19 April, 2024
Source:
Title:
Agenda i
Documer

3GPP RAN1 Meeting #116-bis R1-2403280
Changsha, China, 15 April – 19 April, 2024
Sourc
Title:
Agend
Docur

3GPP TSG RAN1 Meeting #116-bis R1-2403285
Changsha, China, 15 April – 19 April, 2024

Source:	BUPT, CMCC
Title:	Discussion on modeling near-field propagation and spatial non-stationarity in TR38.901 for 7-24GHz
Agenda item:	9.8.2
Document for:	Discussion and Decision

Proposal at 3GPP RAN1 Meeting in Apr. 2024

[1] RP-234018. Study on channel modelling enhancements for 7-24 GHz for NR. Edinburgh: 3GPP, Dec. 2023.
[2] R1-2403261. Changes to TR38.901. Changsha: 3GPP, Apr. 2024.
[3] R1-2403280. Discussion on channel model validation of TR38.901 for 7-24GHz. Changsha: 3GPP, Apr. 2024.
[4] R1-2403285. Discussion on modeling near-field propagation and spatial non- stationarity in TR38.901 for 7-24GHz. Changsha: 3GPP, Apr. 2024.

The First White Paper on Near-Field Communications

- The **first white paper** on near-field technologies released at **Global 6G Conference 2024**
- Contributed by **200+** people from **40+** global entities of **12** countries

The first white paper

Released at the Global 6G Conference, 2024

Consultants

Tiejun Cui (tjcui@seu.edu.cn), Southeast University

Ping Zhang (pzhang@bupt.edu.cn), Beijing University of Posts and Telecommunications

Xiaohu You (xhyu@seu.edu.cn), Southeast University

Yonina Eldar (yonina.eldar@weizmann.ac.il), Weizmann Institute of Science

Editors in Chief

Yajun Zhao (zhao.yajun1@zte.com.cn), ZTE Corporation

Linglong Dai (daill@tsinghua.edu.cn), Tsinghua University

Jianhua Zhang (jhzhang@bupt.edu.cn), Beijing University of Posts and Telecommunications

QR code for download

Y. Zhao, L. Dai, J. Zhang, *et al*. "6G near-field technologies white paper," FuTURE Forum, Nanjing, China, Apr. 2024.

Part 2: Fundamentals of Near-Field Communications

清華大學 Tsinghua University
南京郵電大學 Nanjing University of Posts and Telecommunications
WEIZMANN INSTITUTE OF SCIENCE

Far-Field vs. Near-Field

- **Far-field**: the EM waves impinging on the antenna array can be approximately modeled as **planar waves**, where the phase of the EM wave is a **linear function** of the antenna index
- **Near-field**: the EM waves have to be accurately modeled as **spherical waves**, where the phase of the EM wave is a **non-linear function** of the antenna index

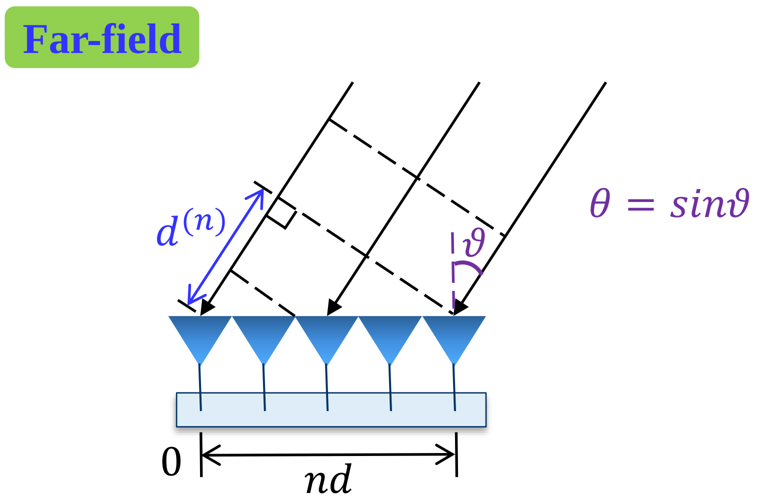

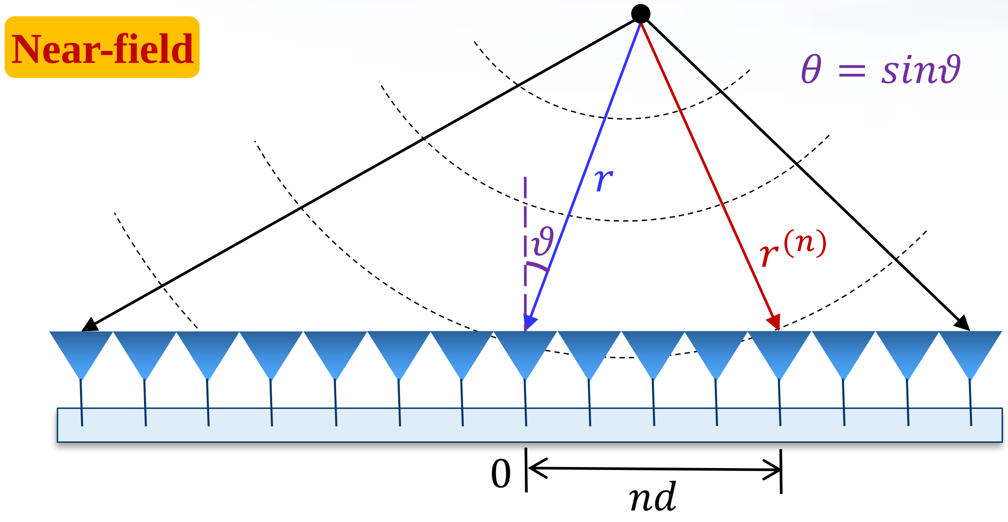

Distance: $d^{(n)} = nd\theta$ **Linear**

Phase: $\phi_n^{\text{far}} = -\frac{2\pi d^{(n)}}{\lambda} = -\frac{2\pi}{\lambda} nd\theta$

Distance: $r^{(n)} = \sqrt{r^2 + n^2 d^2 - 2ndr\theta}$ **Non-linear**

Phase: $\phi_n = \frac{2\pi\left(r^{(n)} - r\right)}{\lambda} = \frac{2\pi}{\lambda}\left(\sqrt{r^2 + n^2 d^2 - 2ndr\theta} - r\right)$

Antenna index: $n \in [-N, \cdots, 0, \cdots, N]$ **Antenna number:** $M = 2N + 1$

Definition of Rayleigh Distance

- **The metric to determine the boundary between the far-field and near-field regions is the Rayleigh distance**

Rayleigh distance: The planar waves are a long-distance approximation of the spherical waves. When the largest phase error $\Delta_n = \left|\phi_n - \phi_n^{\text{far}}\right|$ between the accurate phase ϕ_n and the approximated phase ϕ_n^{far} is $\max_n \Delta_n = \pi/8$, then the Tx-Rx distance is the Rayleigh distance (RD), satisfying

$$\text{RD} = \frac{2D^2}{\lambda},$$

where D denotes the array aperture, and λ is the wavelength.

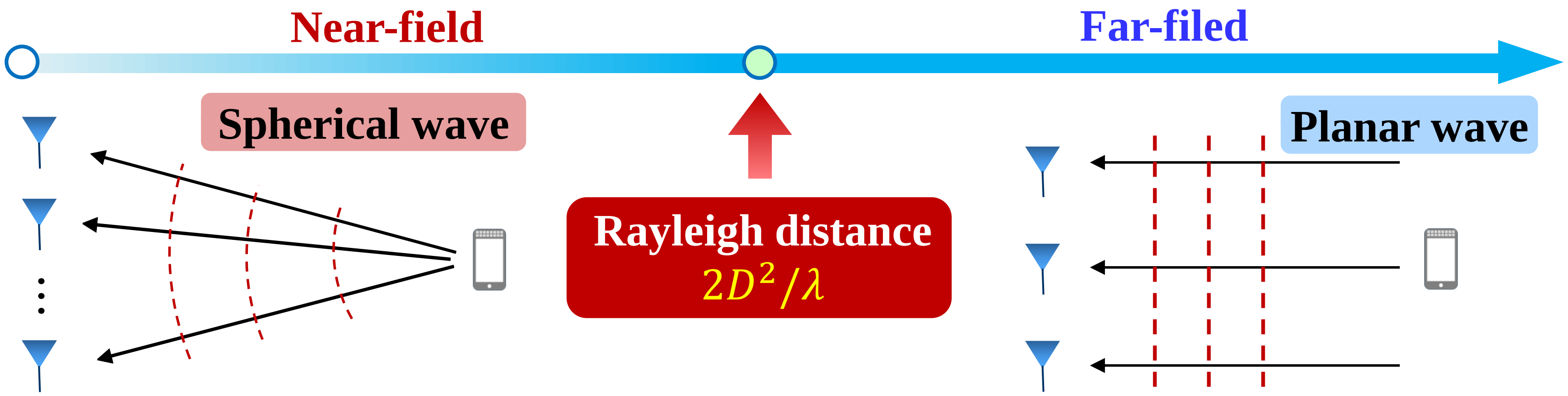

J. Sherman, "Properties of focused apertures in the Fresnel region," *IRE Trans. Antennas Propag.*, vol. 10, no. 4, pp. 399–408, Jul. 1962.

Derivation of Rayleigh Distance

- **To derive the Rayleigh distance, it is essential to derive the specific value of phase error $\Delta_n = \left|\phi_n - \phi_n^{\mathrm{far}}\right|$, where $\phi_n = \frac{2\pi}{\lambda}\left(\sqrt{r^2 + n^2 d^2 - 2ndr\theta} - r\right)$ and $\phi_n^{\mathrm{far}} = -\frac{2\pi}{\lambda} nd\theta$**

$$\phi_n = \frac{2\pi}{\lambda} r \left(\sqrt{1 + \frac{n^2 d^2}{r^2} - \frac{2nd\theta}{r}} - 1\right) = \frac{2\pi}{\lambda} r \left(1 - \frac{nd\theta}{r} + \frac{(1-\theta^2) n^2 d^2}{2r^2} + o\left(\frac{1}{r^2}\right) - 1\right)$$

$$= \underbrace{-\frac{2\pi}{\lambda} nd\theta}_{\text{Far-field phase } \phi_n^{\mathrm{far}}} + \underbrace{\frac{1-\theta^2}{\lambda r} \pi n^2 d^2 + o\left(\frac{1}{r}\right)}_{\text{Phase error } \Delta_n} \Rightarrow \text{Phase error } \Delta_n \approx \frac{1-\theta^2}{\lambda r} \pi n^2 d^2$$

- **ϕ_n^{far} is the approximation of ϕ_n through first-order Taylor expansion. Therefore, the phase error Δ_n is mainly determined by the second-order Taylor expansion**
- **By maximizing the phase error Δ_n across the entire array**

$$\max_n \Delta_n = \frac{1-\theta^2}{\lambda r} \pi N^2 d^2 = \frac{1-\theta^2}{\lambda r} \frac{\pi D^2}{4} = \frac{\pi}{8} \Rightarrow r = \frac{2D^2(1-\theta^2)}{\lambda} \xrightarrow{\theta = 0} \mathrm{RD} = \frac{2D^2}{\lambda}$$

Near-Field Ranges for Typical Scenarios

- **The near-field range of SIMO/MISO is exactly determined by the classical Rayleigh distance** $\frac{2D^2}{\lambda}$
- **For the MIMO scenario, both the BS array aperture** D_1 **and the UE array aperture** D_2 **contribute to the Rayleigh distance** $\frac{2(D_1+D_2)^2}{\lambda}$
- **For the RIS scenario, the near-field range is determined by the harmonic mean of the BS-RIS distance** r_1 **and RIS-UE distance** r_2

Communication scenario	**SIMO/MISO** 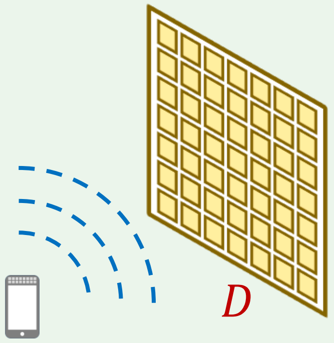	**MIMO** 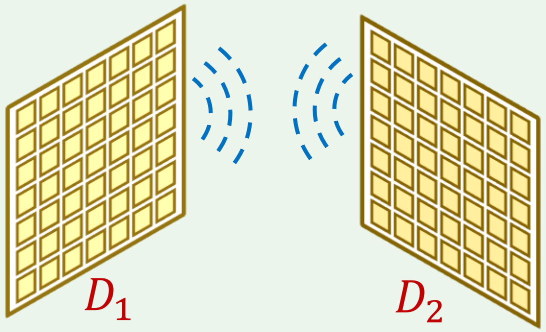	**RIS** 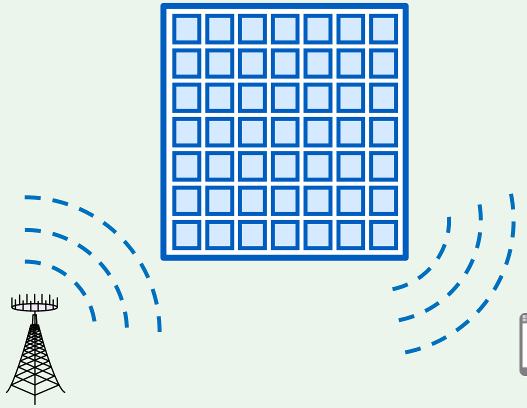
Near-field range	$r < \frac{2D^2}{\lambda}$	$r < \frac{2(D_1+D_2)^2}{\lambda}$	$\frac{r_1 r_2}{r_1+r_2} < \frac{2D^2}{\lambda}$

M. Cui, Z. Wu, Y. Lu, X. Wei, and L. Dai, "Near-field MIMO communications for 6G: Fundamentals, challenges, potentials, and future directions," *IEEE Commun. Mag.*, vol. 61, no. 1, pp. 40-46, Jan. 2023.

Near-Field LoS Channel Model

- **Base station (BS) antenna number $M = 2N + 1$, antenna spacing $d = \lambda/2$, array aperture $D = (M-1)d$, the location of the n-th antenna is $(0, nd)$, where $n \in [-N, \cdots, 0, \cdots, N]$**
- **The channel between the n-th antenna and the user located at $(r\cos\vartheta, r\sin\vartheta)$ is**

$$h_n = \underbrace{\boxed{\tilde{g}_n}}_{\text{Complex gain}} e^{-j\frac{2\pi}{\lambda}r^{(n)}} = \underbrace{\boxed{g_n}}_{g_n = \tilde{g}_n e^{j\frac{2\pi}{\lambda}r}} e^{-j\underbrace{\boxed{\frac{2\pi}{\lambda}\left(r^{(n)} - r\right)}}_{\text{Near-field phase } \phi_n}}$$

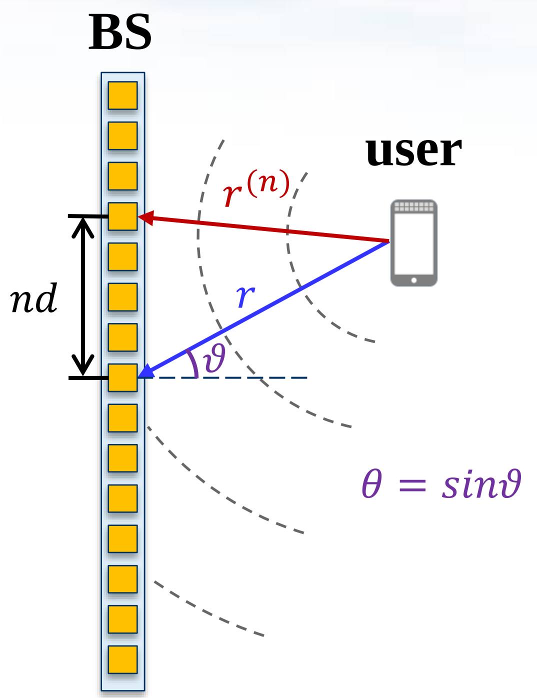

- **Generally, the complex gains are very similar when $r > 1.2D$**

$$g_{-N} \approx \cdots \approx g_0 \approx \cdots \approx g_N \approx g$$

- **Therefore, the LoS channel is**

$$\boldsymbol{h} = [h_{-N}, \cdots, h_0, \cdots, h_N]^T = g\left[e^{-j\frac{2\pi}{\lambda}\left(r^{(-N)} - r\right)}, \cdots, e^{-j\frac{2\pi}{\lambda}\left(r^{(N)} - r\right)}\right]^T$$
$$= g\underbrace{\boxed{\boldsymbol{a}(r, \theta)}}_{\text{Near-field array response vector}}$$

E. Björnson, Ö. T. Demir, and L. Sanguinetti, "A primer on near-field beamforming for arrays and reconfigurable intelligent surfaces," in *Proc. 2021 55th Asilomar Conference on Signals, Systems, and Computers*, pp. 105-112, Oct. 2021.

Near-Field Multi-Path Channel Model

- **The multi-path channel can be represented as the sum of L near-field array response vectors.**

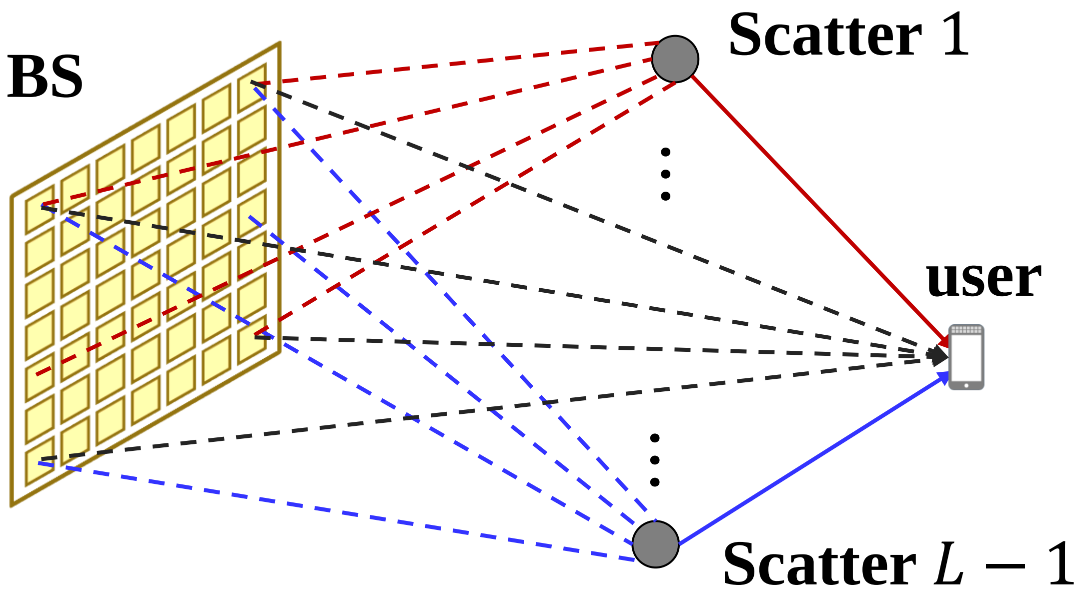

distance between the BS and the l-th scatter

$$\boldsymbol{h} = \underbrace{g_0 \boldsymbol{a}(r_0, \theta_0)}_{\text{LoS path}} + \underbrace{\sum_{l=1}^{L-1} g_l \boldsymbol{a}(\boxed{r_l}, \boxed{\theta_l})}_{\text{NLoS paths}}$$

angle between the BS and the l-th scatter

X. Yin, S. Wang, N. Zhang, and B. Ai, "Scatterer localization using large-scale antenna arrays based on a spherical wave-front parametric model," *IEEE Trans. Wireless Commun.*, vol. 16, no. 10, pp. 6543-6556, Oct. 2017.

Far-Field Beamsteering vs. Near-Field Beamfocusing

- **Far-field beamsteering (Far-field beamforming): the transmitter can only steer the radiated signal energy towards a specific angle**
- **Near-field beamfocusing (near-field beamforming): the spherical wave is able to focus the radiated signal energy in a specific spatial location**

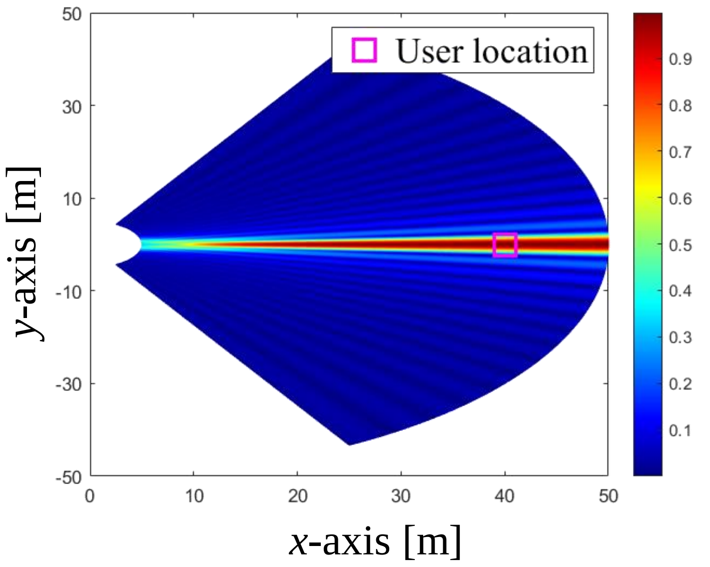

Far-Field Beamsteering

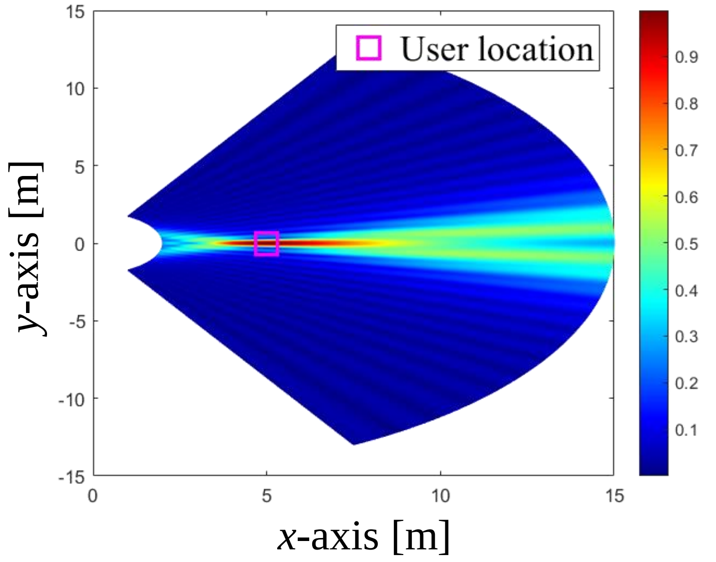

Near-Field Beamfocusing

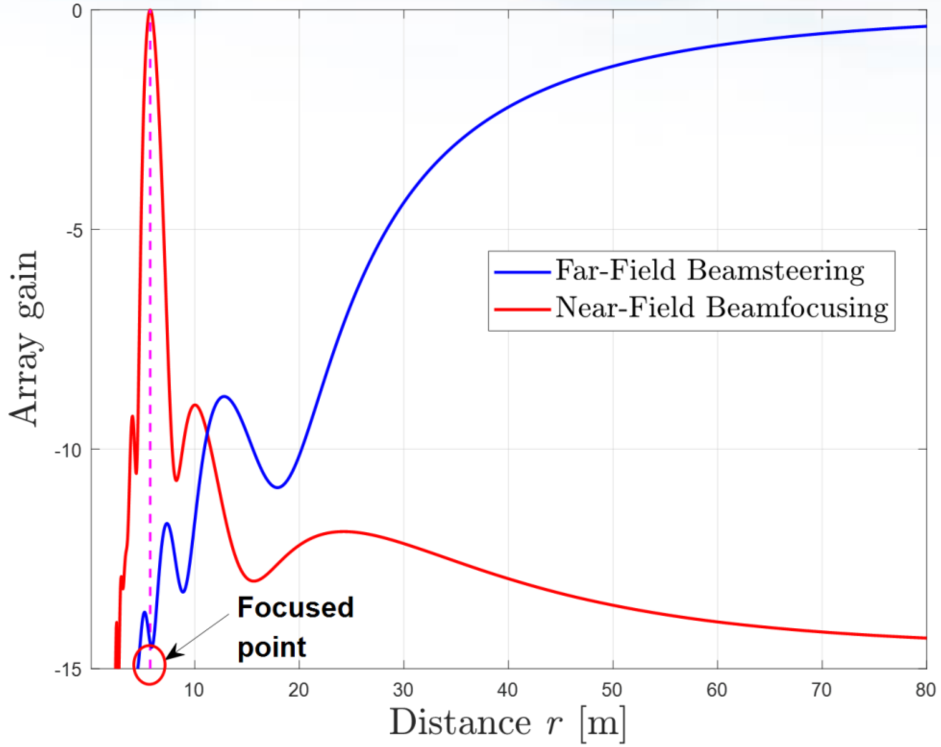

H. Zhang, N. Shlezinger, F. Guidi, D. Dardari, M. F. Imani, and Y. C. Eldar, "Beam focusing for near-field multiuser MIMO communications," *IEEE Trans. Wireless Commun.*, vol. 21, no. 9, pp. 7476–7490, Sep. 2022.

Array Gain of Near-Field Beamfocusing (1)

- **Array gain provided by beamfocusing on the same angle but different distances.**
  - **Assume a user is located at $(\bar{r},\theta)$, then the corresponding LoS channel is**

$$\boldsymbol{h}(\bar{r},\theta) = g\boldsymbol{a}(\bar{r},\theta) = g\left[e^{-jk\left(\bar{r}^{(-N)}-\bar{r}\right)},\cdots,e^{-jk\left(\bar{r}^{(0)}-\bar{r}\right)},\cdots,e^{-jk\left(\bar{r}^{(N)}-\bar{r}\right)}\right]^T$$

  where $M=2N+1$ and $k=2\pi/\lambda$ denote the wave number.

  - **The purpose of beamfocusing is to compensate for the phase variation between antennas, therefore, the beamfocusing vector aligned with the location $(\bar{r},\theta)$ is**

$$\boldsymbol{w}(\bar{r},\theta) = \frac{1}{\sqrt{M}}\boldsymbol{a}^*(\bar{r},\theta) = \frac{1}{\sqrt{M}}\left[e^{jk\left(\bar{r}^{(-N)}-\bar{r}\right)},\cdots,e^{jk\left(\bar{r}^{(0)}-\bar{r}\right)},\cdots,e^{jk\left(\bar{r}^{(N)}-\bar{r}\right)}\right]^T$$

  - **Then, the normalized array gain achieved by $\boldsymbol{w}=\boldsymbol{a}^*(\bar{r},\theta)$ at any other user located at (r,θ) is**

$$f(r,\bar{r},\theta) = \frac{\left\|\boldsymbol{h}(r,\theta)^T\boldsymbol{w}(\bar{r},\theta)\right\|}{\left\|\boldsymbol{h}(r,\theta)\right\|\left\|\boldsymbol{w}(\bar{r},\theta)\right\|} = \frac{1}{M}\left|\sum_{n=-N}^{N} e^{jk\left(\bar{r}^{(n)}-r^{(n)}\right)}\right|$$

Array Gain of Near-field Beamfocusing (2)

Lemma 1: the normalized array gain achieved by $\boldsymbol{w} = \boldsymbol{a}^*(\bar{r},\theta)$ at the user location (r,θ) is obtained through Fresnel approximation as

$$f(r,\bar{r},\theta) = \frac{1}{M}\left|\sum_{n=-N}^{N} e^{jk(\bar{r}^{(n)}-r^{(n)})}\right| \approx |G(\beta)| = \left|\frac{C(\beta)+jS(\beta)}{\beta}\right|$$

where $\beta = \sqrt{\frac{M^2 d^2 (1-\theta^2)}{2\lambda}\left|\frac{1}{r}-\frac{1}{\bar{r}}\right|}$. $C(\beta) = \int_0^\beta \cos\left(\frac{\pi}{2}t^2\right)\mathrm{d}t$ **and** $S(\beta) = \int_0^\beta \sin\left(\frac{\pi}{2}t^2\right)\mathrm{d}t$ **are Fresnel functions.**

- **Proof:**
  - **Based on the second-order Tayler expansion,** $\bar{r}^{(n)}$ **and** $r^{(n)}$ **can be approximated as**

$$r^{(n)} = \sqrt{r^2 - 2ndr\theta + n^2 d^2} \approx r - nd\theta + \frac{1-\theta^2}{2r}n^2 d^2 \qquad \bar{r}^{(n)} \approx \bar{r} - nd\theta + \frac{1-\theta^2}{2\bar{r}}n^2 d^2$$

  - **Then we have** $k\left(\bar{r}^{(n)} - \bar{r}\right) - k\left(r^{(n)} - r\right) = \pi n^2 \frac{d^2(1-\theta^2)}{\lambda}\left(\frac{1}{\bar{r}} - \frac{1}{r}\right) = \pi n^2 x$, **therefore**

$$f(r,\bar{r},\theta) \approx \frac{1}{M}\left|\sum_{n=-N}^{N} e^{j\pi n^2 x}\right| \approx \frac{1}{2N}\left|\int_{-N}^{N} e^{j\pi n^2 x}\,\mathrm{d}n\right| = \left|\frac{\int_0^{\sqrt{2x}N} e^{j\frac{\pi}{2}t^2}\mathrm{d}t}{\sqrt{2x}N}\right| = \left|\frac{C(\beta)+jS(\beta)}{\beta}\right|$$

M. Cui and L. Dai, "Channel estimation for extremely large-scale MIMO: Far-field or near-field?," *IEEE Trans. Commun.*, vol. 70, no. 4, pp. 2663-2677, Apr. 2022.

Array Gain of Near-Field Beamfocusing (3)

- **Near-field array gain of planar arrays and RIS**
  - **A similar result with that of the linear arrays**

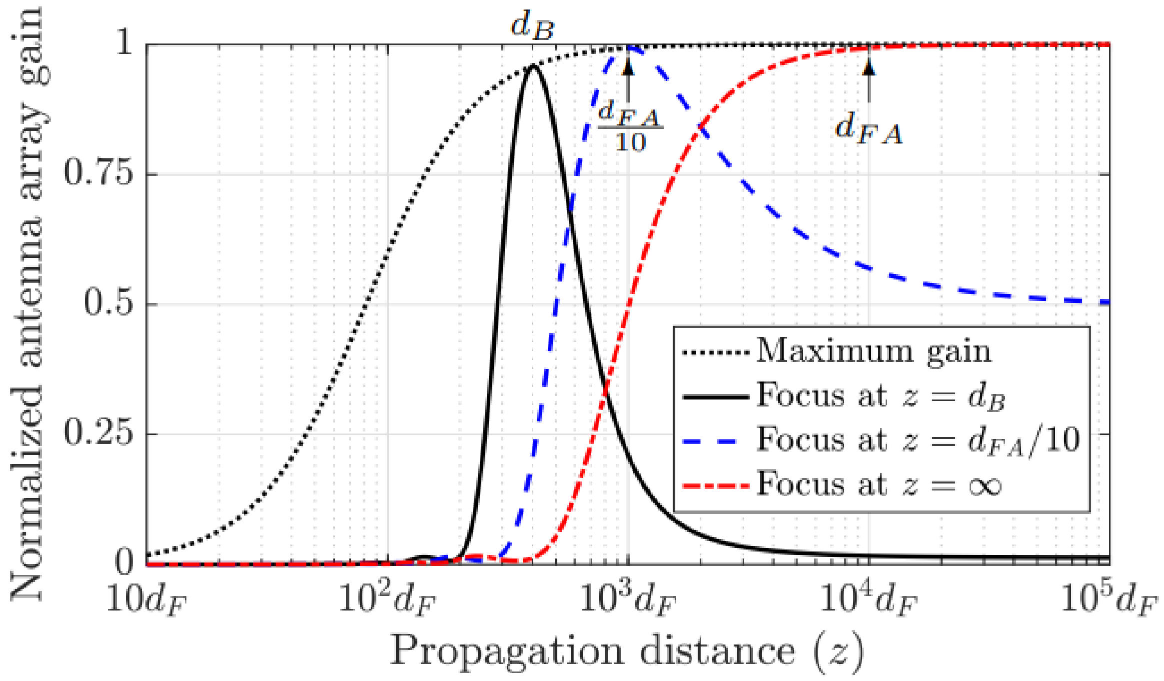

$$
\begin{aligned}
G_{\text{antenna}} &\approx \left(\frac{2}{D^2}\right)^2 \left| e^{-\mathrm{j}\frac{2\pi}{\lambda}z} \int_{\mathcal{A}} e^{-\mathrm{j}\frac{2\pi}{\lambda}\left(\frac{x^2}{2z}+\frac{y^2}{2z}\right)} dx\, dy \right|^2 \\
&= \left(\frac{2}{D^2}\right)^2 \left| \int_{-D/\sqrt{8}}^{D/\sqrt{8}} e^{-\mathrm{j}\frac{\pi}{\lambda}\frac{x^2}{z}} dx \right|^4 \\
&= \left(\frac{8z}{d_F}\right)^2 \boxed{\left(C^2\left(\sqrt{\frac{d_F}{8z}}\right) + S^2\left(\sqrt{\frac{d_F}{8z}}\right)\right)^2}
\end{aligned} \tag{9}
$$

Fresnel functions

E. Björnson, Ö. T. Demir, and L. Sanguinetti, "A primer on near-field beamforming for arrays and reconfigurable intelligent surfaces," in *Proc. 2021 55th Asilomar Conference on Signals, Systems, and Computers*, pp. 105-112, Oct. 2021.

Characteristics of Near-Field Beamfocusing

- **The beamfocusing gain depends on the function $G(\beta) = \left|\frac{C(\beta)+S(\beta)}{\beta}\right|$ and the parameter β**
- **Distance window**
  - $|G(\beta)|$ **shows a significant downward trend**
  - **To guarantee the array gain is larger than Γ, we have**

$$f(r,\bar{r},\theta) \approx G(\beta) = \left|\frac{C(\beta)+S(\beta)}{\beta}\right|$$

$$\beta = \sqrt{\frac{M^2 d^2 (1-\theta^2)}{2\lambda}\left|\frac{1}{r}-\frac{1}{\bar{r}}\right|}$$

$$|G(\beta)| \geq \Gamma \Rightarrow \beta = \sqrt{\frac{M^2 d^2 (1-\theta^2)}{2\lambda}\left|\frac{1}{r}-\frac{1}{\bar{r}}\right|} \leq \beta_\Gamma \quad |G(\beta_\Gamma)| = \Gamma$$

$$\left|\frac{1}{r}-\frac{1}{\bar{r}}\right| \leq \frac{2\lambda\beta_\Gamma^2}{M^2 d^2(1-\theta^2)} = \frac{2\lambda\beta_\Gamma^2}{D^2(1-\theta^2)} = \frac{4\beta_\Gamma^2}{\mathrm{RD}(1-\theta^2)}$$

distance window $\quad r \in \left[\frac{\bar{r}\mathrm{RD}(1-\theta^2)}{\mathrm{RD}(1-\theta^2)+4\beta_\Gamma^2\bar{r}}, \frac{\bar{r}\mathrm{RD}(1-\theta^2)}{\mathrm{RD}(1-\theta^2)-4\beta_\Gamma^2\bar{r}}\right]$

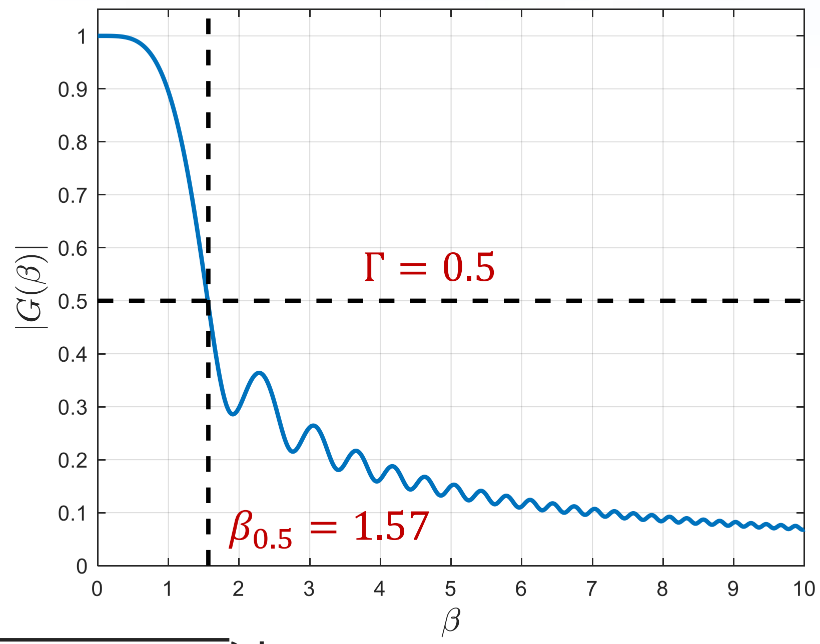

- **Limit performance analysis:**
  - **Array gain at zero distance:** $\lim_{r\to 0}|G(\beta)| = |G(+\infty)| = 0$
  - **Array gain at infinite distance:** $\lim_{r\to +\infty}|G(\beta)| = \left|G\left(\sqrt{M^2 d^2(1-\theta^2)/(2\lambda\bar{r})}\right)\right|$

Simulation Results of Near-Field Beamfocusing

- **Limit performance analysis:**
  - **Array gain at zero distance:** $\lim_{r\to 0}|G(\beta)| = |G(+\infty)| = 0$
  - **Array gain at infinite distance:** $\lim_{r\to +\infty}|G(\beta)| = \left|G\left(\sqrt{M^2d^2(1-\theta^2)/(2\lambda\bar{r})}\right)\right|$
- **Distance window**

$$r \in \left[\frac{\bar{r}\mathrm{RD}(1-\theta^2)}{\mathrm{RD}(1-\theta^2)+4\beta_\Gamma^2\bar{r}},\ \frac{\bar{r}\mathrm{RD}(1-\theta^2)}{\mathrm{RD}(1-\theta^2)-4\beta_\Gamma^2\bar{r}}\right]$$

- **Parameters**

Parameters	Values
Carrier	30 GHz
Array structure	256-ULA
θ	$\pi/8$
$\bar{r}$	15 meters
Γ	0.5

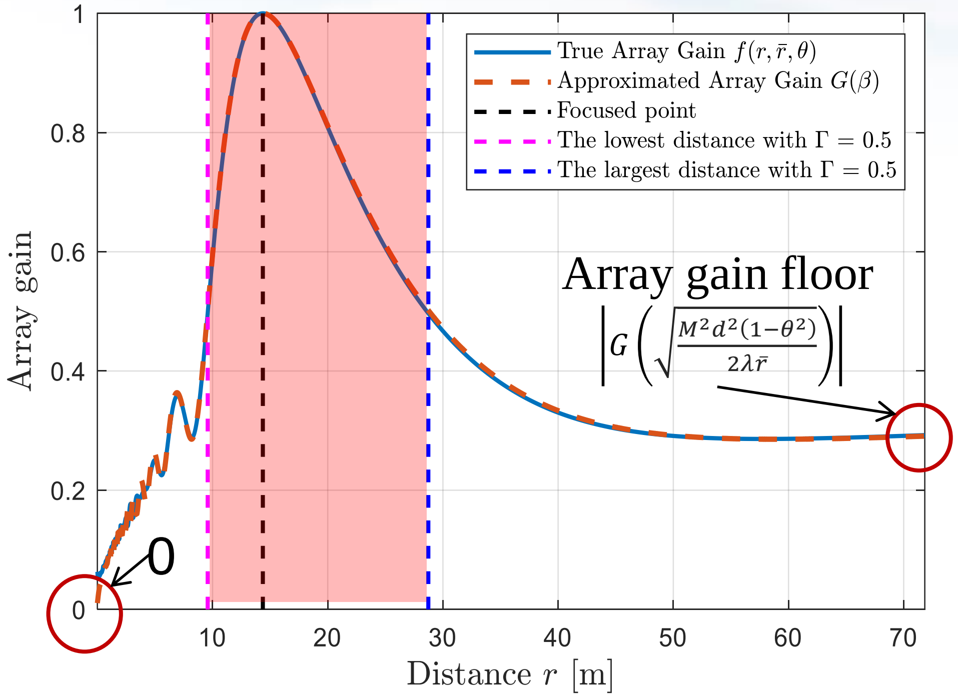

[1] M. Cui and L. Dai, "Channel estimation for extremely large-scale MIMO: Far-field or near-field?," *IEEE Trans. Commun.*, vol. 70, no. 4, pp. 2663-2677, Apr. 2022.
[2] E. Björnson, Ö. T. Demir, and L. Sanguinetti, "A primer on near-field beamforming for arrays and reconfigurable intelligent surfaces," in *Proc. 2021 55th Asilomar Conference on Signals, Systems, and Computers*, pp. 105-112, Oct. 2021.

Proposed Effective Rayleigh Distance

- **Derive the effective Rayleigh distance from the view of array gain loss**

Classical Rayleigh distance (RD)

➢ **Definition: When the largest phase error between the planar wave and spherical wave is $\pi/8$, the Tx-Rx distance is**

$$\mathrm{RD} = \frac{2D^2}{\lambda}$$

Effective Rayleigh distance (ERD)

➢ **Definition: When the array gain loss of the far-field beam in the near-field region is 5%, the Tx-Rx distance is**

$$\mathrm{ERD} = 0.367\cos^2\vartheta\,\mathrm{RD}$$

Distance window

$$r \in \left[\frac{\bar{r}\mathrm{RD}(1-\theta^2)}{\mathrm{RD}(1-\theta^2)+4\beta_\Gamma^2\bar{r}}, \frac{\bar{r}\mathrm{RD}(1-\theta^2)}{\mathrm{RD}(1-\theta^2)-4\beta_\Gamma^2\bar{r}}\right]$$

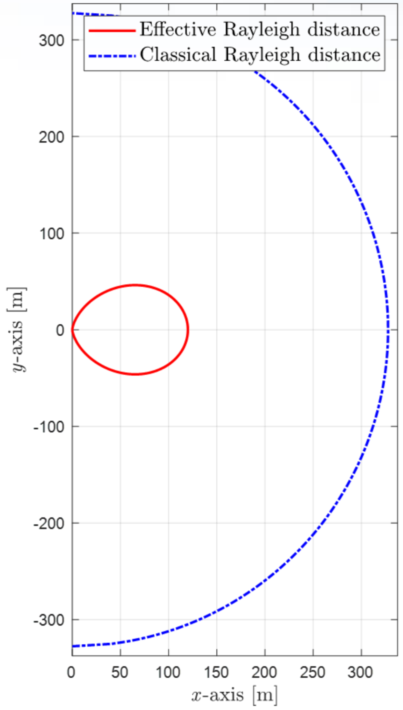

M. Cui, L. Dai, R. Schober, and L. Hanzo, "Near-field wideband beamforming for extremely large antenna array," *IEEE Trans. Wireless Commun.*, early access, May 2024.

Part 3: Opportunities of Near-Field Communications

清華大學 Tsinghua University
南京郵電大學 Nanjing University of Posts and Telecommunications
WEIZMANN INSTITUTE OF SCIENCE

Outline of Part 3

- Near-Field Single-User MIMO Capacity Enhancement
- Near-Field Location Division Multiple Access
- Near-Field DMA Assisted Multi-User Communications
- Near-Field Wireless Power Transfer
- Near-Field Assisted Localization
- Near-Field Physical-Layer Security
- Near-Field Region Enlargement with Circular Arrays

Limited DoFs for Far-Field LoS Channel

- **Based on planar wave assumptions, degrees of freedom (DoF) are limited in line-of-sight (LoS) far-field channel**

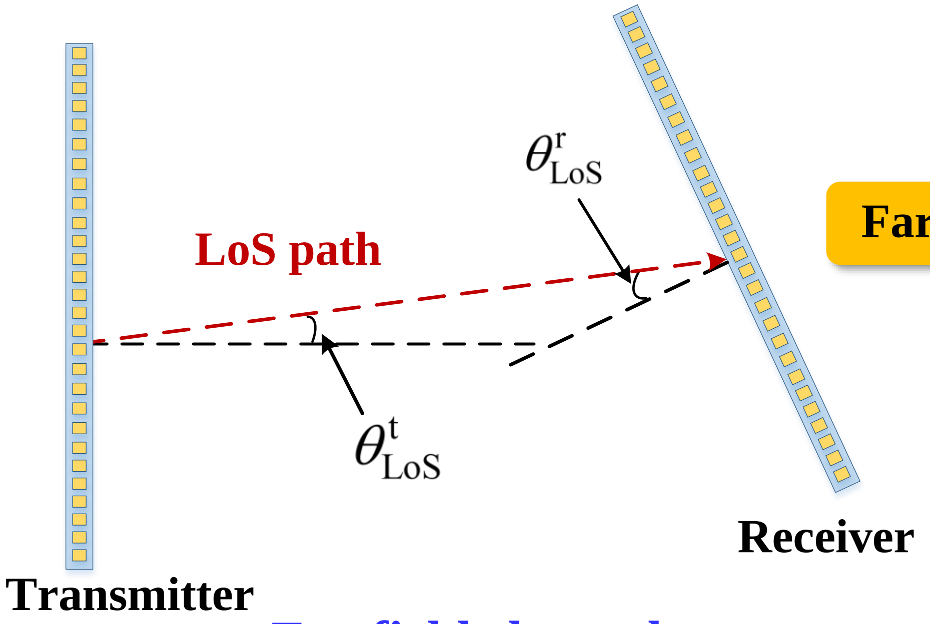

Far-field channel

Distance: $d^{(n)} = nd\theta$

Phase: $\phi_n^{\mathrm{far}} = -\frac{2\pi d^{(n)}}{\lambda} = -\frac{2\pi}{\lambda} nd\theta$

Far-field steering vector

$$\mathbf{a}(\phi) = \frac{1}{\sqrt{N}}\left[1, e^{j\frac{2\pi}{\lambda}d\sin\phi}, \cdots, e^{j(2N)\frac{2\pi}{\lambda}d\sin\phi}\right]^T$$

$$\mathbf{H}_{\mathrm{LoS}} = \alpha_{\mathrm{LoS}} \underbrace{\mathbf{a}_{\mathrm{r}}(\theta_{\mathrm{LoS}}^{\mathrm{r}})\, \mathbf{a}_{\mathrm{t}}^{H}(\theta_{\mathrm{LoS}}^{t})}_{\text{Rank-one matrix}}$$

The rank-one LoS channel can only support one data stream

O. Ayach, S. Rajagopal, S. Abu-Surra, Z. Pi, and R. W. Heath, "Spatially sparse precoding in millimeter wave MIMO systems," *IEEE Trans. Wireless Commun.*, vol. 13, no. 3, pp. 1499–1513, Jan. 2014.

From rank-one channel to highly ranked channel

- The rank-one far-field LoS channel is not valid any more in the near-field region
- Based on **spherical waves**, the near-field LoS channel becomes **highly ranked**

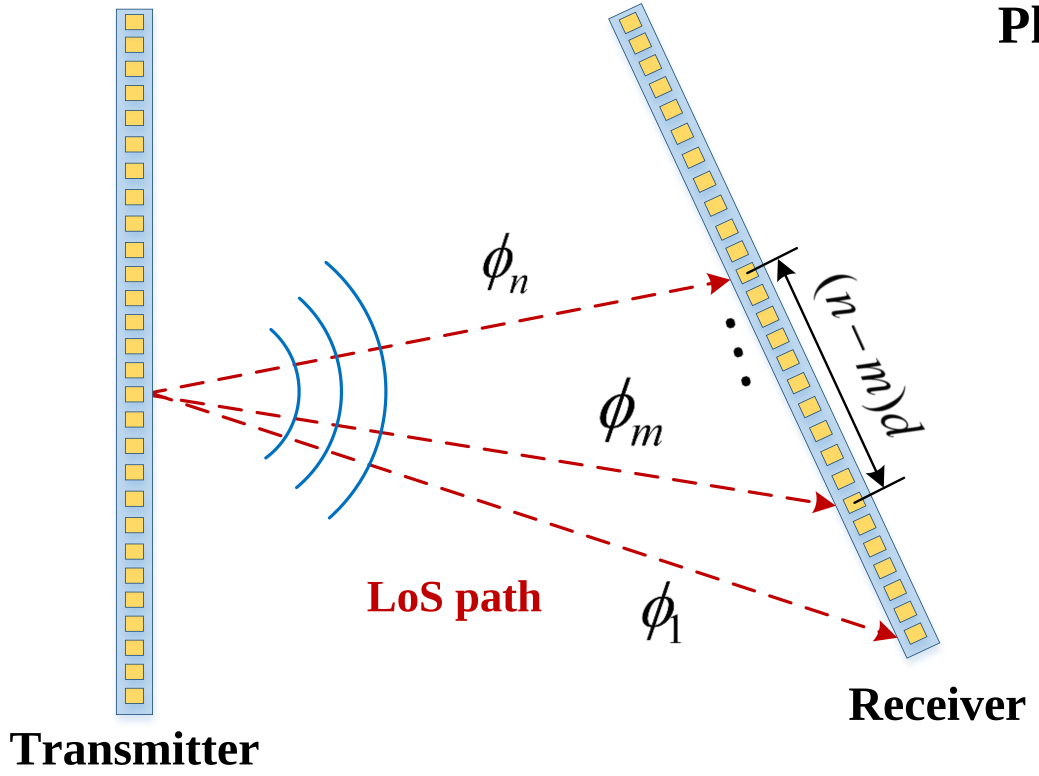

Near-field channel

Phase: $\phi_n = \frac{2\pi\left(r^{(n)}-r\right)}{\lambda} = \frac{2\pi}{\lambda}\left(\sqrt{r^2 - 2ndr\theta + n^2 d^2} - r\right)$

$$\overset{r > RD}{\approx} \underbrace{-\frac{2\pi}{\lambda} nd\theta}_{}$$

Far-field phase ϕ_n^{far}

✖ Not valid in near-field region

Near-field LoS channel

$$\mathbf{H}_{\text{LoS}} = \underbrace{\begin{bmatrix} \alpha_{1,1} e^{-j2\pi r_{1,1}/\lambda} & \cdots & \alpha_{1,N_2} e^{-j2\pi r_{1,N_2}/\lambda} \\ \vdots & \ddots & \vdots \\ \alpha_{N_2,1} e^{-j2\pi r_{N2,1}/\lambda} & \cdots & \alpha_{N_2,N_1} e^{-j2\pi r_{N_2,N_1}/\lambda} \end{bmatrix}}_{\text{Significantly increased rank}}$$

Increased DoFs for Near-Field LoS Channel

- The **DoFs can significantly increase** in the near-field region when both BS and UE are equipped with ELAAs

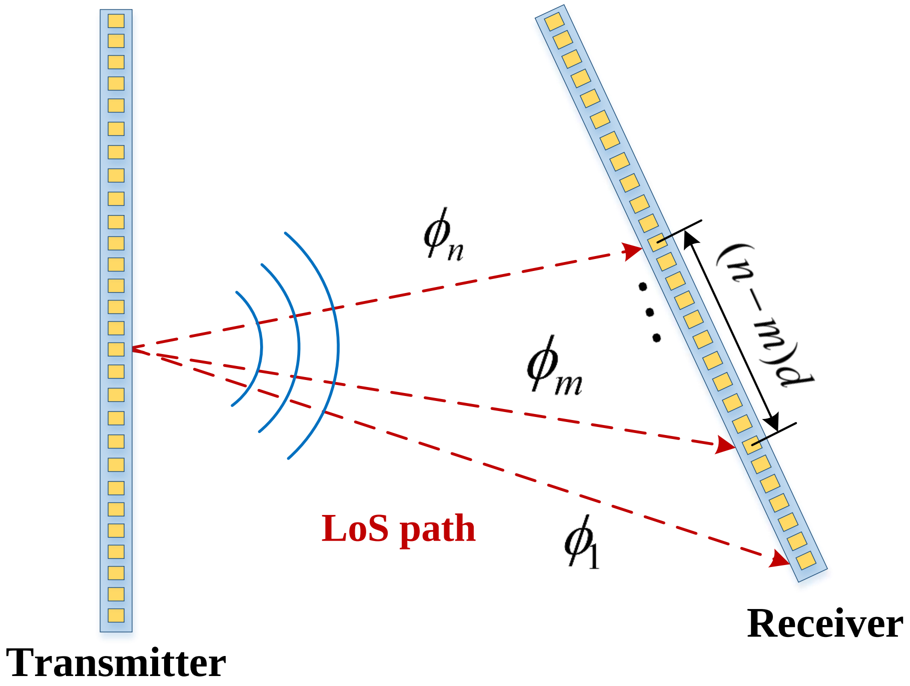

Near-field LoS channel

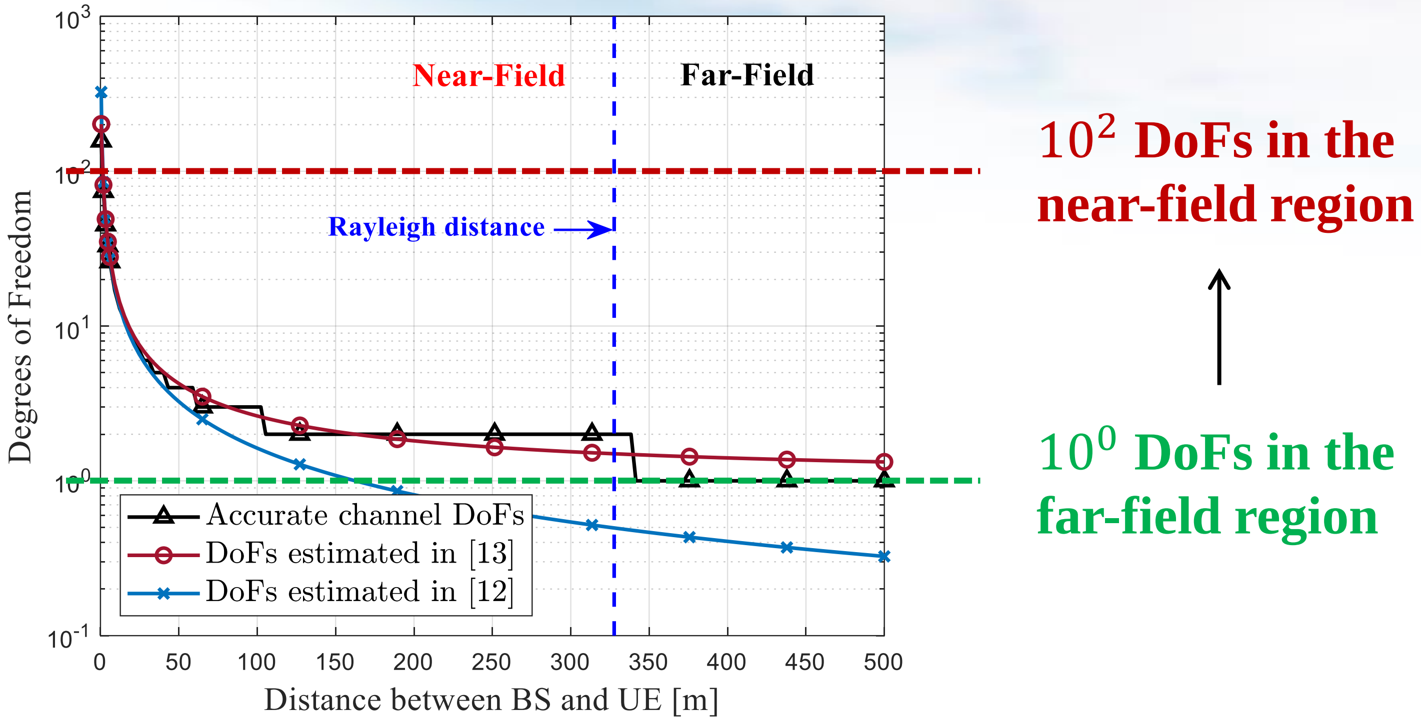

The capacity is expected to be significantly enhanced with increased DoFs

[12] D. A. Miller, "Waves, modes, communications, and optics: A tutorial," *Adv. in Opt. and Photon.*, vol. 11, no. 3, pp. 679–825, Sep. 2019.
[13] N. Decarli and D. Dardari, "Communication modes with large intelligent surfaces in the near field," *IEEE Access*, vol. 9, pp. 165 648–165 666, Sep. 2021.

Limitation of hybrid precoding architecture

- **However, limited by the small number of RF chains, the classical hybrid precoding can not efficiently utilize the increased DoFs to enhance the capacity**

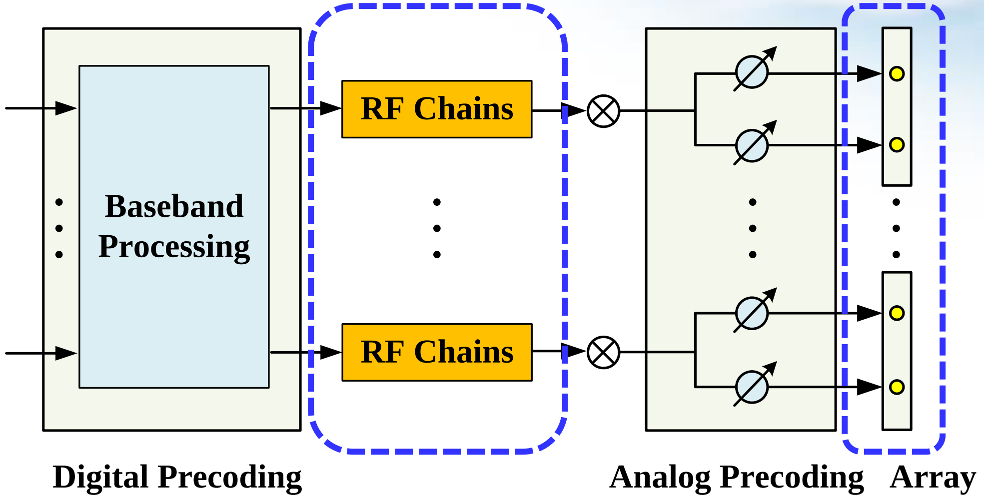

Precoding	Region	Spatial DoFs	RF chains	Spectral Efficiency
Hybrid Precoding	Far-Field	Low	RF Chains $\approx$ DoFs	Near Optimal
	Near-Field	High	RF Chains $\ll$ Distance-Related DoFs	Far From Optimal

How to efficiently utilize the significantly increased DoFs in near field

Distance-Aware Precoding Architecture

- Based on the distance-related DoFs in the near-field region, the distance-aware precoding architecture is proposed
- The number of activated RF chains can be configured to match the increased DoFs in the near-field region

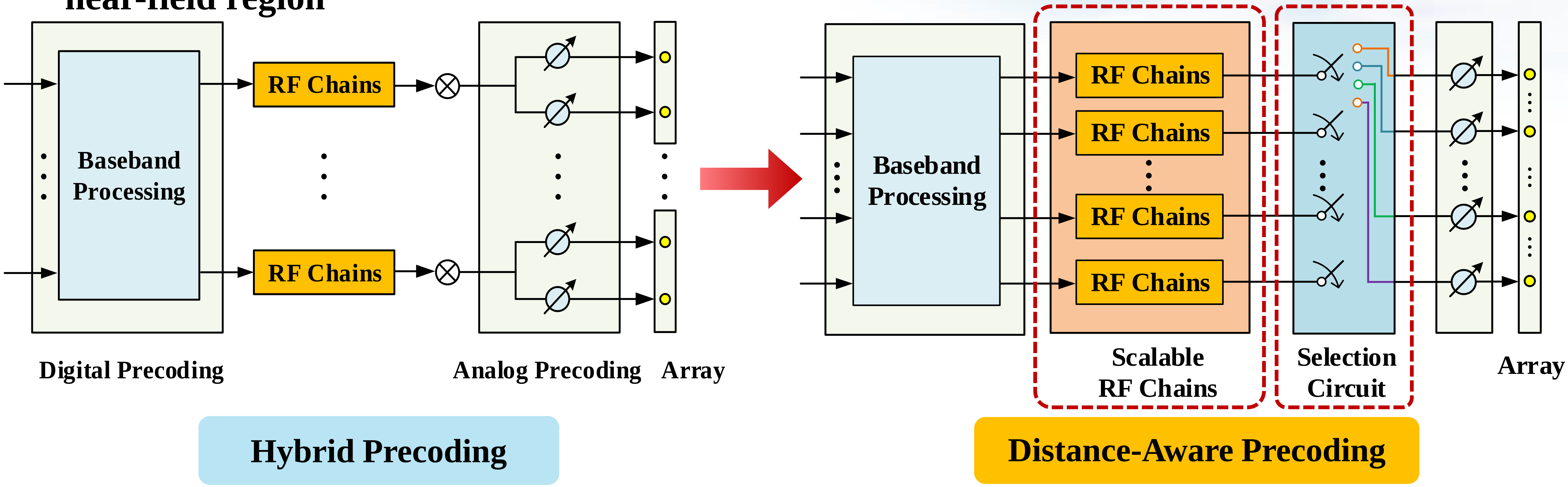

Z. Wu, M. Cui, Z. Zhang, and L. Dai, "Distance-aware precoding for near-field capacity improvement in XL-MIMO," in *Proc. IEEE 95th Veh. Technol. Conf. (IEEE VTC'22 Spring)*, Helsinki, Finland, Jun. 2022.

Simulation Results

- In the distance-aware precoding architecture, the number of RF chains can be flexibly adjusted to match the spatial DoFs
- The spectral efficiency can be significantly enhanced in the near-field region

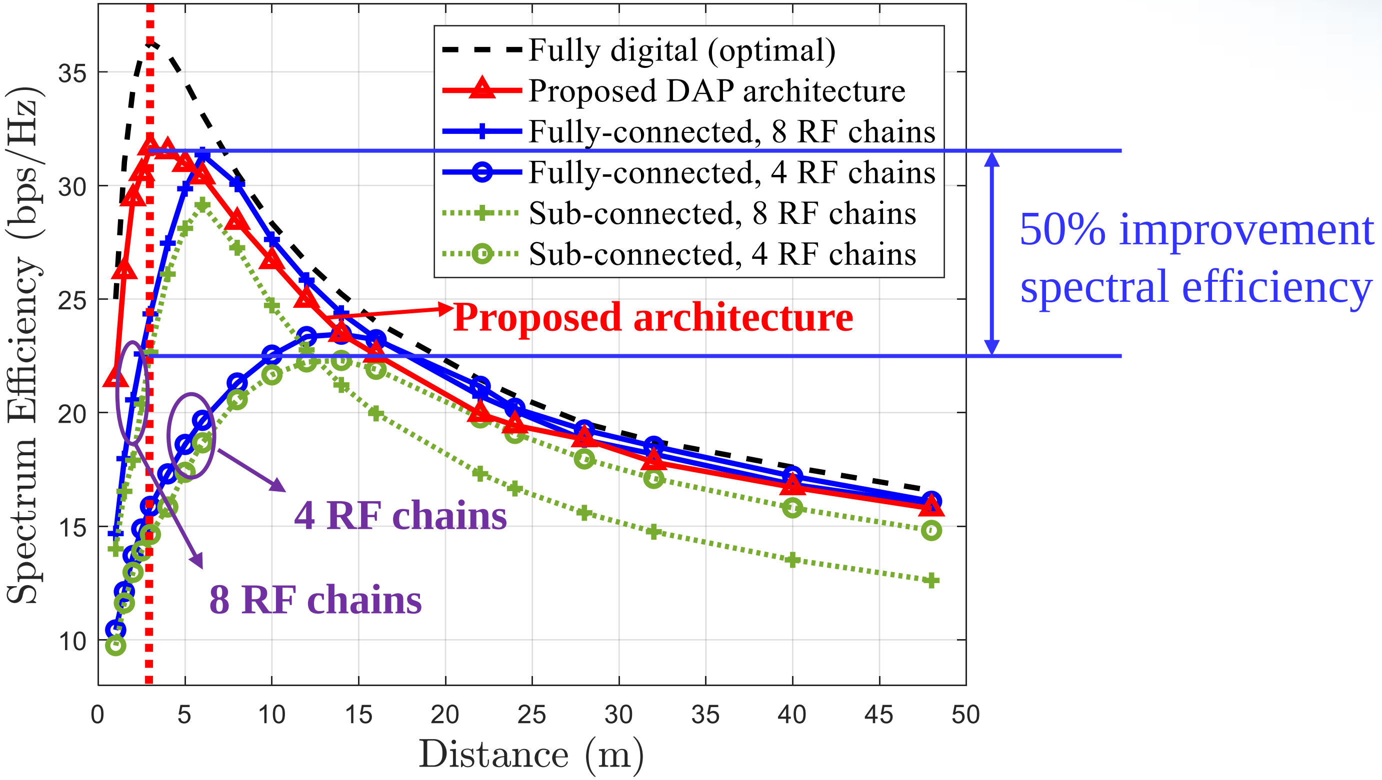

Parameters	Values
Carrier	100 GHz
BS antennas	256
MS antennas	256
SNR	30 dB

[1] X. Gao, L. Dai, S. Han, C.-L. I, and R. W. Heath, "Energy-efficient hybrid analog and digital precoding for mmwave MIMO systems with large antenna arrays," *IEEE J. Sel. Areas Commun.*, vol. 34, no. 4, pp.998–1009, Apr. 2016.

[2] X. Yu, J. Z. J. Shen, and K. B. Letaief, "Alternating minimization algorithms for hybrid precoding in millimeter wave MIMO systems," *IEEE J. Sel. Areas Commun.*, vol. 10, no. 3, pp. 485–500, Apr. 2016.

Outline of Part 3

- **Near-Field Single-User MIMO Capacity Enhancement**
- **Near-Field Location Division Multiple Access**
- **Near-Field DMA Assisted Multi-User Communications**
- **Near-Field Wireless Power Transfer**
- **Near-Field Assisted Localization**
- **Near-Field Physical-Layer Security**
- **Near-Field Region Enlargement with Circular Arrays**

Challenge of SDMA for Far-Field Communication

- **Spatial division multiple access (SDMA)** is employed by **massive MIMO** to multiplex data streams to different users for improving spectral efficiency
- In massive MIMO systems, **far-field beamsteering** vectors only focus on specific angles, which enables the multiple access for users at different angles

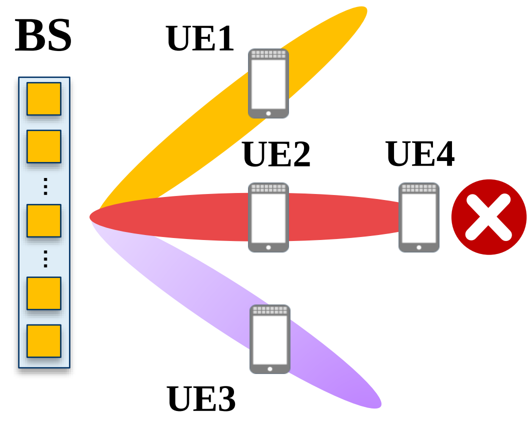

SDMA for far-field communications

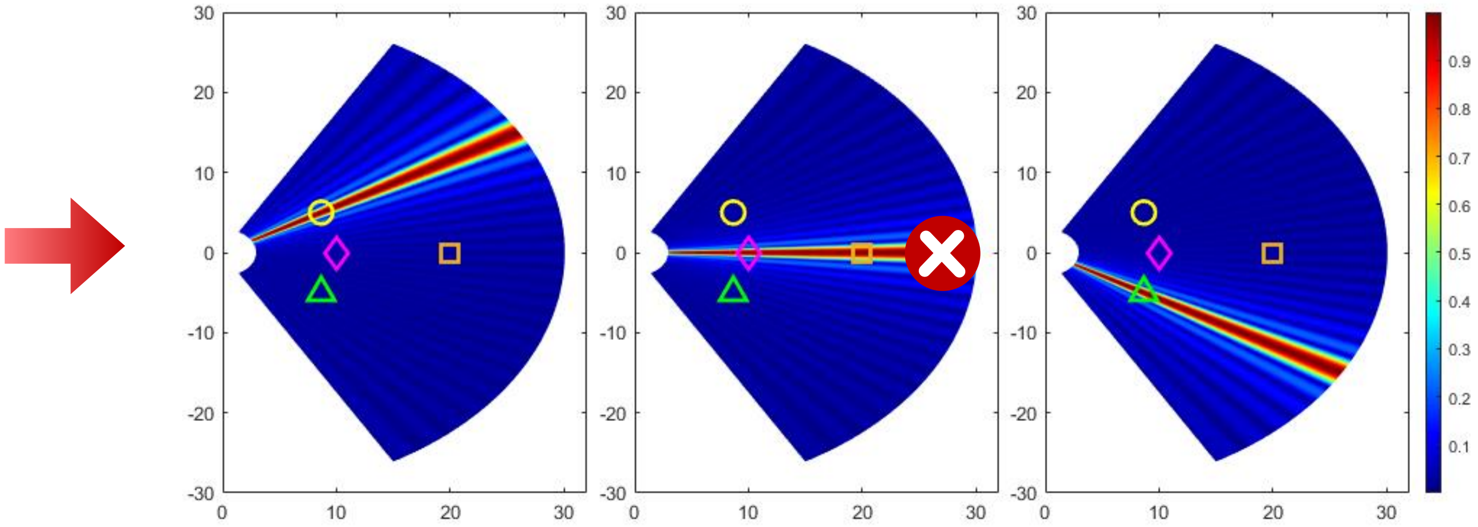

Users at the same angle cannot be simultaneously served by massive MIMO with SDMA

Mitigated Interference with Near-Field Beamfocusing

- **Far-field beamsteering** vectors focus on specific spatial **angle**
- **Near-field beamfocusing** is capable to focus on specific **location**, which could be leveraged to mitigate **inter-user interferences**

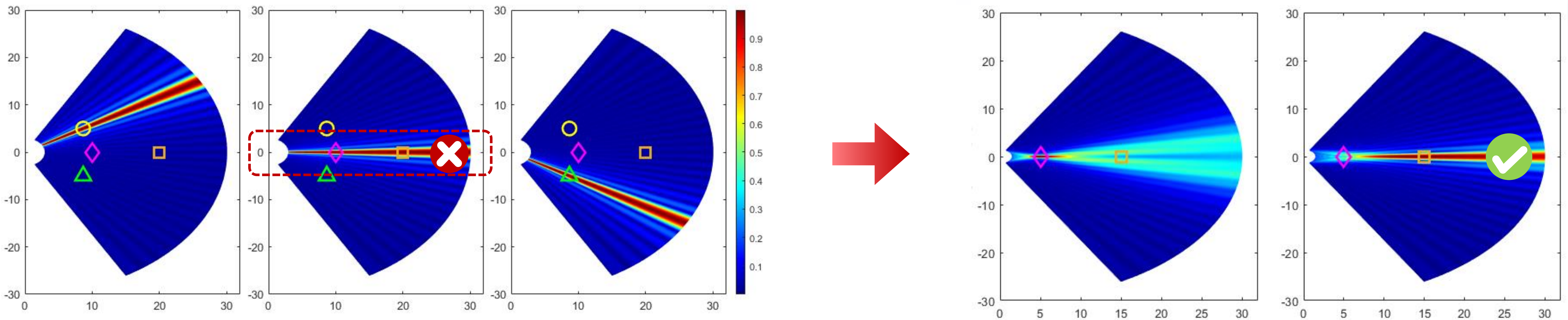

Near-field beamfocusing has the potential to serve users at the same spatial angle

H. Zhang, N. Shlezinger, F. Guidi, D. Dardari, M. F. Imani, and Y. C. Eldar, "Beam focusing for near-field multiuser MIMO communications," *IEEE Trans. Wireless Commun.*, vol. 21, no. 9, pp. 7476–7490, Sep. 2022.

Multiple Access for Near-Field Communications: SDMA or LDMA?

- **Far-field SDMA**: Users at different **angles** can be served by orthogonal far-field beams
- **Near-field location division multiple access (LDMA)**: Users at different **locations** can be simultaneously served due to property of near-field beam focusing

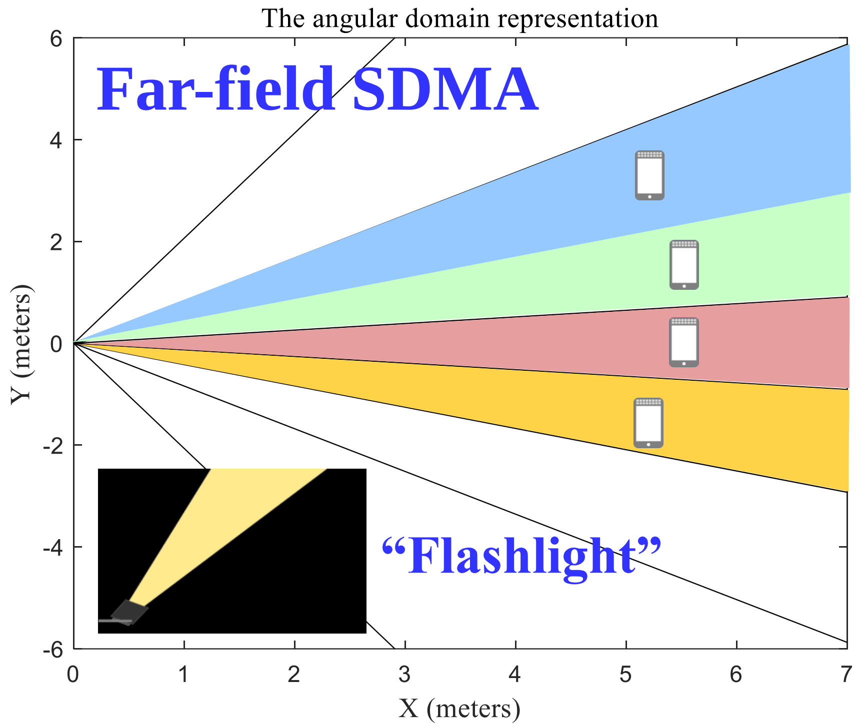

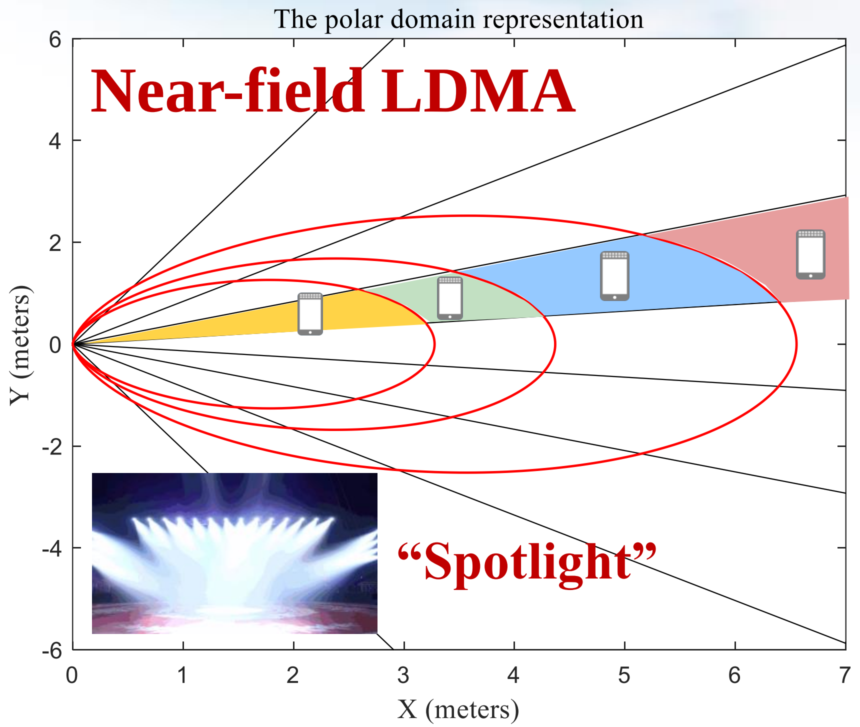

Compared with far-field SDMA, near-field LDMA provides a new dimension for capacity improvement

Z. Wu and L. Dai, "Multiple access for near-field communications: SDMA or LDMA? " *IEEE J. Sel. Areas Commun.*, vol. 41, no. 6, pp. 1918-1935, Jun. 2023.

Distance Domain Asymptotic Orthogonality

- **Far-field orthogonality in angular domain**

  Phase: $\phi_n^{\text{far}}(\theta) = -\frac{2\pi}{\lambda} nd\theta$

  Correlation: $f^{\text{far}} = |\mathbf{a}^H(\theta_1)\mathbf{a}(\theta_2)| = \frac{1}{N}\left|\frac{\sin(\frac{1}{2}Nkd(\sin\theta_1 - \sin\theta_2))}{\sin(\frac{1}{2}kd(\sin\theta_1 - \sin\theta_2))}\right|$

  As $N \to \infty$, interference from different angles $I^{\text{far}} \to 0$ $(\theta_1 \neq \theta_2)$

- **Lemma 2: Near-field orthogonality in distance domain**

  Phase: $\phi_n^{\text{near}}(\theta) = -\frac{2\pi}{\lambda} nd\theta + \frac{1-\theta^2}{\lambda r}\pi n^2 d^2$

  Correlation: $f^{\text{near}} = |\mathbf{a}^H(\theta, r_1)\mathbf{a}(\theta, r_2)| \approx |G(\beta)| = \left|\frac{C(\beta)+jS(\beta)}{\beta}\right|$

  where $\beta = \sqrt{\frac{N^2 d^2(1-\theta^2)}{2\lambda}\left|\frac{1}{r} - \frac{1}{\bar{r}}\right|}$

  As $N \to \infty$, interference from different distances $I^{\text{near}} \to 0$ $(\forall\theta, r_1 \neq r_2)$

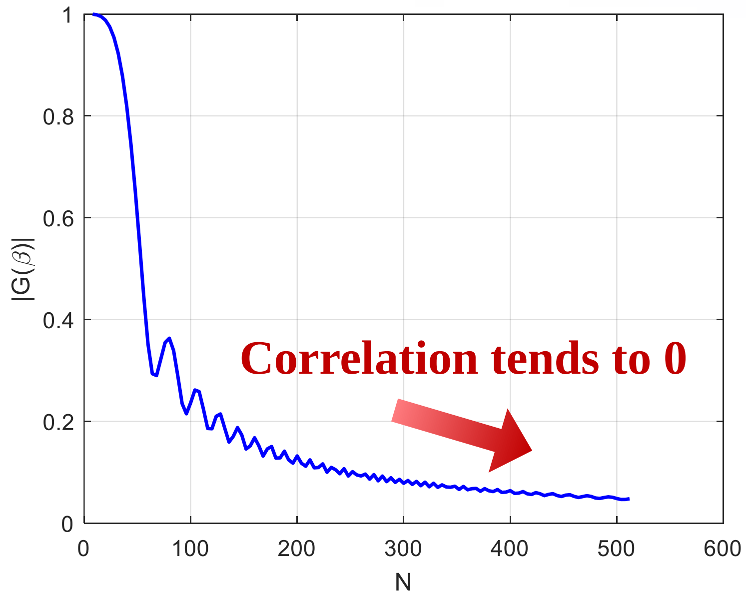

Correlation with increasing antennas

Simulation Results for LDMA

- **Scenario 1: Users are linearly distributed along the same direction**
- **Scenario 2: Users are uniformly distributed within a cell**

BS Antennas	UE Antennas	Frequency	UE Numbers	Elevation/ Azimuth Angle Range	Distance Range
256	1	30 GHz	20	$[-\pi/2, \pi/2]$	[4m, 100m]

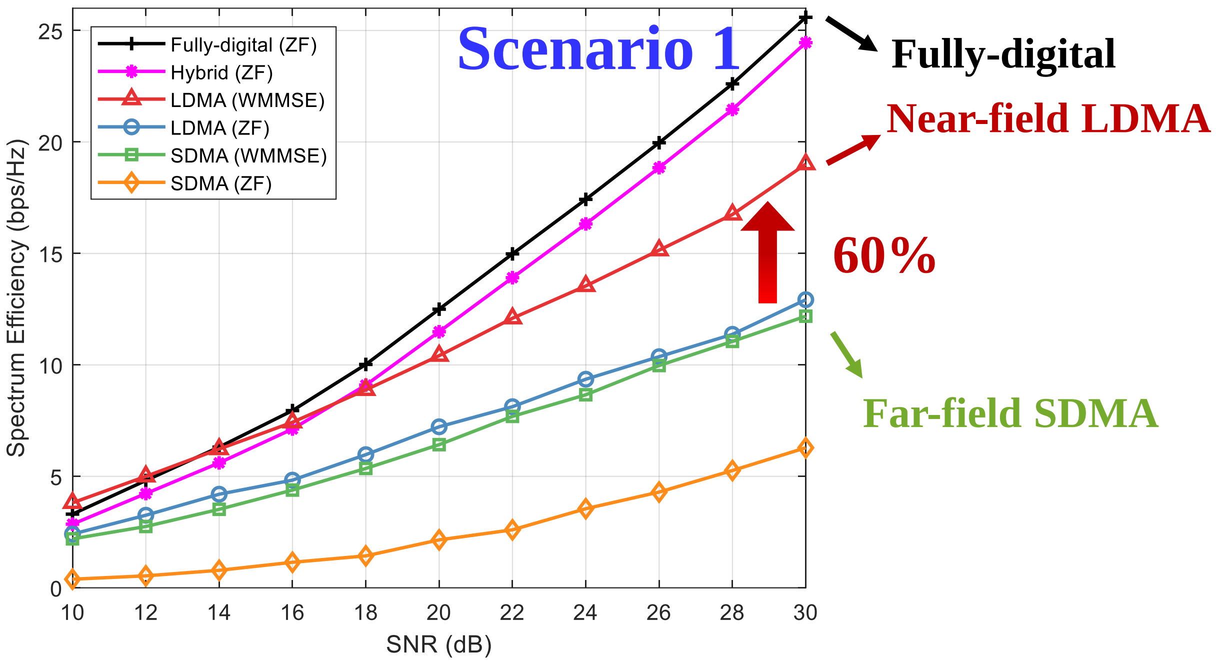

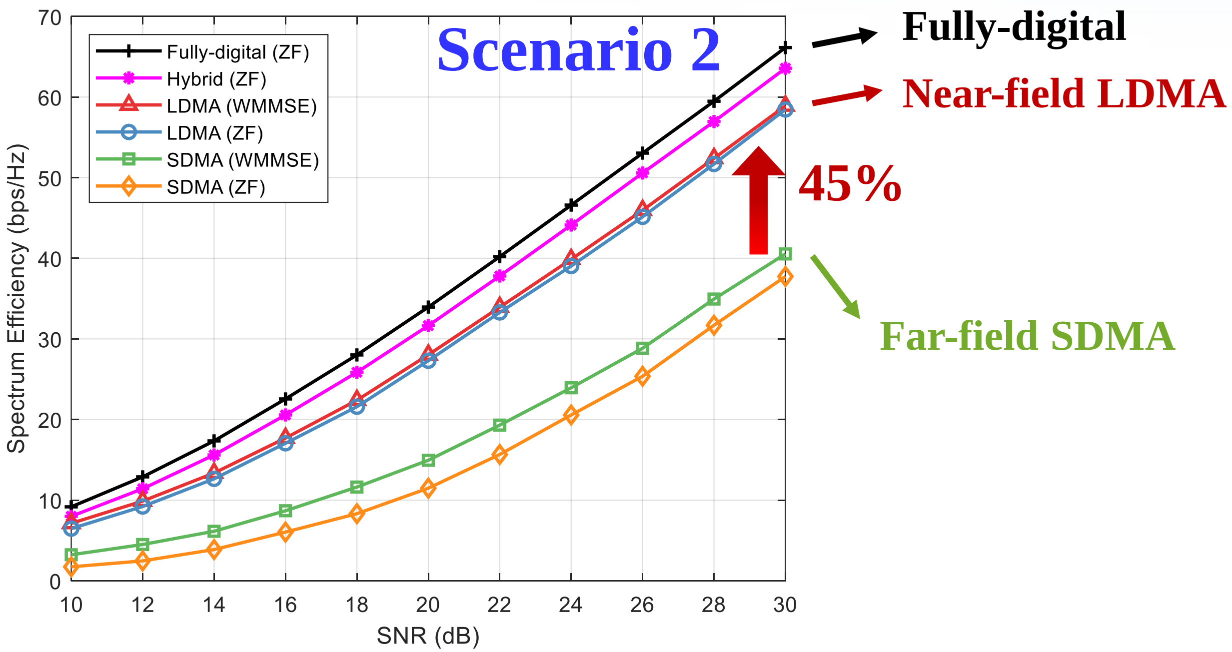

Z. Wu and L. Dai, "Multiple access for near-field communications: SDMA or LDMA? " *IEEE J. Sel. Areas Commun.*, vol. 41, no. 6, pp. 1918-1935, Jun. 2023.

Outline of Part 3

- **Near-Field Single-User MIMO Capacity Enhancement**
- **Near-Field Location Division Multiple Access**
- **Near-Field DMA Assisted Multi-User Communications**
- **Near-Field Wireless Power Transfer**
- **Near-Field Assisted Localization**
- **Near-Field Physical-Layer Security**
- **Near-Field Region Enlargement with Circular Arrays**

Emerging Dynamic Metasurface Antennas

- Emerging antenna technology
  - Scalable
  - Low power
- Dynamically configurable radiation pattern
- Applications
  - Microwave imaging
  - Radar systems
  - Satellite communications
- Intelligent reflective surfaces

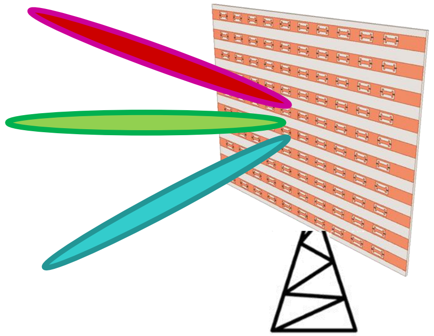

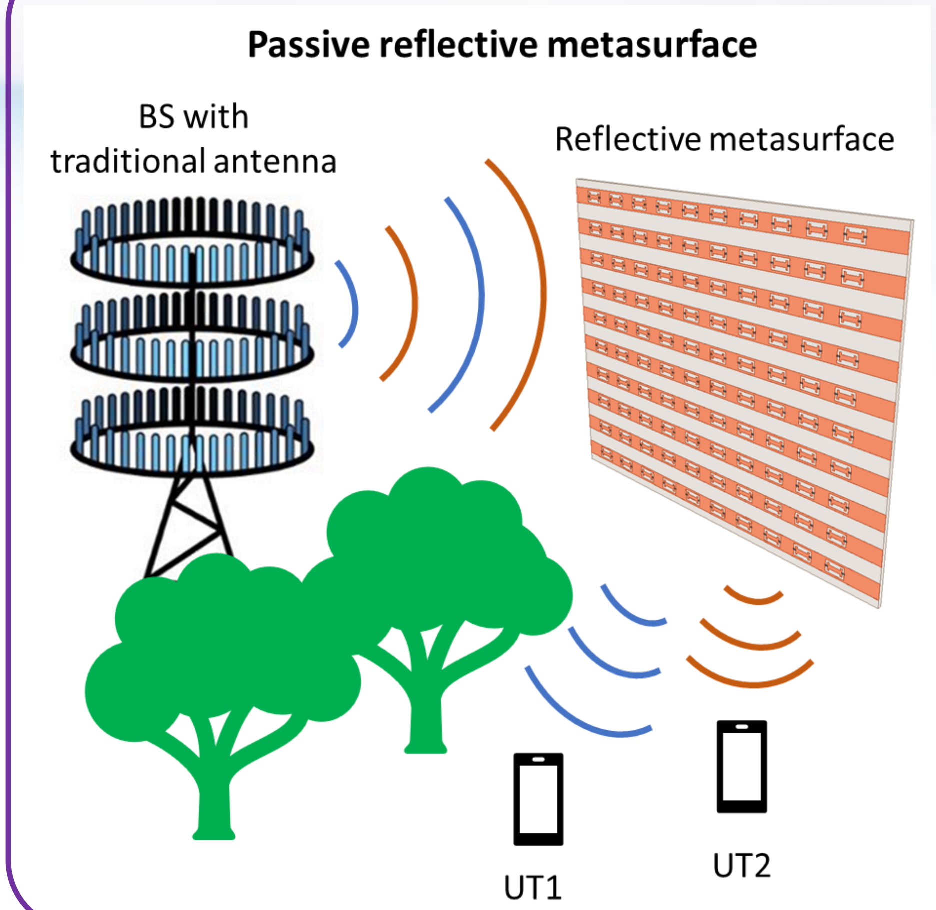

- Shlezinger et. al 19-20
- Collaboration with the group of Prof. David Smith

Dynamic Metasurface (Analog Precoders)

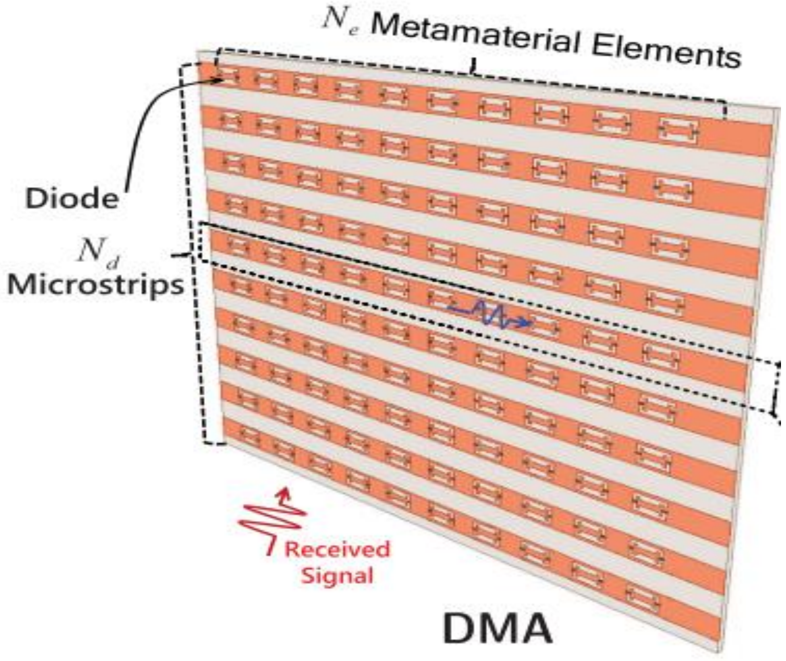

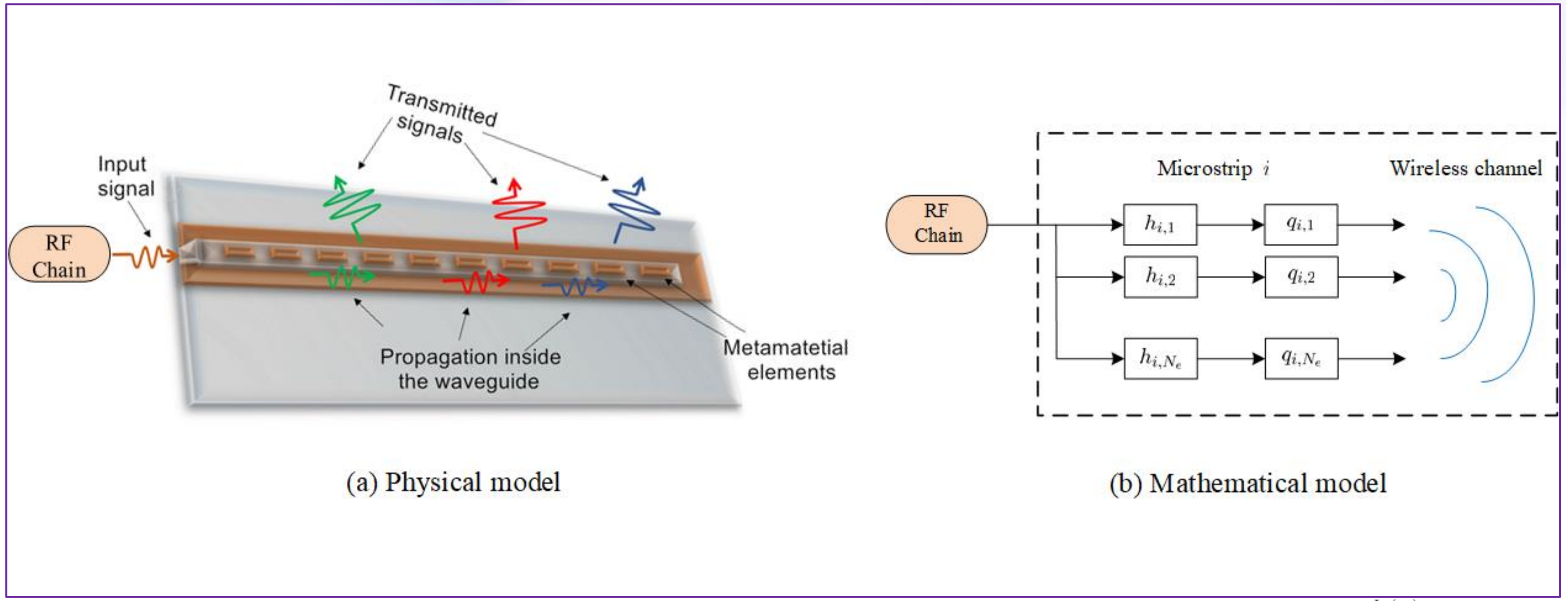

(a) Physical model

(b) Mathematical model

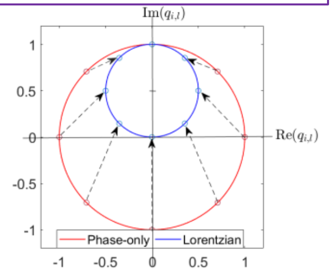

Lorentzian-constrained frequency response: $q_{i,l} \in \mathcal{Q} = \left\{\frac{j+e^{j\phi}}{2} \middle| \phi \in [0,2\pi]\right\}$

[1] N. Shlezinger, O. Dicker, Y. C. Eldar, I. Yoo, M. F. Imani, and D. R. Smith, "Dynamic metasurface antennas for uplink massive MIMO systems," IEEE TWC, 2019.
[2] H. Wang, N. Shlezinger, Y. C. Eldar, S. Jin, M. F. Imani, I. Yoo, and D. R. Smith, "Dynamic metasurface antennas for MIMO-OFDM receivers with Bit-Limited ADCs," IEEE TCOM, 2021.

Near-field Channel Model with UPA

- **We consider a downlink multi-user MIMO system where the BS employs a uniform planar array (UPA)**
- **The signal received by the mth user, located at $\mathbf{p}_m = (x_m, y_m, z_m)$ is given by**

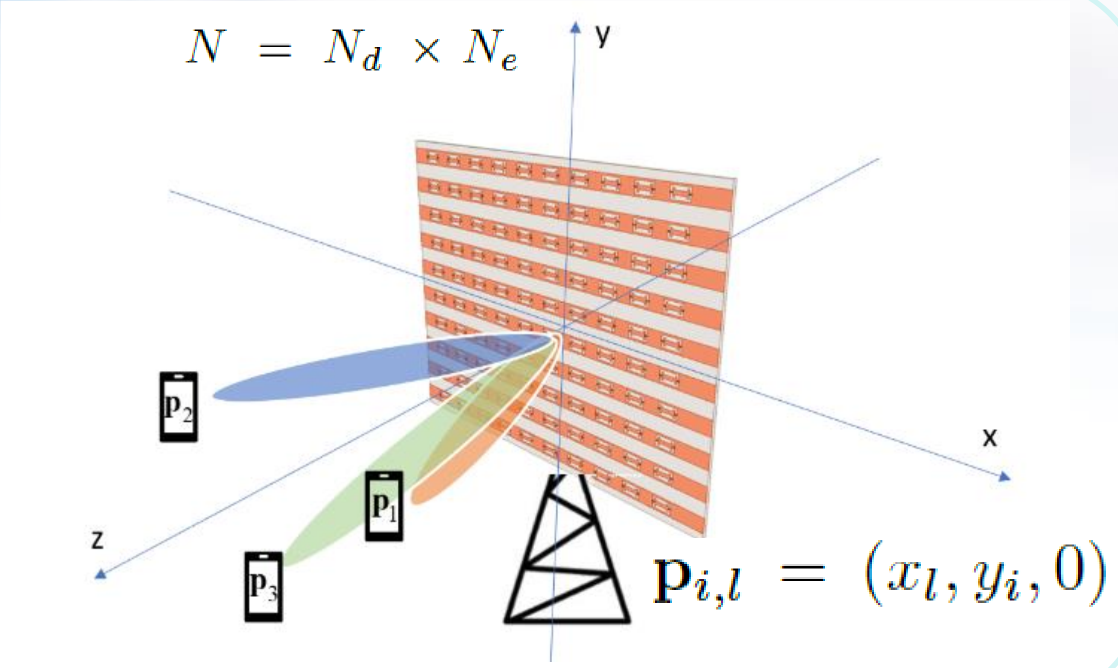

$$r(\mathbf{p}_m) = \sum_{i=1}^{N_d} \sum_{l=1}^{N_e} \boxed{A_{i,l}(\mathbf{p}_m)\, e^{-\jmath k |\mathbf{p}_m - \mathbf{p}_{i,l}|}}\, s_{i,l} + n_m$$

Near-Field Channel

$$A_{i,l}(\mathbf{p}_m) = \sqrt{F(\Theta_{i,l,m})} \frac{\lambda}{4\pi |\mathbf{p}_m - \mathbf{p}_{i,l}|}$$

Channel Gain

$$F(\Theta_{i,l,m}) = \begin{cases} 2(b+1)\cos^b(\theta_{i,l,m}) & \theta_{i,l,m} \in [0, \pi/2], \\ 0 & \text{otherwise.} \end{cases}$$

Radiation profile

H. Zhang, N. Shlezinger, F. Guidi, D. Dardari, M.F. Imani, and Y. C. Eldar, "Beam focusing for near-field multi-user MIMO communications," *IEEE Trans. Wireless Commun.*, 2022.

Near-Field Communications with DMAs

- **Near-field multi-user communications with DMA**
- **The aim is to design the transmission beam pattern to maximize the achievable sum-rate**

$$\max_{\{\mathbf{w}_m\},\mathbf{Q}} \sum_{m=1}^{M} \log_2\left(1+\frac{\left|\mathbf{a}_m^H\,\mathbf{H}\mathbf{Q}\,\mathbf{w}_m\right|^2}{\sum_{j\neq m}\left|\mathbf{a}_m^H\,\mathbf{H}\mathbf{Q}\,\mathbf{w}_j\right|^2+\sigma^2}\right)$$

$$s.t. \quad \boxed{(13)}, \quad \boxed{q_{i,l}} \in \mathcal{Q}, \forall i,l, \quad \sum_{m=1}^{M}\|\mathbf{w}_m\|^2 \leq P_{\max}.$$

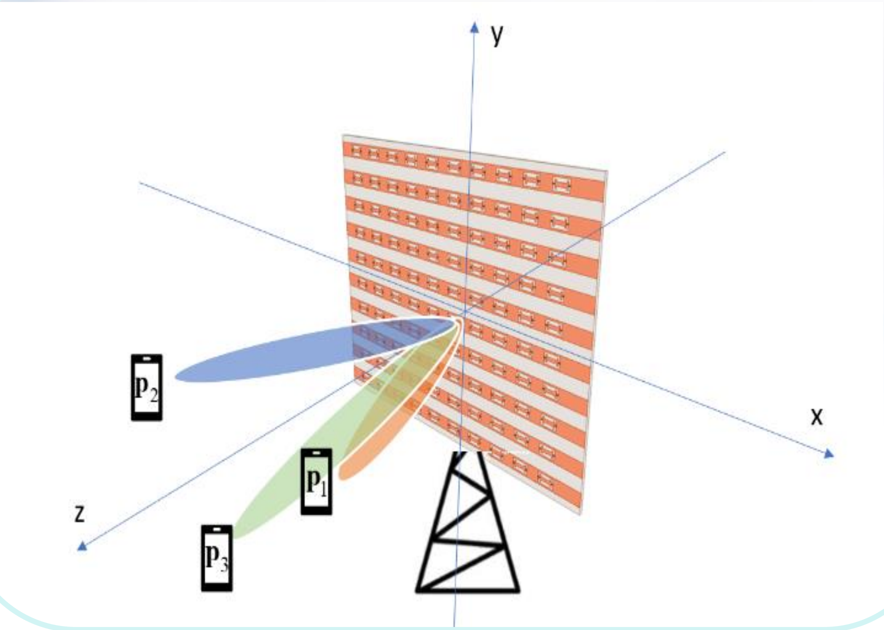

Structure Constraint of DMA

$$\mathbf{Q}_{(i-1)N_e+l,n} = \begin{cases} q_{i,l} & i=n, \\ 0 & i\neq n. \end{cases}$$

Lorentzian constraint of each element of DMA

$$q_{i,l} \in \mathcal{Q} \triangleq \left\{\frac{j+e^{j\phi}}{2}\middle|\phi\in[0,2\pi]\right\}$$

H. Zhang, N. Shlezinger, F. Guidi, D. Dardari, M.F. Imani, and Y. C. Eldar, "Beam focusing for near-field multi-user MIMO communications," *IEEE Trans. Wireless Commun.*, 2022.

Simulation Results

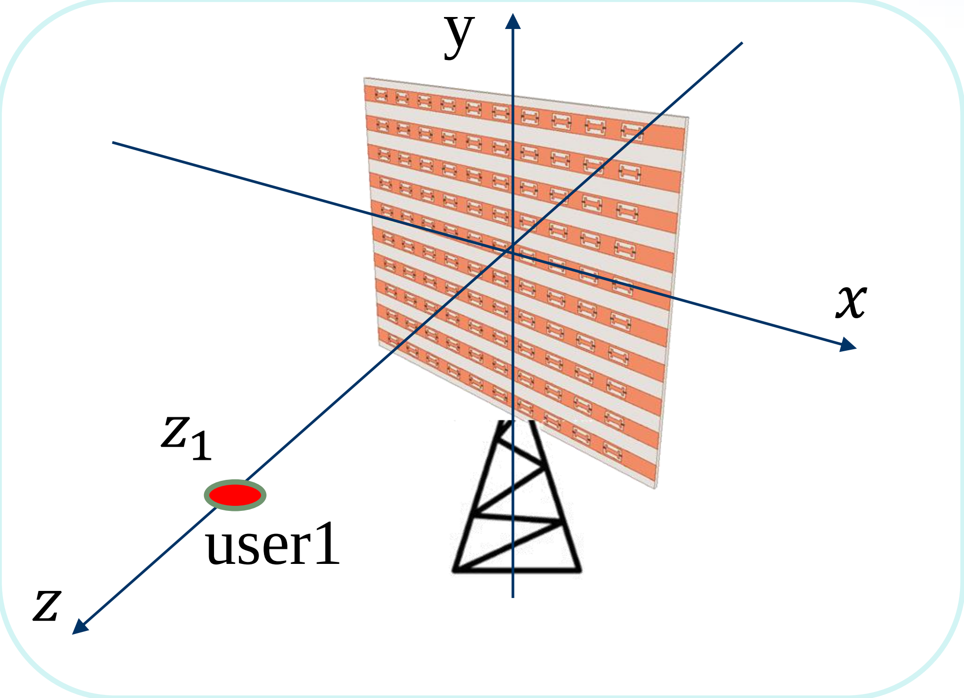

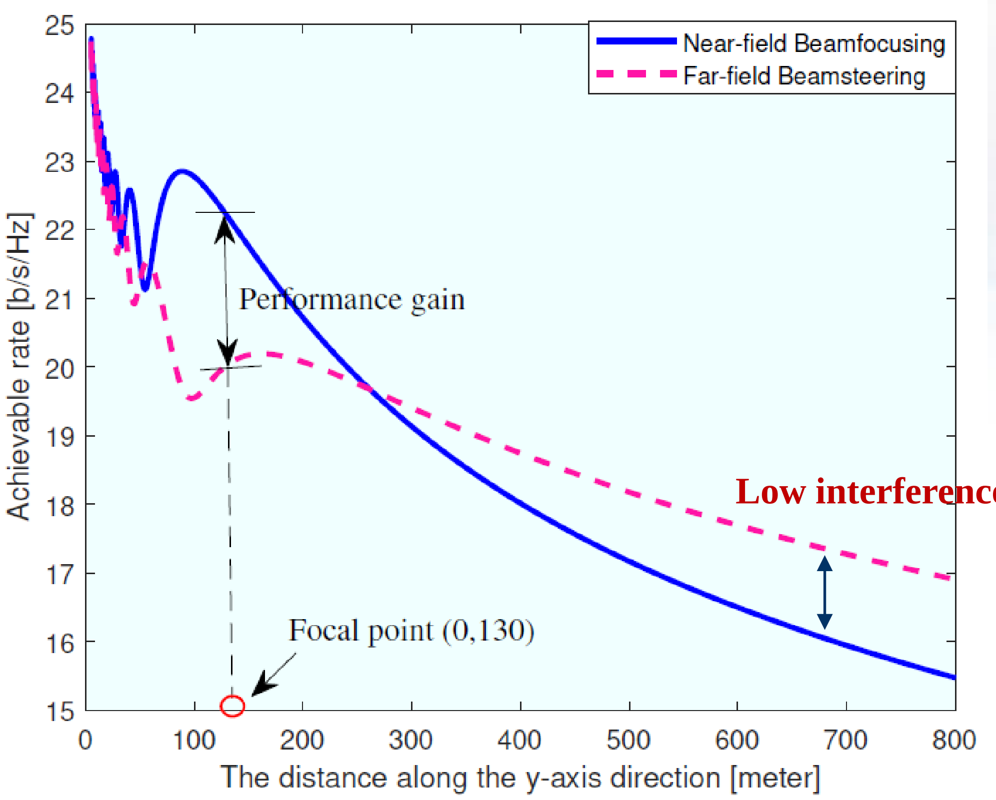

Low interference at far-field region!

Comparison of beam focusing and beam steering in terms of achievable rate

Beam focusing can not only increase the signal strength of the target point but also decrease the interference to other non-target points located in the far field

H. Zhang, N. Shlezinger, F. uidi, D. Dardari, and Y.C. Eldar, "6G wireless communications: From far-field beam steering to near-field beam focusing," *IEEE Commun. Mag.*, Apr. 2023.

Simulation Results

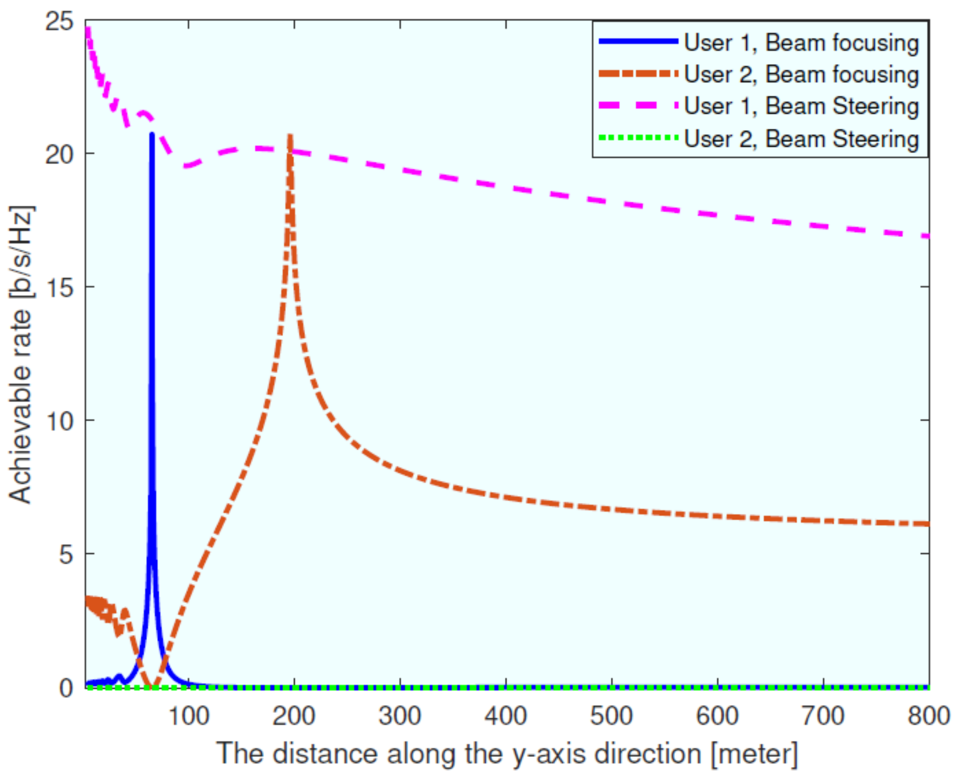

Achievable rates per user versus location along the z-axis.

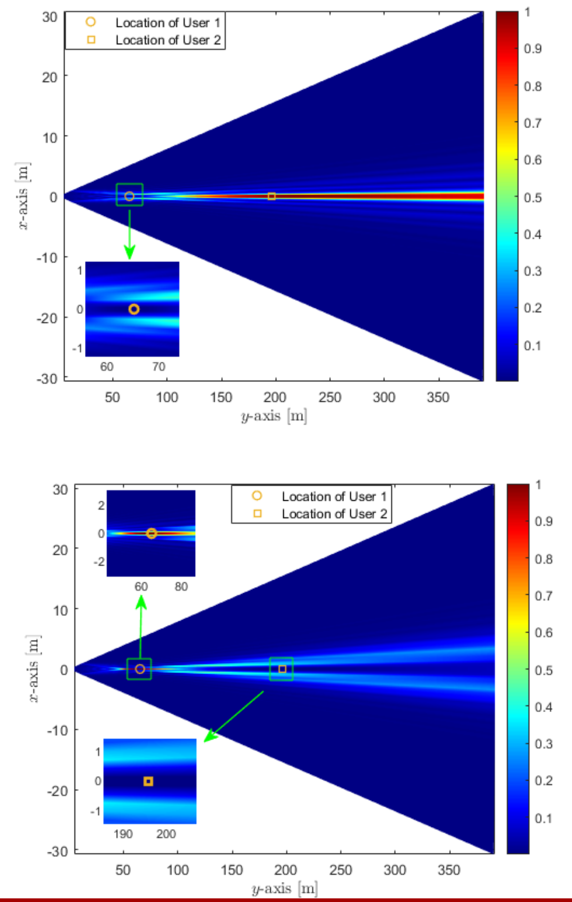

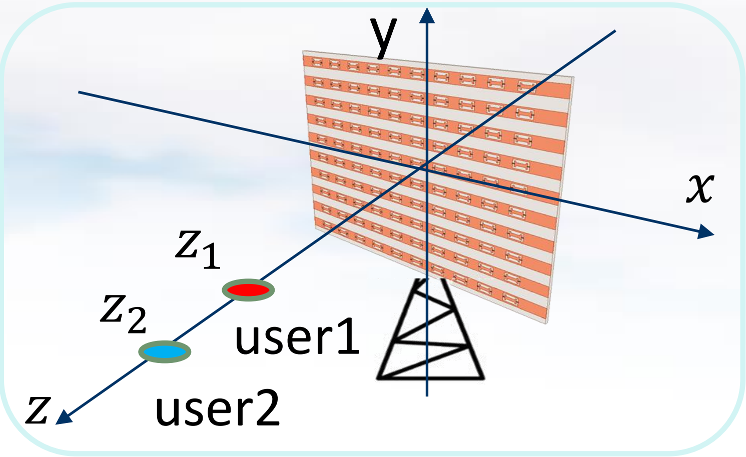

Beam focusing can simultaneously serve multiple users located at the same angular angle, whereas beam steering is unable to distinguish these users

H. Zhang, N. Shlezinger, F. uidi, D. Dardari, and Y.C. Eldar, "6G wireless communications: From far-field beam steering to near-field beam focusing," *IEEE Commun. Mag.*, Apr. 2023.

Outline of Part 3

- Near-Field Single-User MIMO Capacity Enhancement
- Near-Field Location Division Multiple Access
- Near-Field DMA Assisted Multi-User Communications
- Near-Field Wireless Power Transfer
- Near-Field Assisted Localization
- Near-Field Physical-Layer Security
- Near-Field Region Enlargement with Circular Arrays

Radio Frequency (RF)-Based Wireless Power Transfer

- 6G networks are envisioned to support the Internet-of-Everything (IoE) applications such as in-home setups as well as industrial and commercial settings.
- Most of these IoE devices will be either battery-powered or battery-less.
- How to prolong the lifetime of these IoE devices becomes a key challenge.
- RF-based wireless power transfer (WPT) allows to power up or charge wireless devices without requiring a wiring infrastructure.

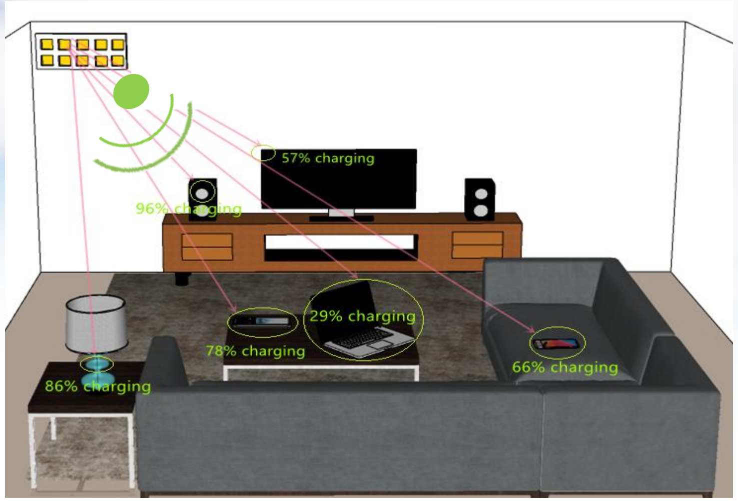

Radio Frequency (RF)-based Wireless Power Transfer

- The generic radiating WPT system and the energy receiver structure are shown below

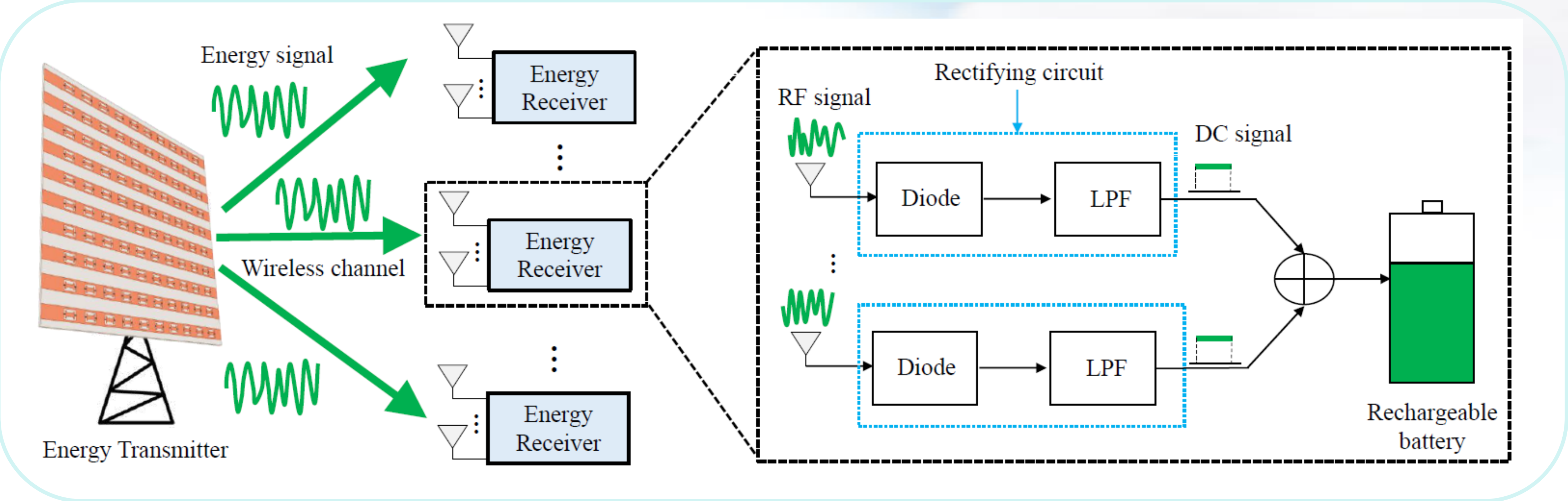

- **Advantages**
  - **Long distances**
  - **Charge multiple devices simultaneously**

R. Zhang and CK Ho, "MIMO Broadcasting for Simultaneous Wireless Information and Power Transfer," *IEEE TWC*, 2013.

Near-field Wireless Power Transfer

- **6G network-based IoE devices are likely operating in the radiating near-field region**

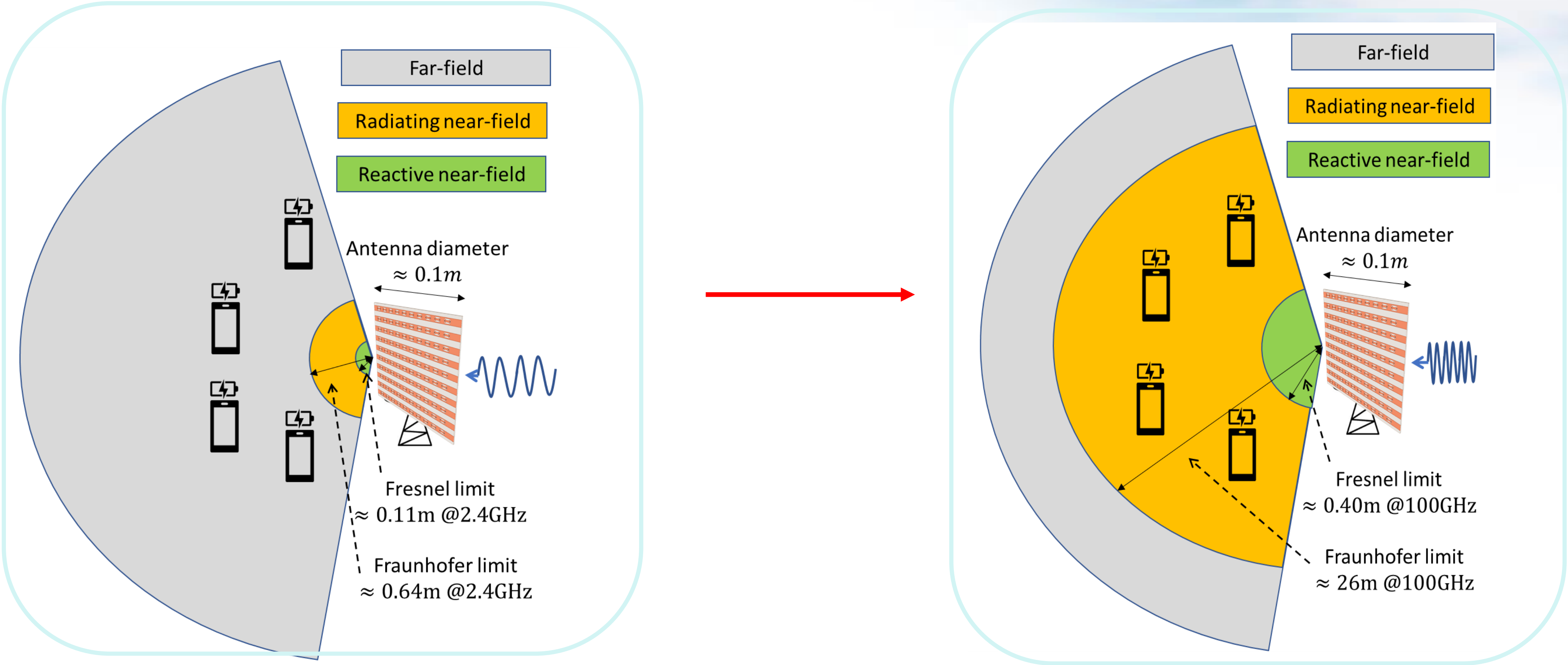

H. Zhang, N. Shlezinger, F. Guidi, D. Dardari, M.F. Imani, and Y. C. Eldar, "Near-field wireless power transfer for 6G Internet of everything mobile networks: Opportunities and challenges," *IEEE Communications Magazine*, 2022

Energy Beam Focusing

- In the near-field, spherical waveform enables the generating of focused energy beams
- Energy focusing brings forth several core advantages to WPT systems:
  - Enhance the energy transfer efficiency
  - Reduce energy pollution and limit human exposure to radiated energy

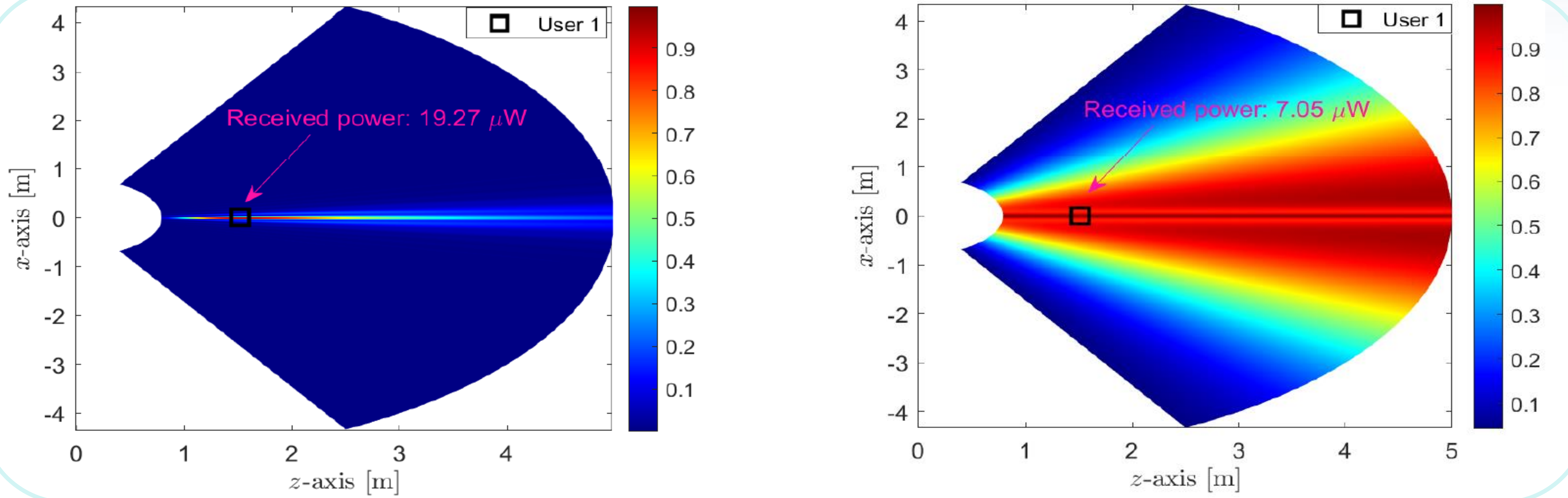

[1] H. Zhang, N. Shlezinger, F. Guidi, D. Dardari, M.F. Imani, Y. C. Eldar, "Near-Field Wireless Power Transfer with Dynamic Metasurface Antennas", IEEE SPAWC, 2022.

[2] H. Zhang, N. Shlezinger, F. Guidi, D. Dardari, M.F. Imani, and Y. C. Eldar, "Near-field Wireless Power Transfer for 6G Internet-of-Everything Mobile Networks: Opportunities and Challenges", IEEE Communications Magazine, 2022

Outline of Part 3

- Near-Field Single-User MIMO Capacity Enhancement
- Near-Field Location Division Multiple Access
- Near-Field DMA assisted Multi-User Communications
- Near-Field Wireless Power Transfer
- Near-Field Assisted Localization
- Near-Field Physical-Layer Security
- Near-Field Region Enlargement with Circular Arrays

Near-field Localization

- In the far-field, source localization adopts two-step approaches, i.e., joint estimation of the angle of arrival (AoA) and time of arrival (ToA), requiring precise synchronization/multiple access points.
- In the near-field (Fresnel) region, radio frequency (RF) signals are spherical wavefronts, which bring forth the possibility to localization based on the curvature of arrival (CoA).

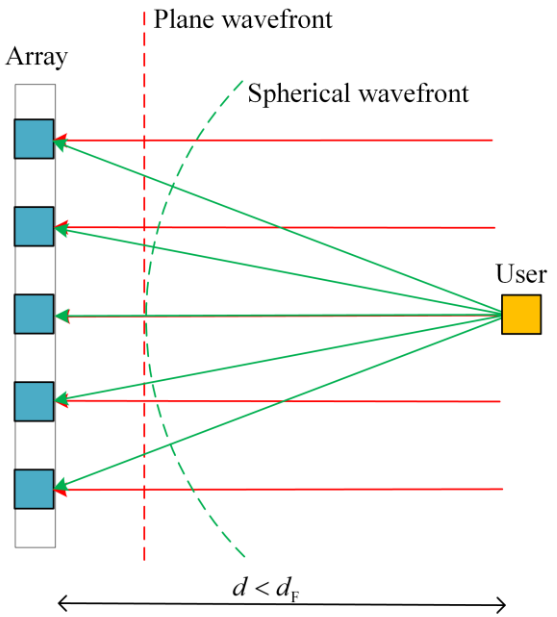

Spherical/plane wavefront of the signal impinging on the array

- For the near-field user source, once we obtain the curvature of the spherical wavefront, we can obtain the corresponding user position.
- Notice, when instead the wavefront is the approximate plane wavefront, it becomes a typical far-field model, the wavefront would lose distance information, making CoA degenerate into AoA.

Near-field Localization with DMA

- **The distance between user and antenna can be expressed by the user position as**

$$d_{m,i,1}\left(d_m,\theta_m,\gamma_m\right)=\sqrt{r_{i,l}^2+d_m^2-2r_{i,l}d_m g\left(\theta_m,\gamma_m\right)}$$

$$g\left(\theta_m,\gamma_m\right)=\sin\varphi_{i,l}\sin\theta_m\sin\gamma_m+\cos\varphi_{i,l}\cos\gamma_m$$

- **The position maximum likelihood estimation(MLE) processing is expressed as:**

$$\underset{\mathbf{p}_{\mathcal{M}}}{\arg\max}\log p\left(\mathbf{y};\mathbf{p}_{\mathcal{M}}\right)\propto\sum_{t=1}^{N_{\mathrm{T}}}\left\|\mathcal{P}\left[\mathbf{S}\left(\mathbf{p}_{\mathcal{M}},\mathbf{Q}\right)\mathbf{y}(t)\right]\right\|^2$$

  - $\mathcal{P}\left[\mathbf{S}\left(\mathbf{p}_{\mathcal{M}},\mathbf{Q}\right)\right.$ **denotes the projection operator.**
  - **One can localize the user when Q is fixed.**

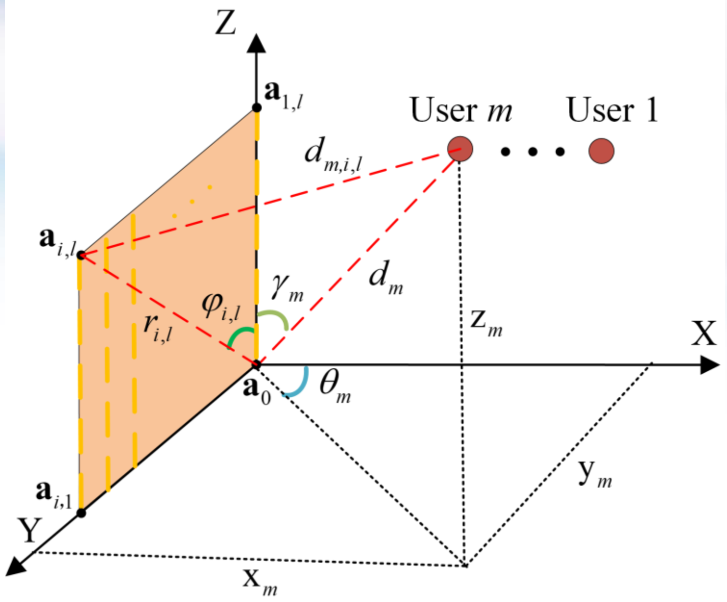

The *m*-th user position:

$$x_m=d_m\sin\gamma_m\cos\theta_m$$
$$y_m=d_m\sin\gamma_m\sin\theta_m$$
$$z_m=d_m\cos\gamma_m$$

[1] Q. Yang, A. Guerra, F. Guidi, N. Shlezinger, H. Zhang, D. Dardari, B. Wang, and Y. C. Eldar, "Near-field Localization with Dynamic Metasurface Antennas", *IEEE ICASSP 2023*.

Simulation Results

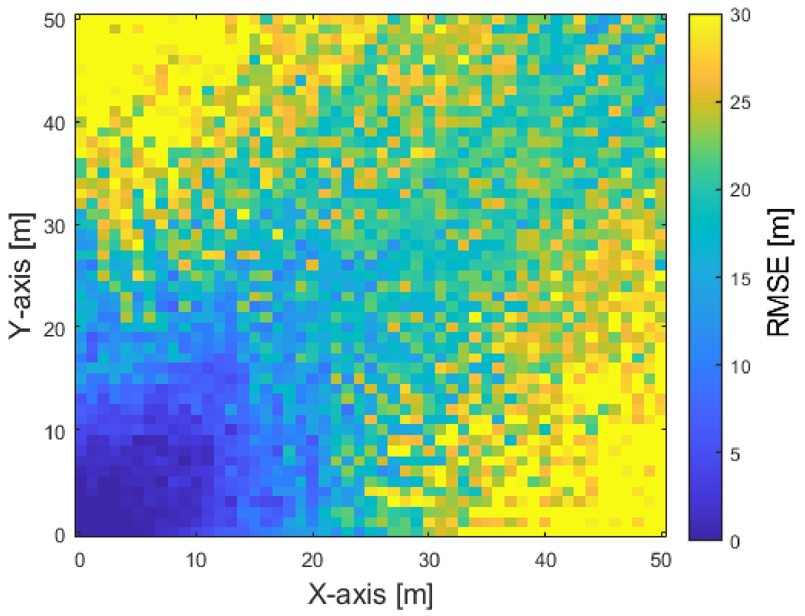

Fig. The heatmap for position estimate RMSE under different user positions. The nearfield distance $d_F = 24$ meters.

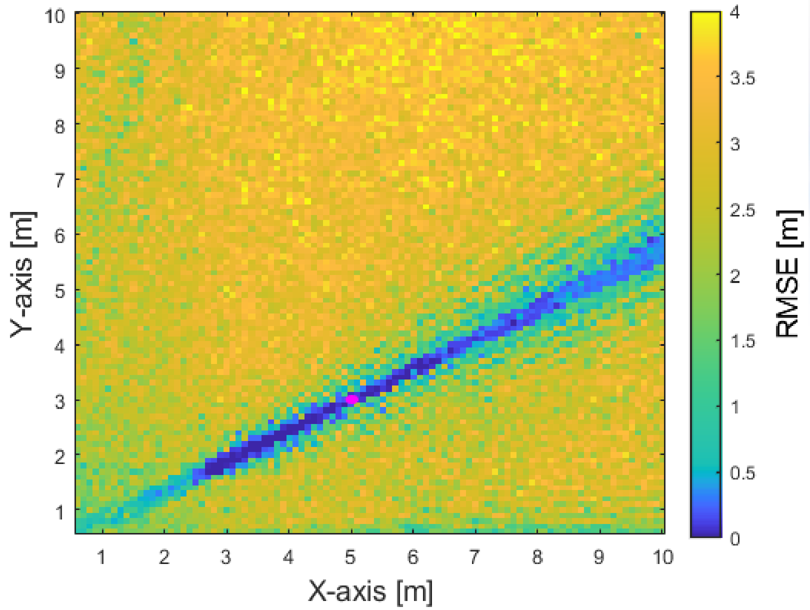

Fig. The heatmap for position estimate RMSE by varying user position. The red point is the hypothetical point that DMA tuning focus on.

DMA tuning design could significantly improve the near-field localization performance without requiring initial position of user.

[1] Q. Yang, A. Guerra, F. Guidi, N. Shlezinger, H. Zhang, D. Dardari, B. Wang, and Y.C. Eldar, "Near-field Localization with Dynamic Metasurface Antennas", *IEEE ICASSP 2023*.

Hybrid RIS-Aided Communications

- **Conventional RIS**

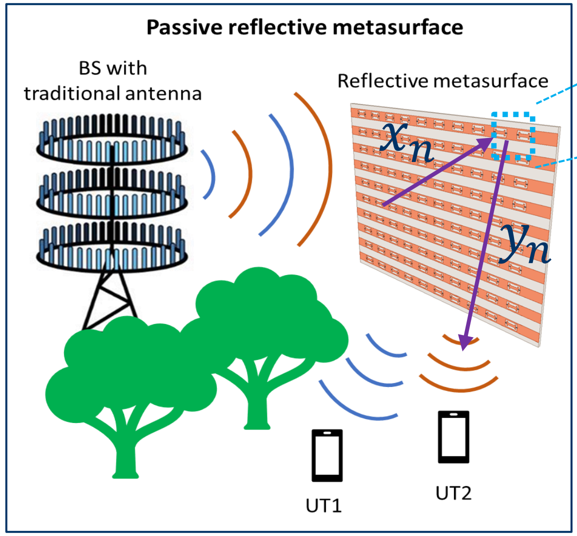

$$y_n = \beta_n e^{j\theta_n} x_n, n = 1, \cdots, N$$
$$where\ \beta_n \in [0,1],\ \ \theta_n \in [0,2\pi)$$

- **Main challenges**
  - **Passive RIS (no RF chains): RIS doesn't have any signal processing ability**
  - **Only cascaded channel is available.**
  - **Large number of channel coefficients**

- **Simultaneous Reflecting and Sensing Reconfigurable Intelligent Metasurfaces**

$$y_l^{RF}(n) = \rho_l e^{j\phi_l} r_l(n)$$

$$y_{r,l}^{RC}(n) = (1-\rho_l) e^{j\varphi_{r,l}} r_l(n)$$

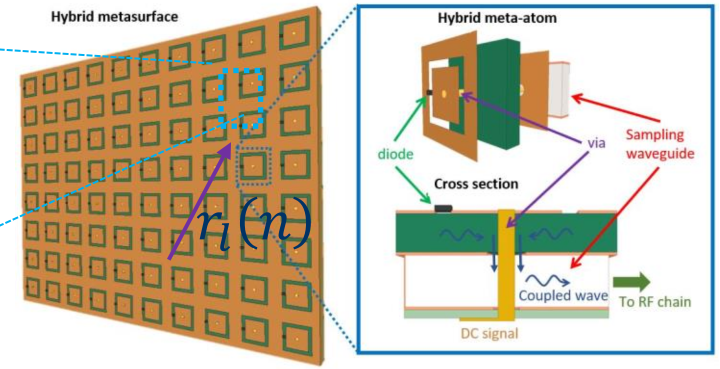

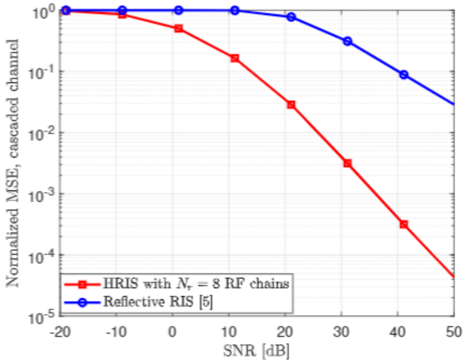

[1] H. Zhang and Y.C. Eldar, et al, "Channel Estimation with Simultaneous Reflecting and Sensing Reconfigurable Intelligent Metasurfaces", *IEEE TCOM*, 2023

Hybrid RIS-Aided Near-Field Localization

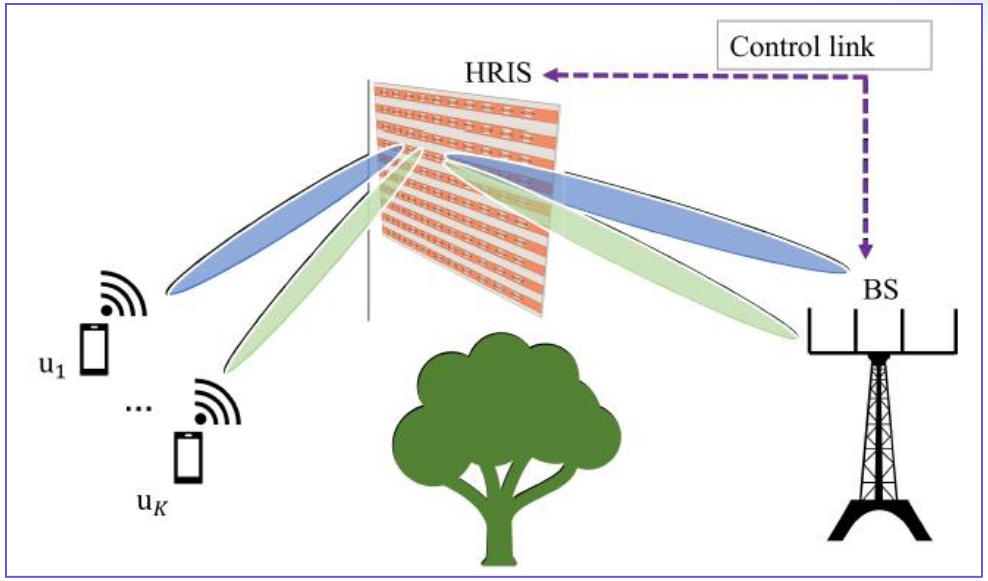

Equivalent received signals:

$$\mathbf{y} = [y_1, \ldots, y_{N_b}, z_1, \ldots, z_{N_f}]^T$$

Problem Formulation:

$$\begin{aligned} \min_{\boldsymbol{\rho},\boldsymbol{\psi},\boldsymbol{\alpha}} \quad & \sum_{\epsilon\in\{r,\phi,\theta\}} J_\epsilon(\boldsymbol{\rho},\boldsymbol{\psi},\boldsymbol{\alpha}) \\ s.t. \quad & \rho_{ij}\in[0,1], \psi_{ij}\in[0,2\pi], \alpha_{k,ij}\in[0,2\pi], \\ & i=1,\ldots,N_c; j=1,\ldots,N_r; k=1,\ldots,N_f. \end{aligned}$$

Received signals at the HRIS and BS:

$$y_b = \frac{ce^{-\jmath\chi_{\text{URB}}}}{4\pi f_c(d+r)} \sum_{i=1}^{N_c}\sum_{j=1}^{N_r} \rho_{ij} e^{\jmath\psi_{ij}} e^{-\jmath 2\pi f_c(\Delta t_{ij}+\Delta t_{b,ij})} + w_b$$

$$z_k = \frac{c}{4\pi f_c r} e^{-\jmath\chi_{\text{UR}}} \sum_{i=1}^{N_c}\sum_{j=1}^{N_r} (1-\rho_{ij}) e^{\jmath\alpha_{k,ij}} e^{-\jmath 2\pi f_c \Delta t_{ij}} + v_k,$$

Algorithm 1 HRIS Configuration for CRLB Minimization

Initialize: $\mathbf{x}^{(0)}$, step size η, and $t \leftarrow 0$.
while the stopping criteria is not satisfied **do**
1. Update the objective value $f(\mathbf{x}^{(t)})$ in (19).
2. Compute the gradients by the AD-based backpropagation algorithm $\Delta_{\mathbf{x}} f(\mathbf{x}^{(t)})$.
3. $\mathbf{x}^{(t+1)} \leftarrow \mathbf{x}^{(t)} - \eta\Delta_{\mathbf{x}} f(\mathbf{x}^{(t)})$.
4. $t \leftarrow t+1$.

end while
Output: $\{\boldsymbol{\rho},\boldsymbol{\psi},\boldsymbol{\alpha}\} \leftarrow \mathbf{x}^{(t)}$.

[1] Xing Zhang and Haiyang Zhang, "Hybrid Reconfigurable Intelligent Metasurfaces-Assisted Near-Field Localization", *IEEE Communications Letters*, 2023.

Simulation Results

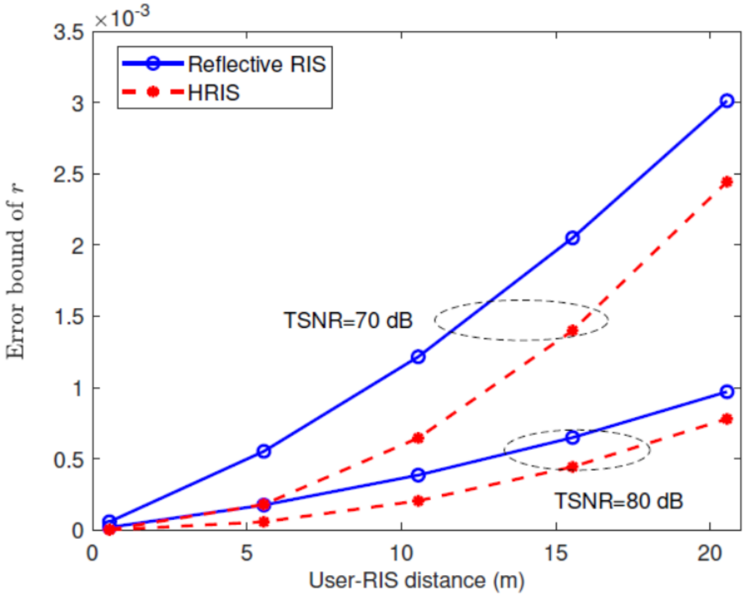

Fig. Distance error bound versus the user-RIS distance

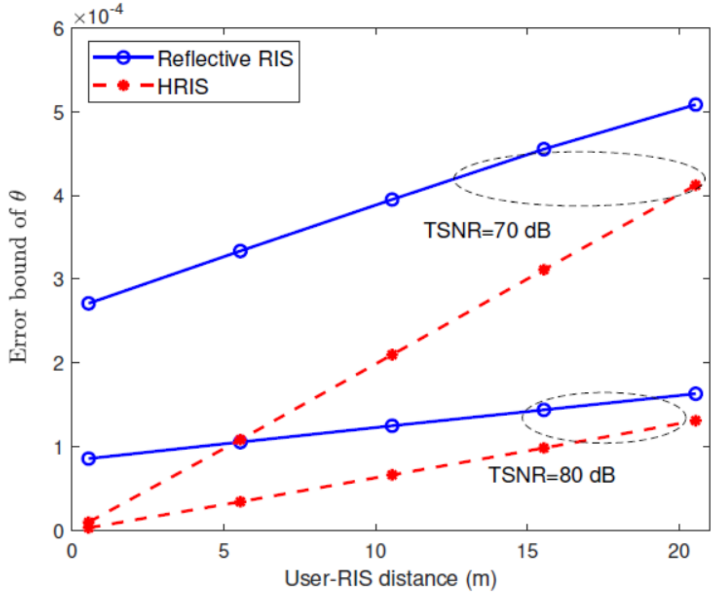

Fig. Elevation angle error bound versus the user-RIS distance

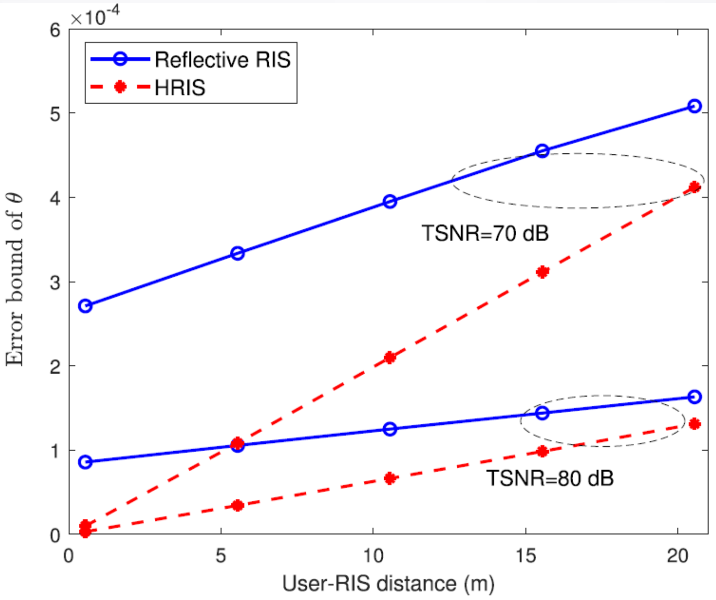

Fig. Azimuth angle error bound versus the user-RIS distance

HRIS is capable of improving the estimation accuracy of near-field parameters significantly

[1] Xing Zhang and Haiyang Zhang, "Hybrid Reconfigurable Intelligent Metasurfaces-Assisted Near-Field Localization", *IEEE Communications Letters*, 2023.

Outline of Part 3

- ☐ **Near-Field Single-User MIMO Capacity Enhancement**
- ☐ **Near-Field Location Division Multiple Access**
- ☐ **Near-Field DMA assisted Multi-User Communications**
- ☐ **Near-Field Wireless Power Transfer**
- ☐ **Near-Field Assisted Localization**
- ☐ **Near-Field Physical-Layer Security**
- ☐ **Near-Field Region Enlargement with Circular Arrays**

Near-Field Beam-Focusing for Physical-Layer Security

- Physical-layer security (PLS) exploits physical properties of wireless channels to provide communications security.
- Most of the existing results on PLS are obtained based on the assumption of far-field communications.

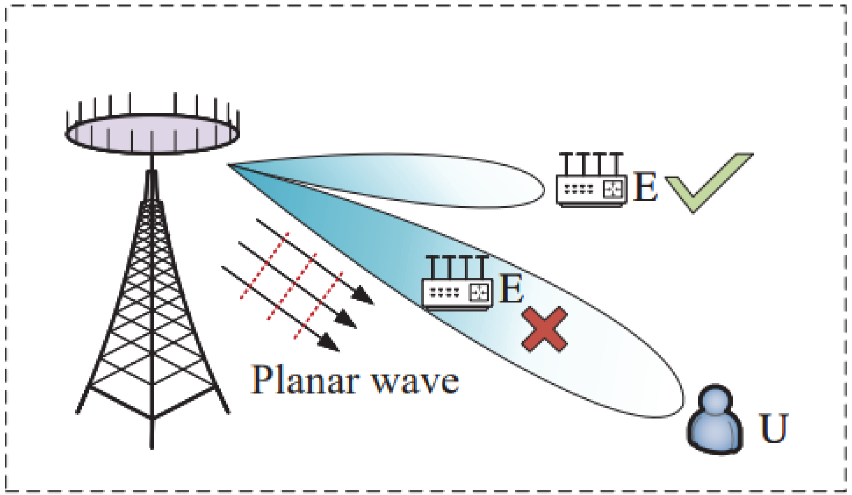

(a) Far-Field beam-steering

- Near-field Spherical wave brings the beam focusing ability that is able to achieve secure communications:
- even if they are with the same angular direction.
- even if the eavesdropper has better channel condition than the legitimate user.

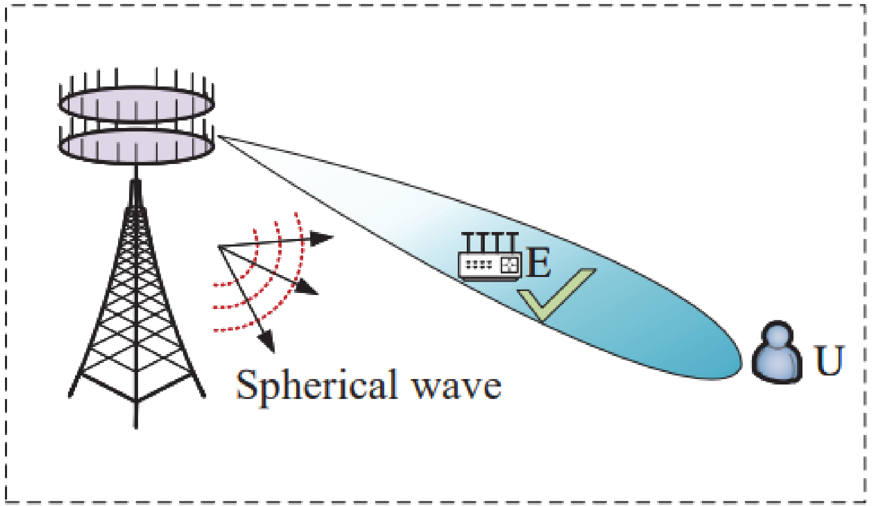

(b) Near-Field beam-focusing

[1] Z. Zhang, Y. Liu, Z. Wang, X. Mu, and J. Chen, "Physical Layer Security in Near-Field Communications", arXiv:2302.04189, 2023.

Analog Near-field Wideband Secure Beamfocusing

- **System model**

Bob and Eve are located in the near-field region of Alice

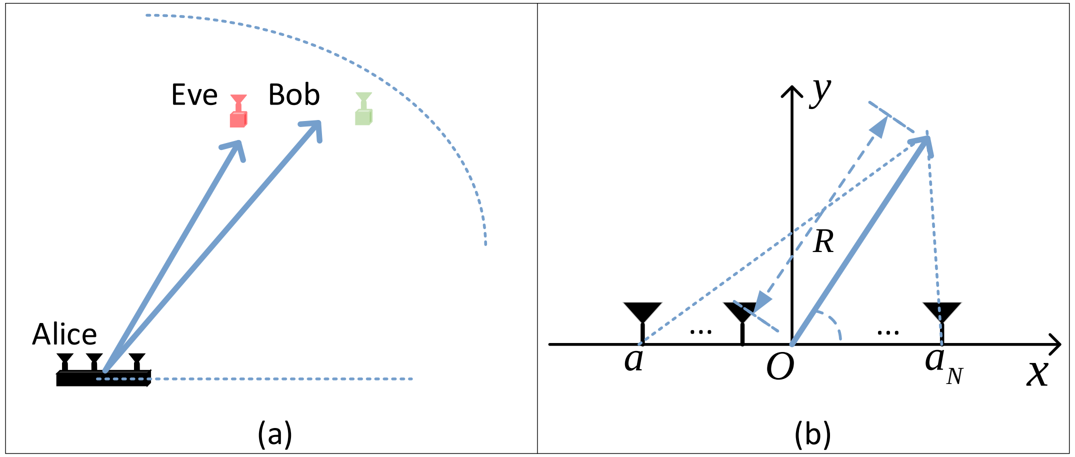

The distance between the n-th antenna and the destination (R, θ) is

$$D_n = \sqrt{a_n^2 + R^2 - 2a_n R \cos\theta}$$

- **Wave path difference is related to both distance and angle**

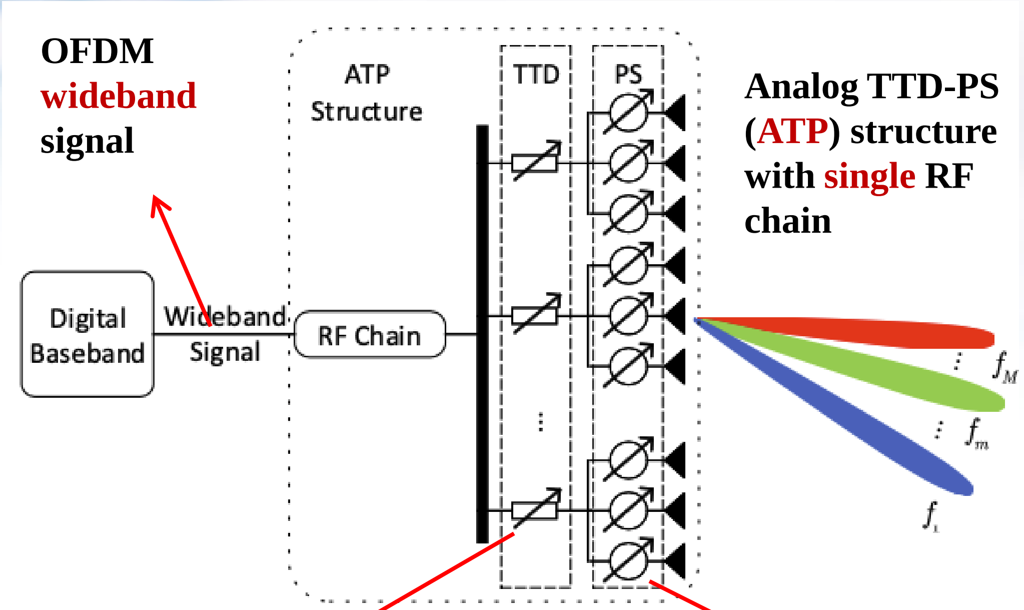

True-time delay (TTD): Introduce frequency-dependent phase

$$\mathbf{t}_m = \Big[\underbrace{e^{-j2\pi f_m \tau_1}, \ldots, e^{-j2\pi f_m \tau_1}}_{\text{The 1st group}}, \ldots, \underbrace{e^{-j2\pi f_m \tau_{N_T}}, \ldots, e^{-j2\pi f_m \tau_{N_T}}}_{\text{The } N_T\text{-th group}}\Big]^T$$

Analog Near-field Wideband Secure Beamfocusing

- **Beamsplit-aware low-complexity approach (BALA)**
  - **Given a specified end point of the near beamsplit trace, the configuration of phase-shift and time-delay can be configured in closed form**
  - **The near beamsplit trace equation can be derived in closed form**

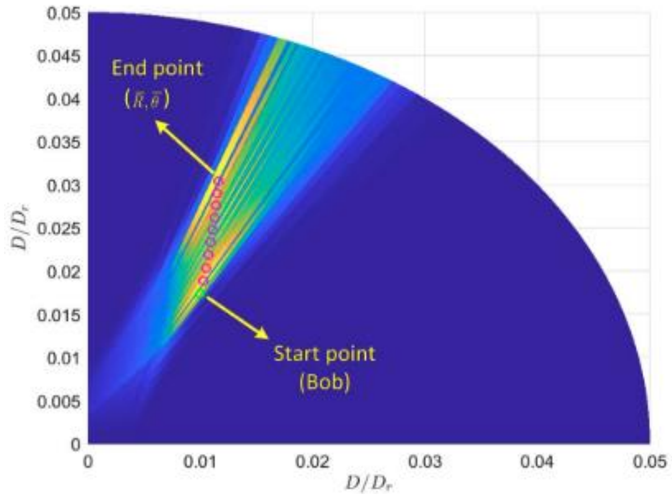

TTD

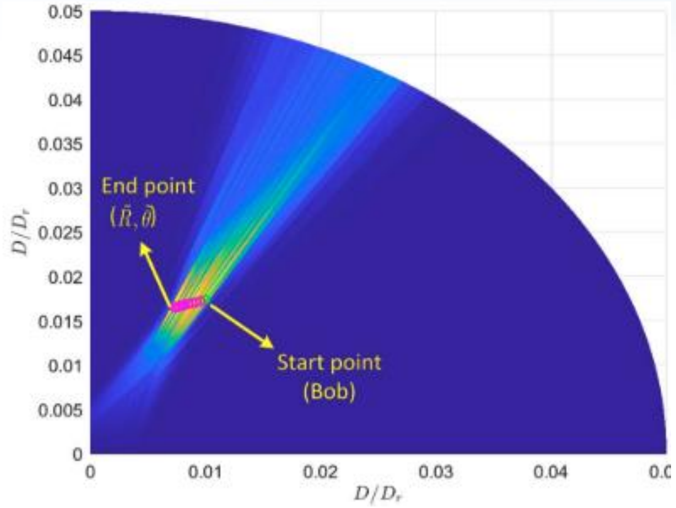

PS: $\phi_n = {2\pi f D_{B,n}}/{c}$

Trace equation: $\theta = \arccos\left(\frac{f_1 \cos\theta_B}{f}\right)$ $R = \left(\frac{f}{f_1 \sin^2\theta_B} - \frac{f_1}{f \tan^2\theta_B}\right) R_B$

PS: $\phi_n = {2\pi f_1 f_M \left(\tilde{D}_n - D_{B,n}\right)}/{cB}$ **TTD:** $\tau_n = {\left(f_M \tilde{D}_n - f_1 D_{B,n}\right)}/{cB}$

Trace equation: $\theta = \arccos\left(\frac{(f - f_1) f_M \cos\tilde{\theta} - (f - f_M) f_1 \cos\theta_B}{Bf}\right)$ $R = 1 \Big/ \left(\frac{(f - f_1) f_M \sin^2\tilde{\theta}}{Bf\tilde{R}\sin^2\theta} - \frac{(f - f_M) f_1 \sin^2\theta_B}{BfR_B \sin^2\theta}\right)$

The near-field beamsplit trace is determined by PS and TTD in closed form

Analog Near-field Wideband Secure Beamfocusing

- **Basic idea of BALA**
  - We perform one-dimensional search to the end point of the near-field beamsplit trace
  - The end point corresponding to the highest secrecy rate is chosen
  - The corresponding PS and TTD are configured in closed form

Proposed

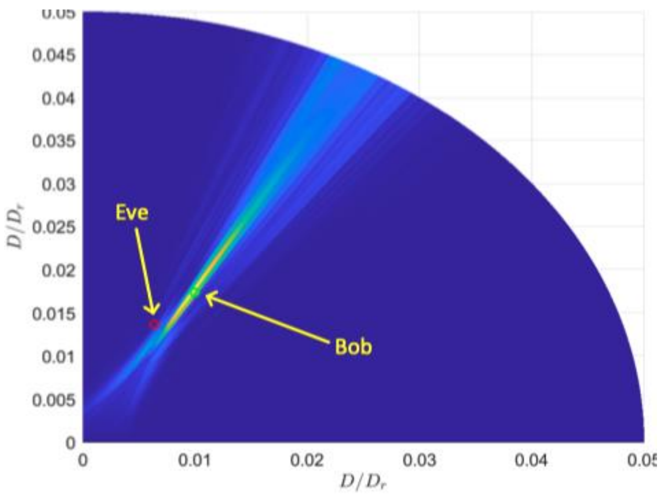

- Leveraging near-field propagation,
- Overcoming wideband beamsplit
- Realizing secure beamfocusing at Bob

Traditional narrowband approach

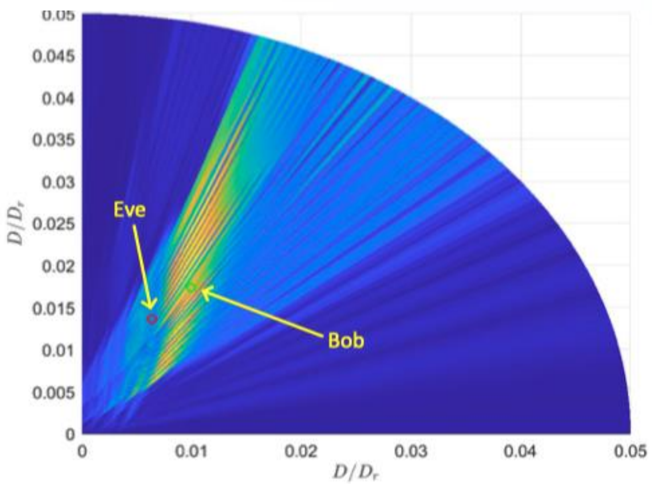

- Suffering from wideband beamsplit
- Significant energy leakage to Bob

Y. Zhang, H. Zhang, S. Xiao, W. Tang and Y. C. Eldar, "Near-Field Wideband Secure Communications: An Analog Beamfocusing Approach," *IEEE TSP*, 2024.

Outline of Part 3

- Near-Field Single-User MIMO Capacity Enhancement
- Near-Field Location Division Multiple Access
- Near-Field DMA assisted Multi-User Communications
- Near-Field Wireless Power Transfer
- Near-Field Assisted Localization
- Near-Field Physical-Layer Security
- Near-Field Region Enlargement with Circular Arrays

Challenge of Limited Near-Field Region

- According to the definition of effective Rayleigh distance, the near-field region dramatically reduces at large angles
- Since users are randomly distributed in the cell, many users located outside the effective Rayleigh distance fail to harvest the benefits of near-field communications

Rayleigh Distance $= \frac{2D^2}{\lambda}$ Effective Rayleigh distance $= \eta \cos^2\theta \, \frac{2D^2}{\lambda}$

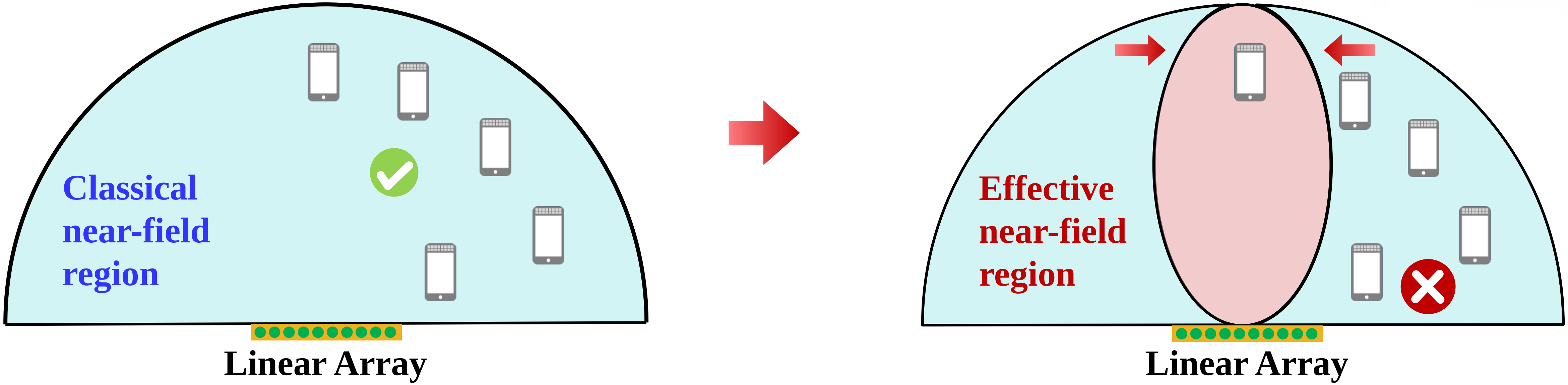

How to enlarge the near-field region to enable more users to benefit from near-field communication?

Key Factor Determining the Near-Field Region

- The reduced near-field region originates from the **reduced effective array aperture**
- To provide an **enlarged** and **uniform** effective array aperture at different directions, the array geometry can be changed from **linear array** to **circular array**

$$\mathrm{ERD} = \eta \frac{2D^2\cos^2\theta}{\lambda}$$

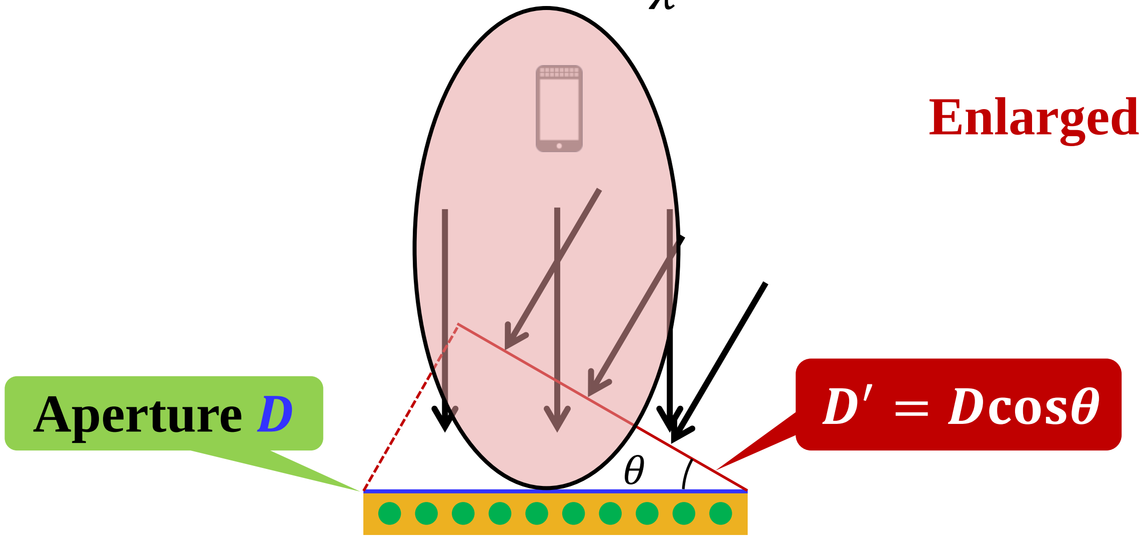

Linear Array

Enlarged near-field region

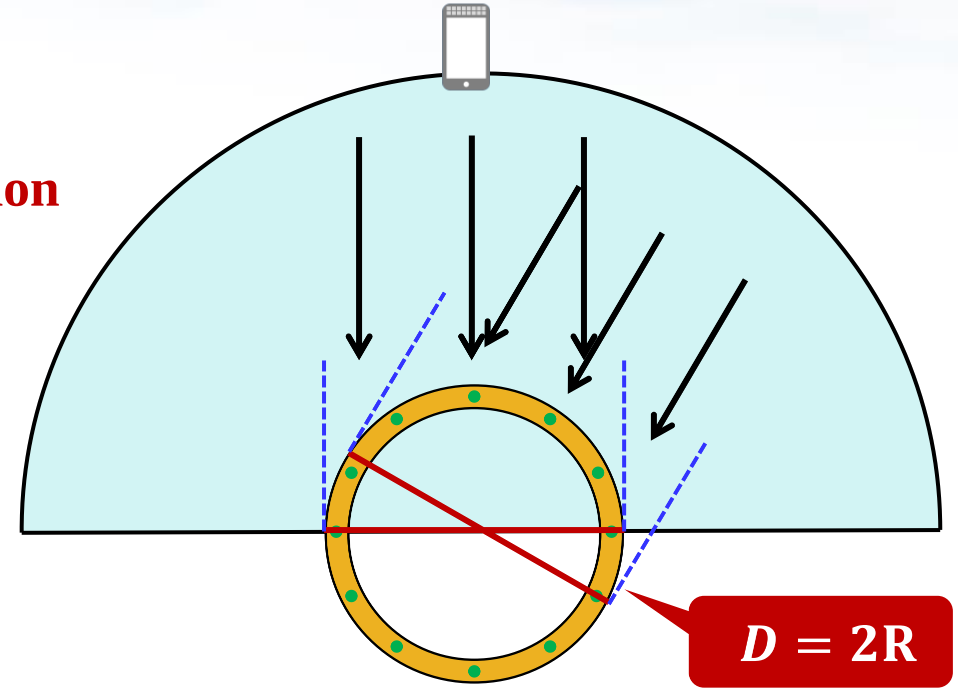

The near-field region is no longer dependent on the position direction

Array Gain of Uniform Circular Array (UCA)

Lemma 1: normalized array gain of ULA achieved by $\boldsymbol{w} = \boldsymbol{a}^*(r_1, \theta)$ at the user location (r_2, θ) is obtained through Fresnel approximation as

$$f(r_1, r_2, \theta) = \frac{1}{M}\left|\sum_{n=-N}^{N} e^{jk\left(r_2^{(n)} - r_1^{(n)}\right)}\right| \approx |G(\beta)| = \left|\frac{C(\beta)+jS(\beta)}{\beta}\right|$$

where $\beta = \sqrt{\frac{M^2 d^2 (1-\theta^2)}{2\lambda}\left|\frac{1}{r_1} - \frac{1}{r_2}\right|}$. $C(\beta) = \int_0^\beta \cos\left(\frac{\pi}{2}t^2\right)\mathrm{d}t$ **and** $S(\beta) = \int_0^\beta \sin\left(\frac{\pi}{2}t^2\right)\mathrm{d}t$ **are Fresnel functions.**

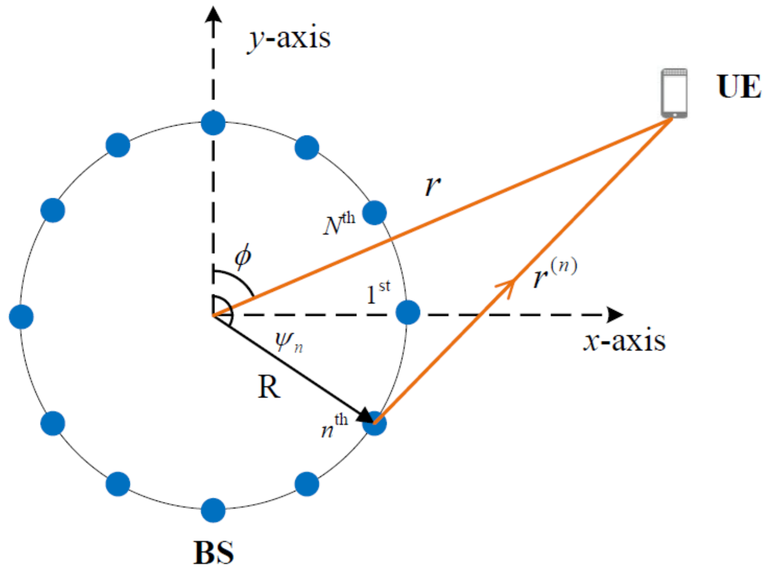

Lemma 3: $f_{\mathrm{UCA}}(r_1, r_2, \theta) = \frac{1}{M}\left|\sum_{m=0}^{M-1} e^{jk\left(r_2^{(m)} - r_1^{(m)}\right)}\right| \approx |J_0(\zeta)|$,

where $r^{(m)} \approx r - R\cos(\phi - \psi_n) + \frac{R^2}{2r}\left(1 - \cos^2(\phi - \psi_m)\right)$,

$$\zeta = \frac{2\pi R^2}{\lambda}\left|\frac{1}{r_1} - \frac{1}{r_2}\right|$$

Bessel function

Independent of θ

Z. Wu, M. Cui, and L. Dai, "Enabling more users to benefit from near-field communications: From linear to circular array," *IEEE Trans. Wireless Commun.*, vol. 23, no. 4, pp. 3735-3748, Apr. 2024.

Comparison of the near-field region

- **Given a predetermined threshold δ, the effective Rayleigh distance of uniform circular array (UCA) exceeds that of ULA of the same aperture.**
- **Different from the polar-domain codebook for ULA, the concentric-ring codebook can be constructed for UCA for beamforming, channel estimation, etc.**

$$\mathrm{ERD_C} = \frac{\pi R^2}{2\lambda J_0^{-1}(1-\delta)}$$

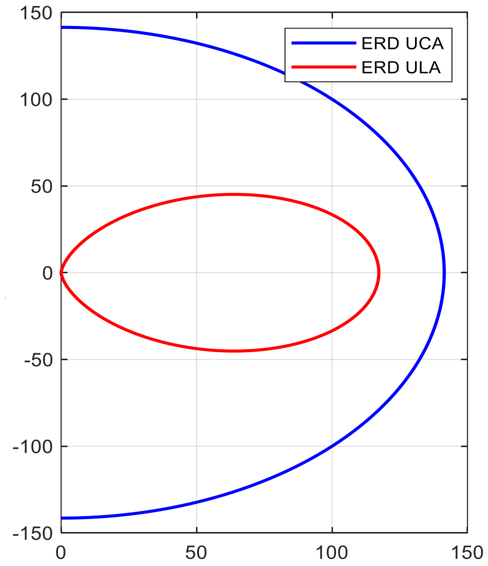

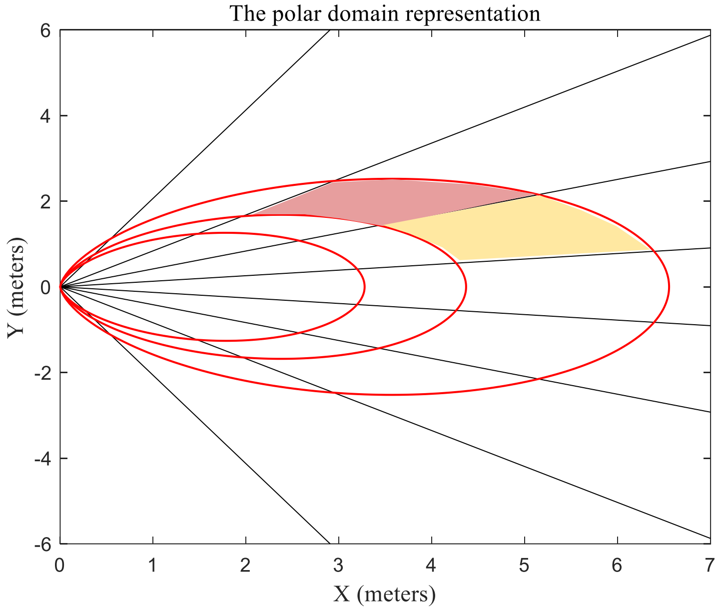

Polar-Domain Codebook

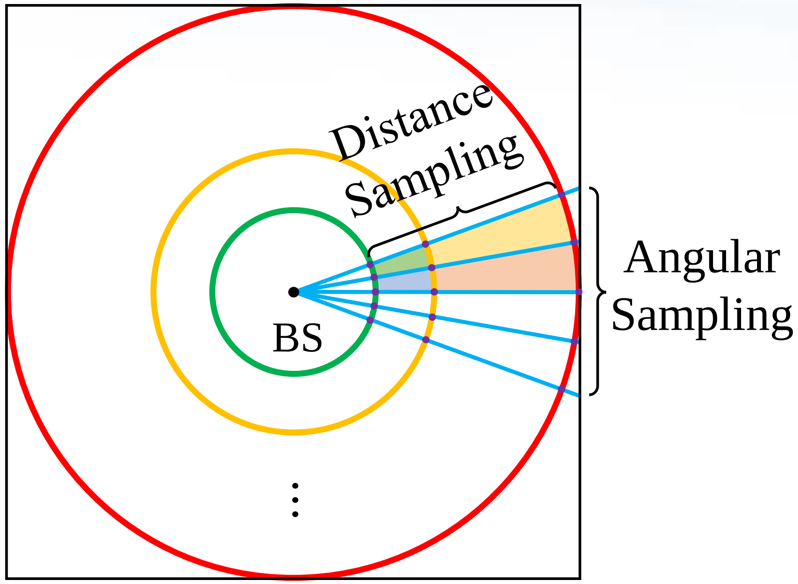

Concentric-Ring Codebook

Z. Wu, M. Cui, and L. Dai, "Enabling more users to benefit from near-field communications: From linear to circular array," *IEEE Trans. Wireless Commun.*, vol. 23, no. 4, pp. 3735-3748, Apr. 2024.

Generalization of Circular Arrays

- Compared with **2D** array geometry such as ULA and UCA, the **3D** array geometry such as uniform planar array (**UPA**) are preferred for practical deployment
- For the ease of deployment, UCA is further generalized into the **3D cylindrical array**, which can be viewed as concatenating M circular arrays in the z-axis

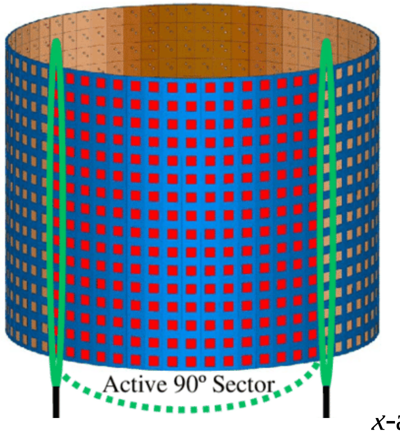

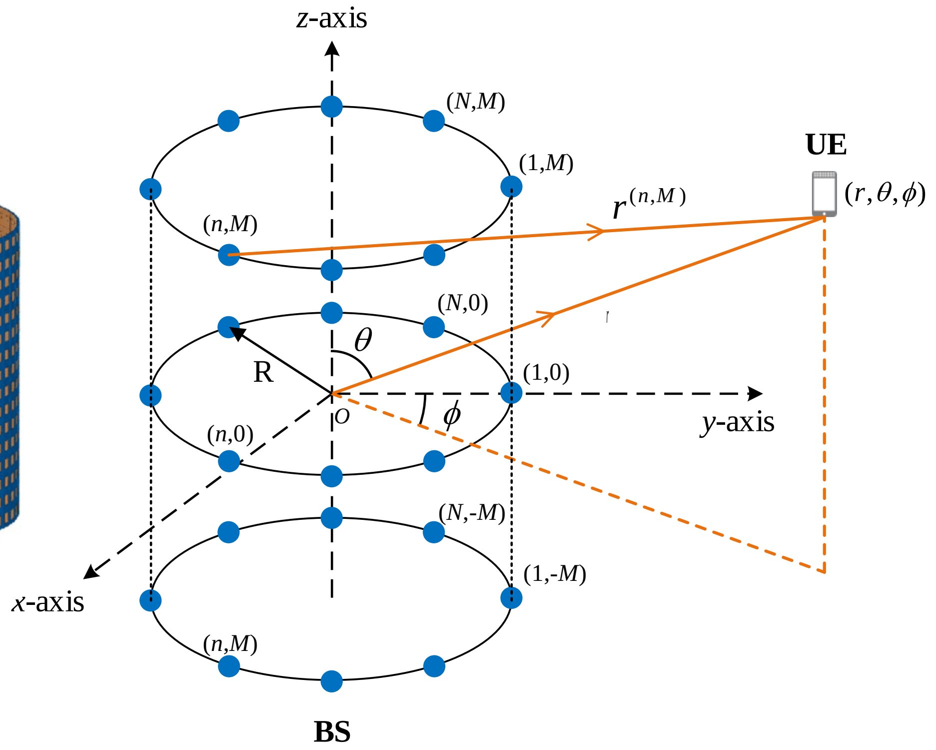

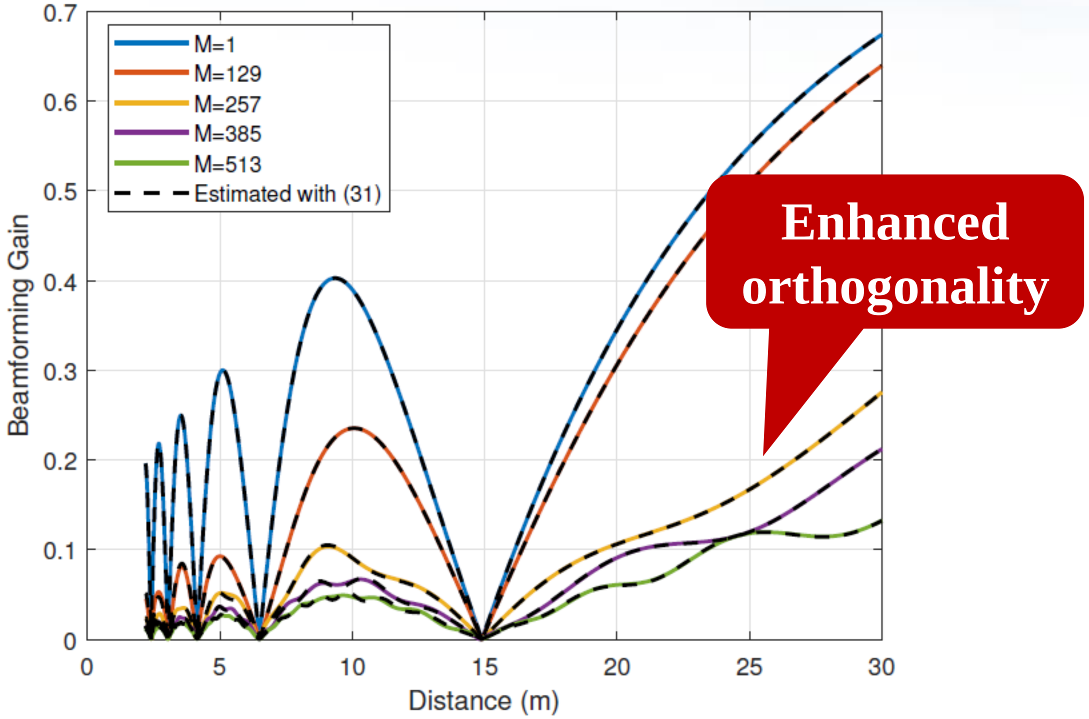

Z. Wu, M. Cui, and L. Dai, "Enabling more users to benefit from near-field communications: From linear to circular array," *IEEE Trans. Wireless Commun.*, vol. 23, no. 4, pp. 3735-3748, Apr. 2024.

Part 4: Challenges of Near-Field Communications

Outline of Part 4

- **Near-Field Channel State Information Acquisition**
  - **Near-field MISO channel estimation**
  - **Near-field MIMO channel estimation**
  - **Near-field EM-based channel model**
  - **Near-field beam training**
- **Near-Field Beam Split**
  - **Phase-delay beam focusing**
  - **Near-field rainbow-based beam training**
  - **Distance-dependent beam split based beam training**

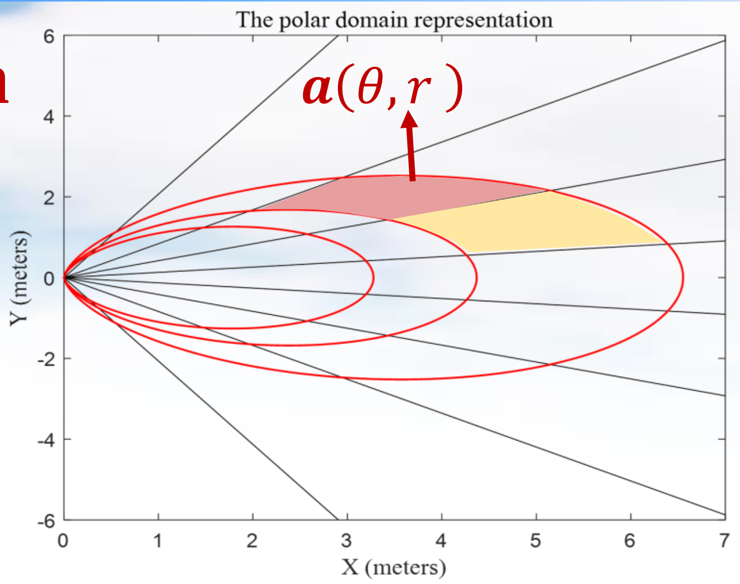

Challenge of Near-Field Channel Estimation

- Existing far-field channel estimation relies on the angle-domain sparsity exploited by the orthogonal angle-domain codebook, i.e., the DFT codebook
- The near-field angle-domain channels suffer from a severe energy spreading problem

Channel h → **Sensing matrix** → Received signal $y = Ah + n$ → **Angle-domain codebook** → Sparse representation $y = AFh_a + n$ → **Sparse signal reconstruction** → $\hat{h}_a$ → **Angle-domain codebook** → $\hat{h} = F\hat{h}_a$

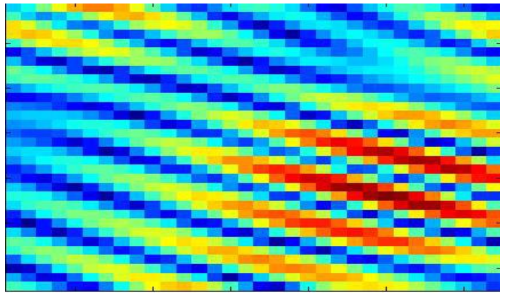

Far-field
antenna-domain

Angle-domain codebook →

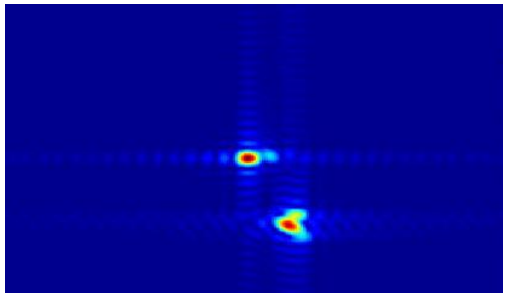

Far-field
angle-domain

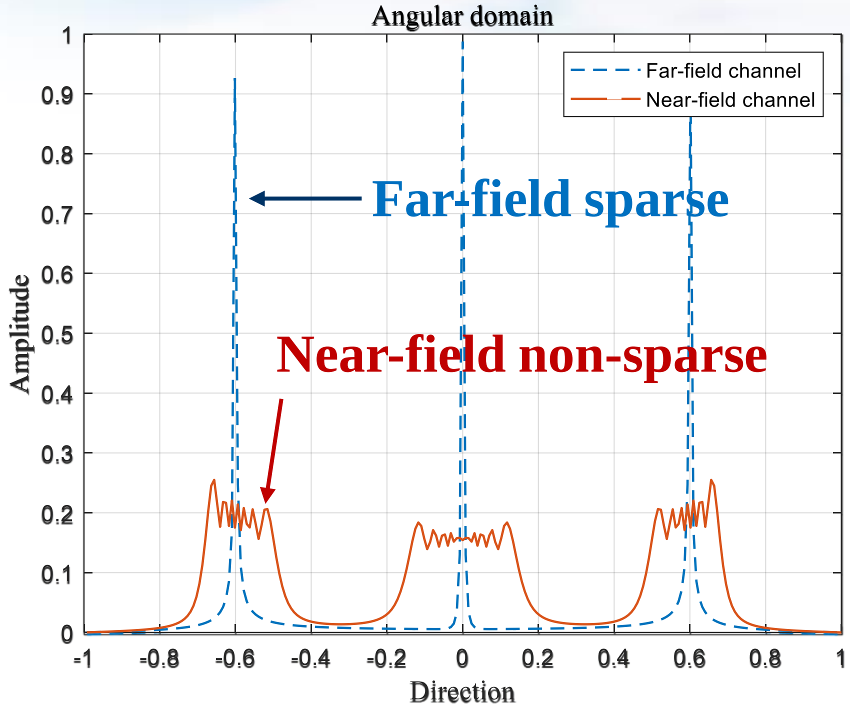

The angle-domain codebook is not appropriate for near-field channel estimation

Near-Field Codebook Design

- **Far-field codebook: samples multiple angle grids in the angle domain**
- **Near-field codebook: samples multiple "angle-distance" grids in the polar domain**

Angle-domain codeword $\boldsymbol{a}(\theta) = \left[e^{jn\pi\theta}\right]_{n=-N}^{N}$

Polar-domain codeword $\boldsymbol{a}(\theta, r) = \left[e^{jk\sqrt{r+n^2d^2-2rnd\theta}}\right]_{n=-N}^{N}$

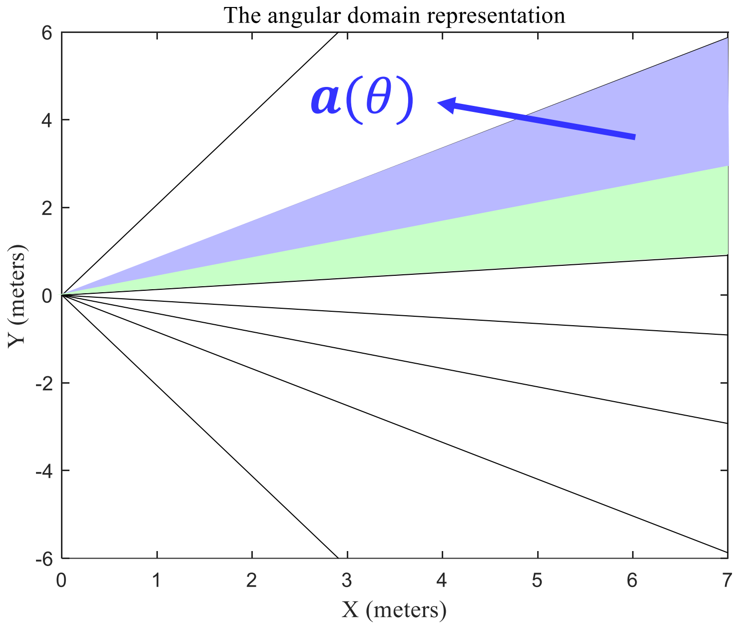

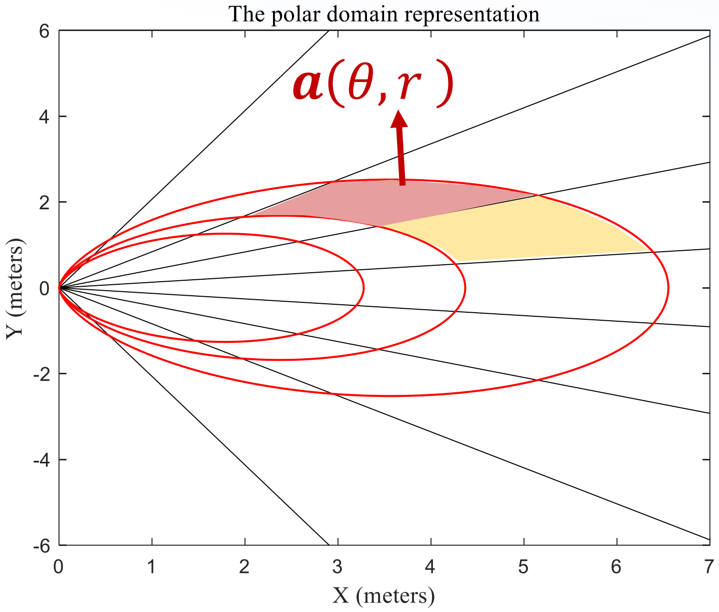

The near field codebook should sample in polar domain instead of angle domain

M. Cui and L. Dai, "Channel estimation for extremely large-scale MIMO: Far-field or near-field?," *IEEE Trans. Commun.*, vol. 70, no. 4, pp. 2663-2677, Apr. 2022.

The Distance-Sampling Criterion

- The grids can be sampled sparsely far away from ELAA, but densely near the ELAA

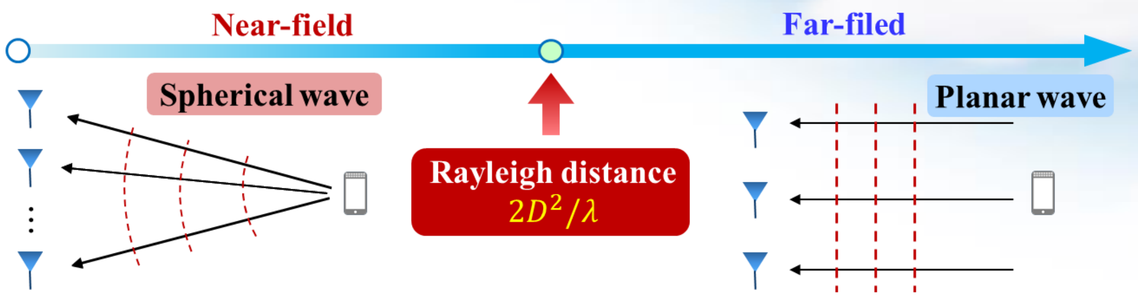

- Codebook design method: Minimizing the maximum coherence of the polar-domain codebook
- Based on the Fresnel approximation, we prove the following sampling criteria

Uniform angle sampling: $\theta_n = -1 + \frac{n+N+1}{2N+1}, \quad n = \{-N, \cdots, 0, \cdots, N\}$

Non-uniform distance sampling: $r_{n,s} = \frac{1}{s}\left(1-\theta_n^2\right)Z_\Gamma, \; s = \{1,2,\cdots,S\}, \; Z_\Gamma = \frac{M^2 d^2}{2\lambda\beta_\Gamma^2}$

The number of sampled distances

Threshold

- The polar-domain codebook can be constructed as

$$\boldsymbol{P}_n = \left[\boldsymbol{a}(\theta_n, r_{n,1}), \boldsymbol{a}(\theta_n, r_{n,2}), \cdots, \boldsymbol{a}(\theta_n, r_{n,S})\right] \qquad \boldsymbol{P} = \left[\boldsymbol{P}_{-N}, \cdots, \boldsymbol{P}_0, \cdots, \boldsymbol{P}_N\right]$$

M. Cui and L. Dai, "Channel estimation for extremely large-scale MIMO: Far-field or near-field?," *IEEE Trans. Commun.*, vol. 70, no. 4, pp. 2663-2677, Apr. 2022.

Polar-Domain Codebook Based Channel Estimation

- Angle-domain codebook is replaced by polar-domain codebook
- Other procedures are similar

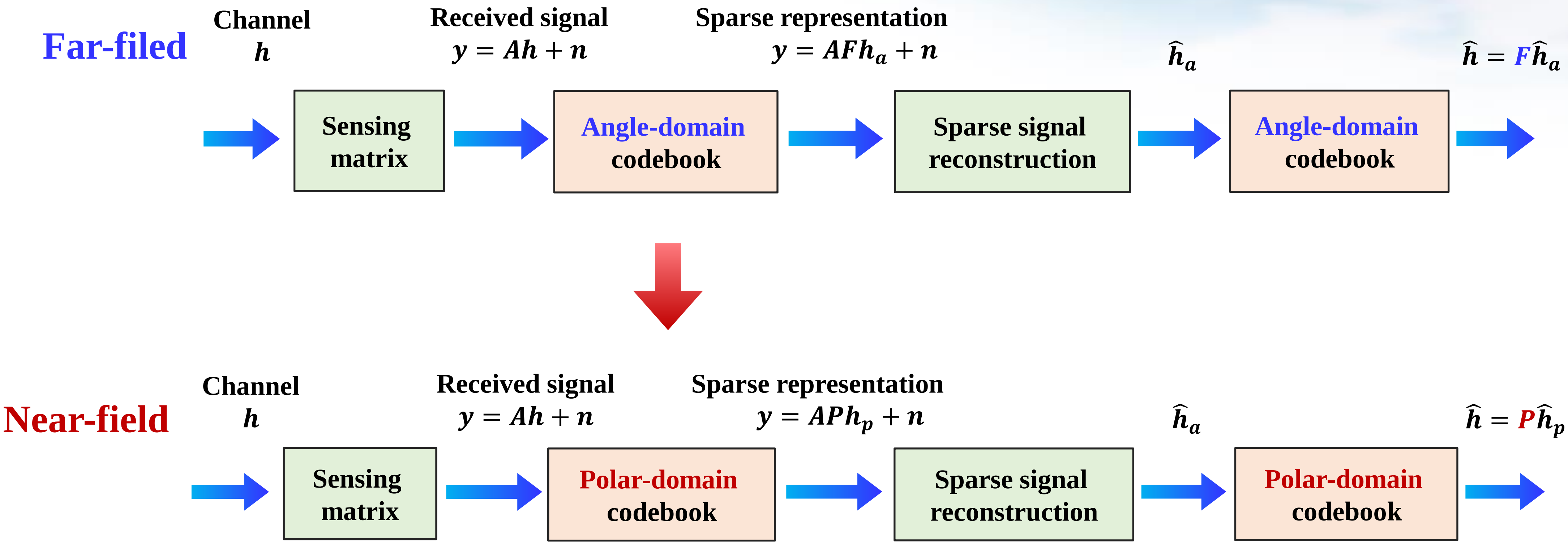

M. Cui and L. Dai, "Channel estimation for extremely large-scale MIMO: Far-field or near-field?," *IEEE Trans. Commun.*, vol. 70, no. 4, pp. 2663-2677, Apr. 2022.

Simulation Results

- **The proposed schemes can accurately estimate the near-field channel**

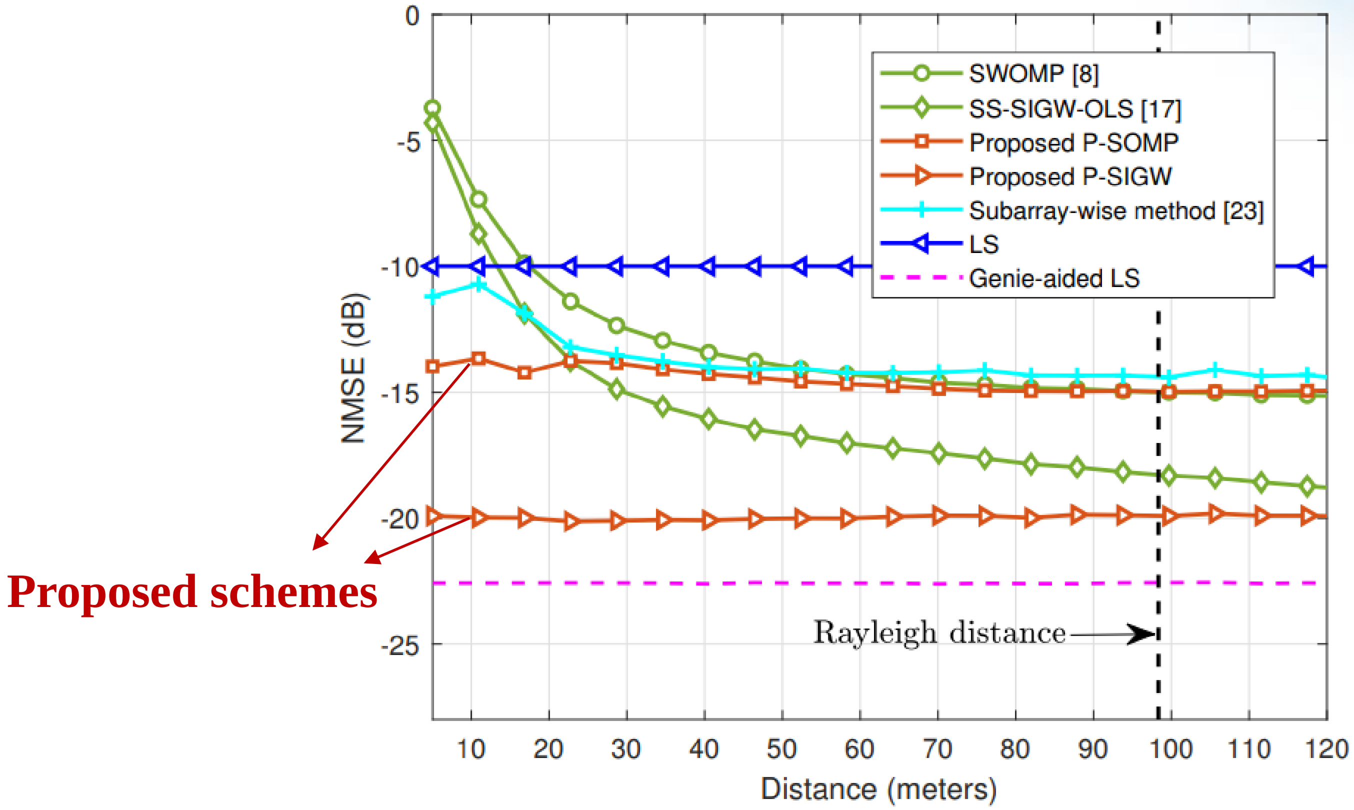

Parameters	Value
Carrier	100 GHz
Bandwidth	400 MHz
Number of carriers	1024
Array Aperture	0.4 m
SNR	10 dB
Pilot compression ratio	0.5

Polar-domain codebook naturally decay to the angle-domain codebook in far field

M. Cui and L. Dai, "Channel estimation for extremely large-scale MIMO: Far-field or near-field?," *IEEE Trans. Commun.*, vol. 70, no. 4, pp. 2663-2677, Apr. 2022.

Near-Field Channel Model

- **Far-field**

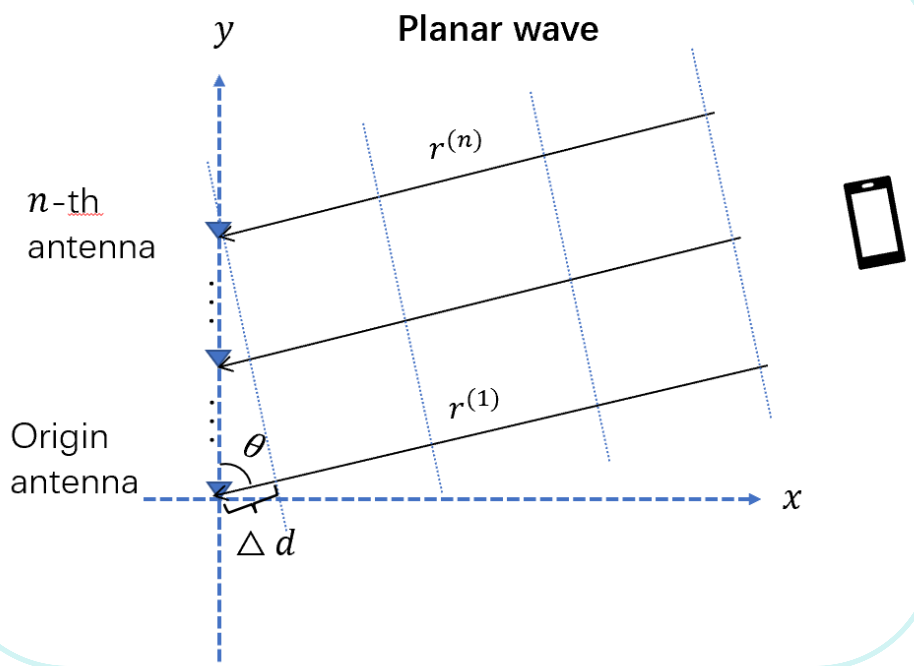

$$\mathbf{a}(\theta) = \left[1, e^{j\pi\cos\theta}, \cdots, e^{j\pi(N-1)\cos\theta}\right]^T$$

- **Near-field**

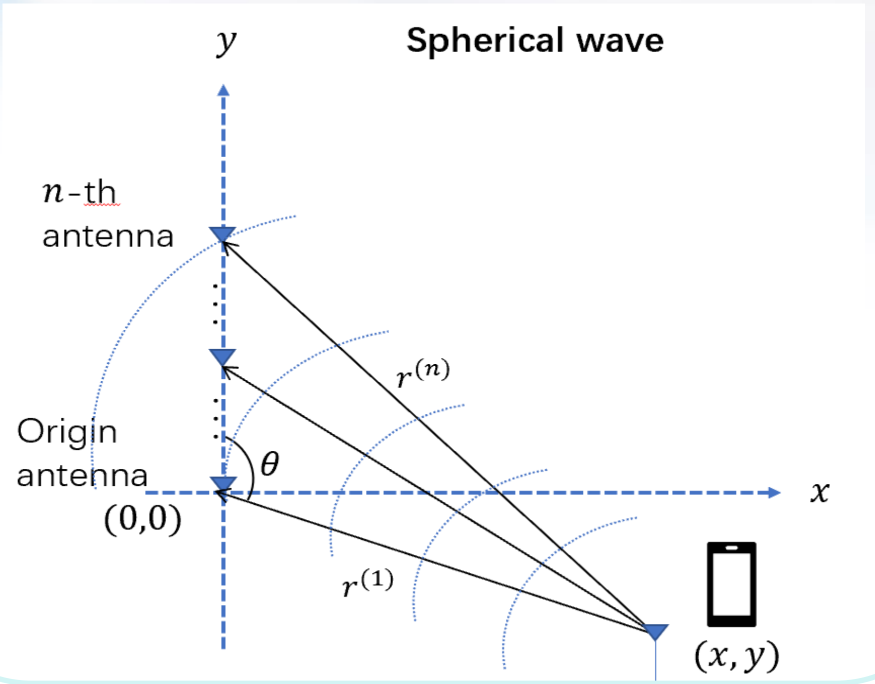

$$\mathbf{b}_N(\theta, r) = \left[1, e^{-j2\pi\frac{f_c}{c}(r^{(2)}-r^{(1)})}, \cdots, e^{-j2\pi\frac{f_c}{c}(r^{(N)}-r^{(1)})}\right]^T$$

In the near-field, the steering vector is a function of both angle and distance

Channel Model: Sparse Representation

- **Far-field channel vector**

$$\mathbf{h}(x,y) = g e^{-j2\pi \frac{f_c}{c} r^{(1)}} \mathbf{a}(\theta)$$

- **Sparse representation:**

$$\mathbf{h}(x,y) = \mathbf{F}\mathbf{s}$$

where s is the angular-domain sparse vector,

F =[a(θ_1),… , a(θ_N)] is the Fourier transform matrix.

- **Near-field channel vector:**

$$\mathbf{h}(x,y) = g e^{-j2\pi \frac{f_c}{c} r^{(1)}} \mathbf{b}_N(\theta, r)$$

- **Sparse representation:**

?

Channel Model: Sparse Representation

Polar-domain representation [1]

- **Sparse representation:**

$$\mathbf{h}(x, y) = \mathbf{D}\mathbf{u}$$

where u is the polar-domain sparse vector, $\mathbf{D} = [\mathbf{b}_N(\theta_1, r_1), \mathbf{b}_N(\theta_1, r_2), \ldots, \mathbf{b}_N(\theta_N, r_M)]$ is an angular-distance 2 dimensional (2D) dictionary

- **The number of columns of D is $N \times M$, N is the sampling number of angle, M is the sampling number of distance**
  - ➢ **High storage burden**
  - ➢ **High coherence between the columns of the dictionary**

Distance-parameterized angular-domain representation [2]

- **Sparse representation:**

$$\mathbf{h}(x, y) = \mathbf{W}(\mathbf{r})\mathbf{s}$$

where s is the angular-domain sparse vector, $\mathbf{W}(\mathbf{r}) = [\mathbf{b}_N(\theta_1, r_1), \mathbf{b}_N(\theta_2, r_2), \ldots, \mathbf{b}_N(\theta_N, r_N)]$ is the distance-parameterized dictionary

- **The number of columns of $\mathbf{W}(\mathbf{r})$ is N, the sampling number of angle**
  - ➢ **Lower storage burden**
  - ➢ **Lower coherence between the columns of the dictionary**

[1] M. Cui and L. Dai, "Channel estimation for extremely large-scale MIMO: Far-field or near-field?", IEEE TCOM, vol. 70, no. 4, pp. 2663-2677, Apr. 2022

[2] X. Zhang, H. Zhang, and Y. C. Eldar, "Near-Field Sparse Channel Representation and Estimation in 6G Wireless Communications", IEEE TCOM, Jan. 2024

Dictionary comparison

Polar-domain dictionary

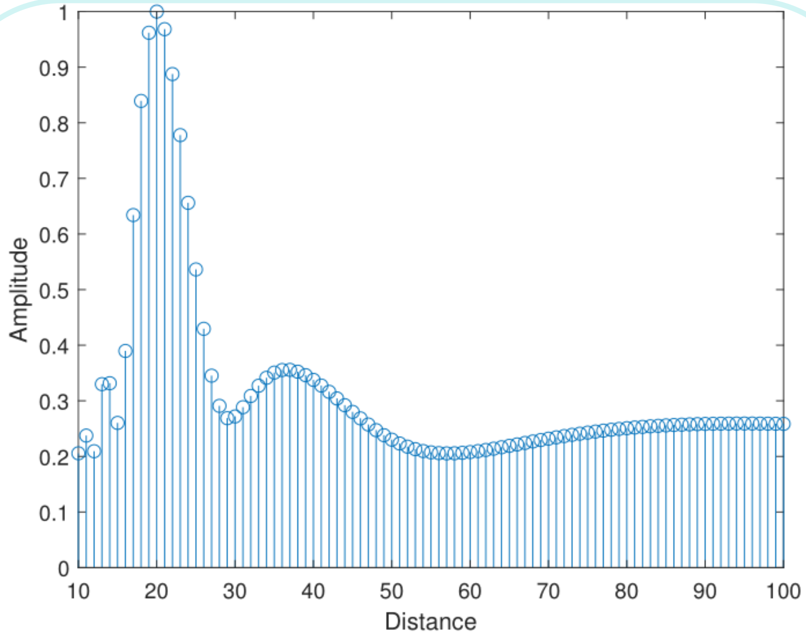

Column coherence of dictionary D with respect to distances (the same angle for each column)

Distance-parameterized angular-domain dictionary

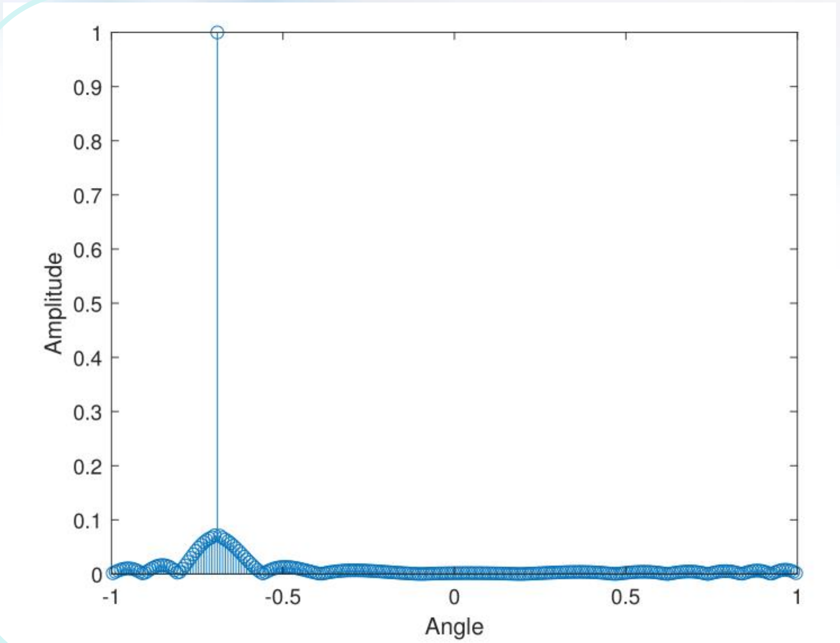

Column coherence of dictionary $\mathbf{W}(\mathbf{r})$ with respect to angles (the same distance for each column)

The column coherence of the proposed dictionary is much lower → higher sparse recovery performance

Channel Estimation

- **Problem formulation: Simultaneously estimate $\mathbf{s}$ and $\mathbf{r}$ based on the channel model $\mathbf{h}(x, y) = \mathbf{W}(\mathbf{r})\mathbf{s}$**

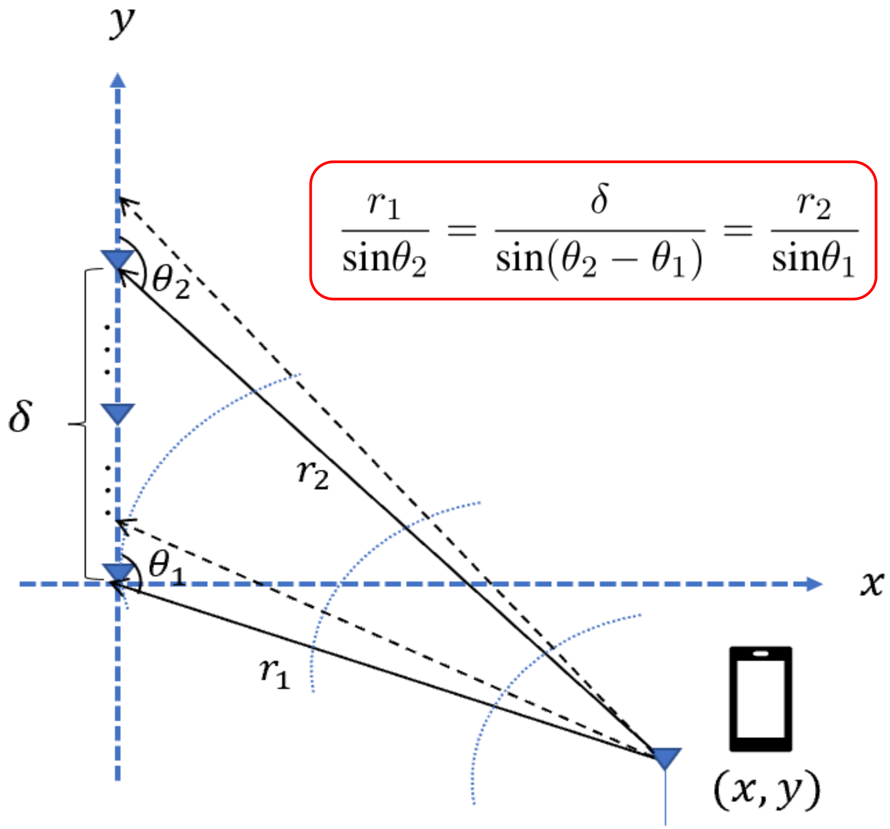

$$\frac{r_1}{\sin\theta_2} = \frac{\delta}{\sin(\theta_2 - \theta_1)} = \frac{r_2}{\sin\theta_1}$$

Illustration of antenna selection for near-field channel estimation

Algorithm 1 The proposed DL-OMP algorithm for near-field LoS channel estimation

Inputs:

Received signal $\mathbf{y}_1$ and $\mathbf{y}_2$; the initial dictionary $\mathbf{W}_1^{\circ}$; the maximum and the minimum distances $r_{\max}$ and $r_{\min}$; antenna spacing between the two subsets δ; dictionary update iterations K_{iter}

Output:

The estimated angle $\hat{\theta}$, distance $\hat{r}$ and the near-field channel $\hat{\mathbf{h}}(x, y)$.

1. **for** $k \in \{1, 2, \cdots, K_{\text{iter}}\}$ **do**
2. Estimating the angle $\hat{\theta}_1$: $\hat{\theta}_1 \leftarrow \mathbf{W}_1^H \mathbf{y}_1$.
3. Constructing the dictionary $\mathbf{W}_2$ based on (25).
4. Estimating the angle $\hat{\theta}_2$: $\hat{\theta}_2 \leftarrow \mathbf{W}_2^H \mathbf{y}_2$.
5. Calculating the distances $\hat{r}_1$: $\hat{r}_1 = \frac{\delta \sin\hat{\theta}_2}{\sin(\hat{\theta}_2 - \hat{\theta}_1)}$.
6. Calculating the updating vector $\boldsymbol{\alpha}_1$ based on (29).
7. Updating the dictionary $\mathbf{W}_1$ as

$$\mathbf{W}_1 = \text{diag}(\boldsymbol{\alpha}_1)\mathbf{W}_1^{\circ}.$$

8. **end for**
9. Refinement of $\hat{r}_1$.
10. Estimating the channel coefficient $\hat{g}$ based on $\hat{\theta} = \hat{\theta}_1$, $\hat{r} = \hat{r}_1$ by (30), and reconstructing the channel vector $\hat{\mathbf{h}}(x, y)$ as in (32).
11. **return** $\hat{\theta}$, $\hat{r}$ and $\hat{\mathbf{h}}(x, y)$.

Simulation results

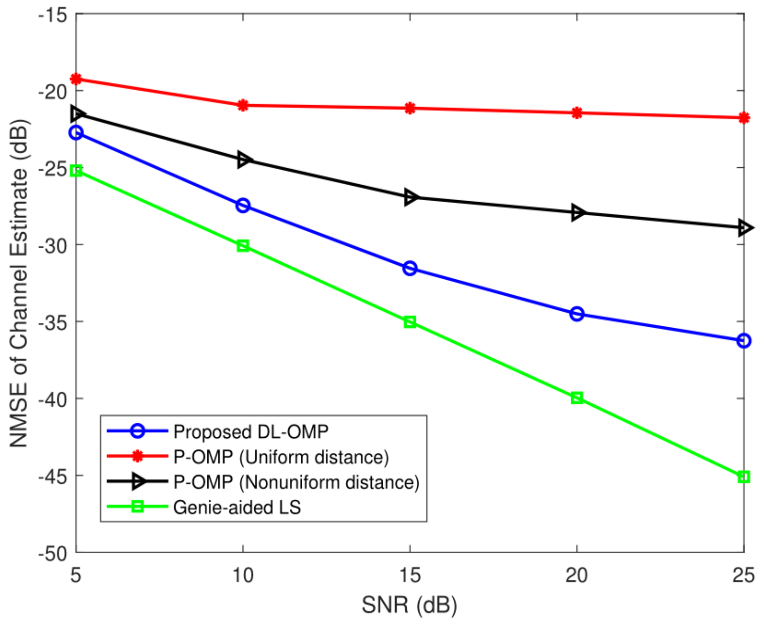

Fig. The NMSE of the channel estimate versus different SNRs

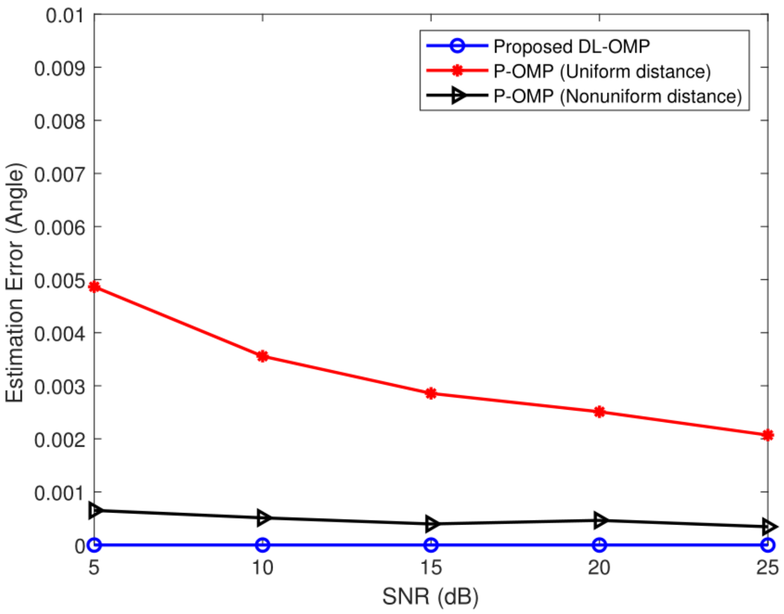

Fig. The estimation error of the angle versus different SNRs

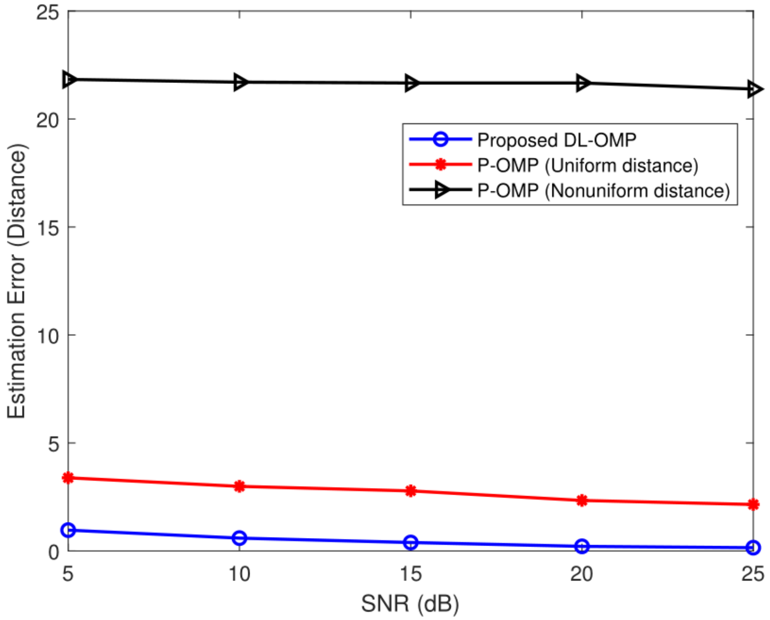

Fig. The estimation error of the distance versus different SNRs

Spherical waveform-based channel estimation achieves significant performance gain with low storage and computational complexity!

Model-based Deep Learning for Near-Field Channel Estimation

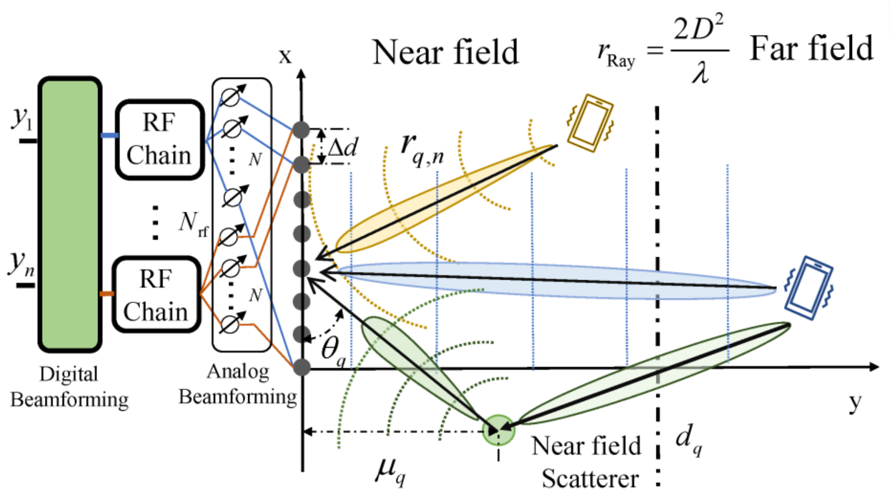

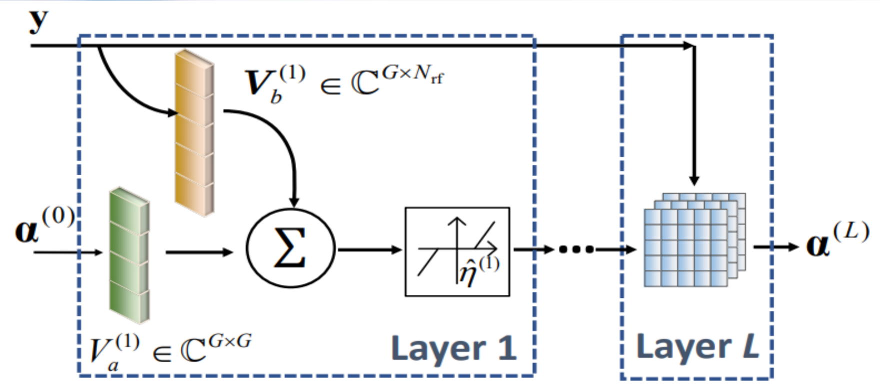

LISTA

Compressed Sensing (CS) theory based near/far-field channel estimation:

Sep1: Sparse representation: $\mathbf{h} \simeq \mathbf{A}\boldsymbol{\alpha},$

Step2: CS Problem formulation: $\min_{\boldsymbol{\alpha}} \|\mathbf{y} - \mathbf{W}\mathbf{A}\boldsymbol{\alpha}\|_2, \quad \text{s.t} \quad \|\boldsymbol{\alpha}\|_0 < \epsilon,$

Step3: Sparse recovery algorithm, e.g., iterative soft thresholding algorithm (ISTA)

$$\boldsymbol{\alpha}^{(t+1)} = h_{(\eta)}\left(\left(\mathbf{I} - \frac{1}{\lambda_{\max}}\boldsymbol{\Psi}^{\mathrm{T}}\boldsymbol{\Psi}\right)\boldsymbol{\alpha}^{(t)} + \frac{1}{\lambda_{\max}}\boldsymbol{\Psi}^{\mathrm{T}}\mathbf{y}\right)$$

Deep Unfolding:
Recast each iteration into a single network layer

[1] X. Zhang, Z. Wang, H. Zhang, and L. Yang, "Near-Field Channel Estimation for Extremely Large-Scale Array Communications: A model-based deep learning approach", *IEEE Communications Letters*, 2023.

[2] V. Monga, Y. Li, and Y. C. Eldar,``Algorithm Unrolling: Interpretable, Efficient Deep Learning for Signal and Image Processing'', *IEEE Signal Proces. Mag.*, 2020

Model-based Deep Learning for Near-field Channel Estimation

- **Existing methods:**
  - ➢ **Fixed sparse dictionary A**
  - ➢ **Non-learning sparse recovery algorithm, e.g., ISTA, OMP.**
- **Motivations:**
  - ➢ **Can we learn a sparse dictionary A ?**
  - ➢ **Can we joint learn a sparse dictionary A and exploiting LISTA do sparse recovery?**

Sparse dictionary learning-LISTA (SDL-LISTA)

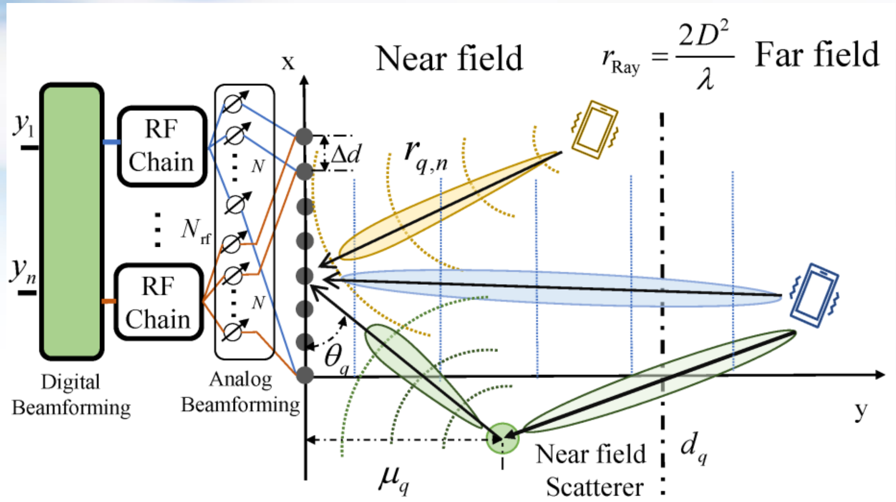

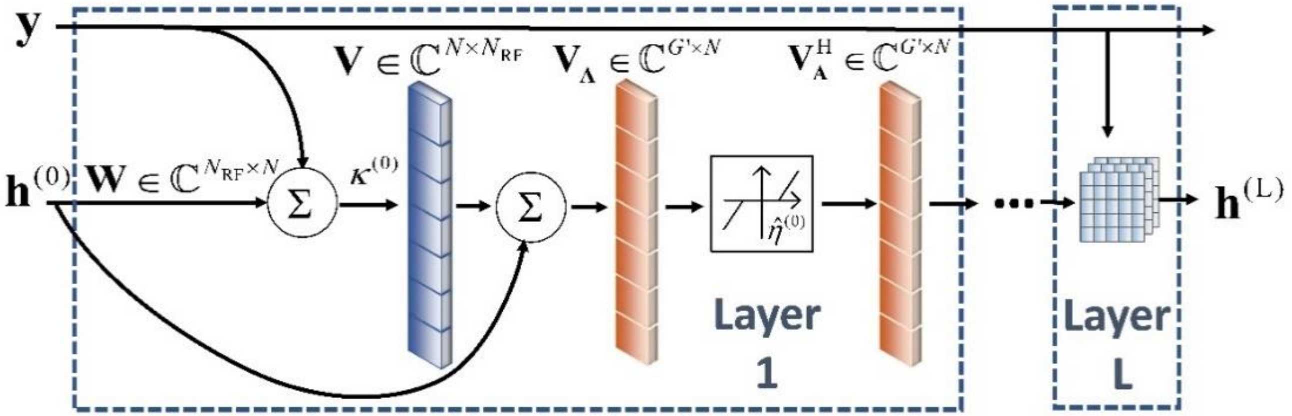

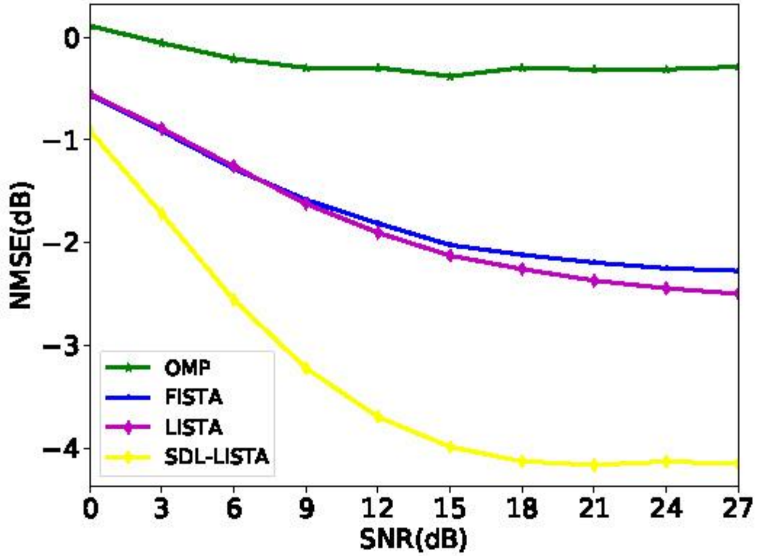

X. Zhang, Z. Wang, H. Zhang, and L. Yang, "Near-field channel estimation for extremely large-scale array communications: A model-based deep learning approach," *IEEE Commun. Lett.*, 2023.

Outline of Part 4

- **Near-Field Channel State Information Acquisition**
  - Near-field MISO channel estimation
  - Near-field MIMO channel estimation
  - Near-field EM-based channel model
  - Near-field beam training
- **Near-Field Beam Split**
  - Phase-delay beam focusing
  - Near-field rainbow-based beam training
  - Distance-dependent beam split based beam training

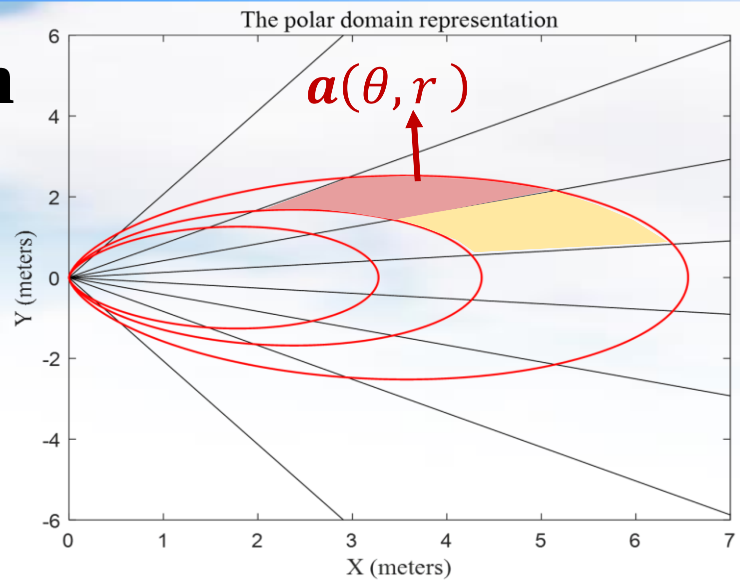

Near-Field Scenario: From MISO to MIMO

- **MISO: Only the BS is equipped with multiple antennas**
- **MIMO: The user is also equipped with multiple antennas**

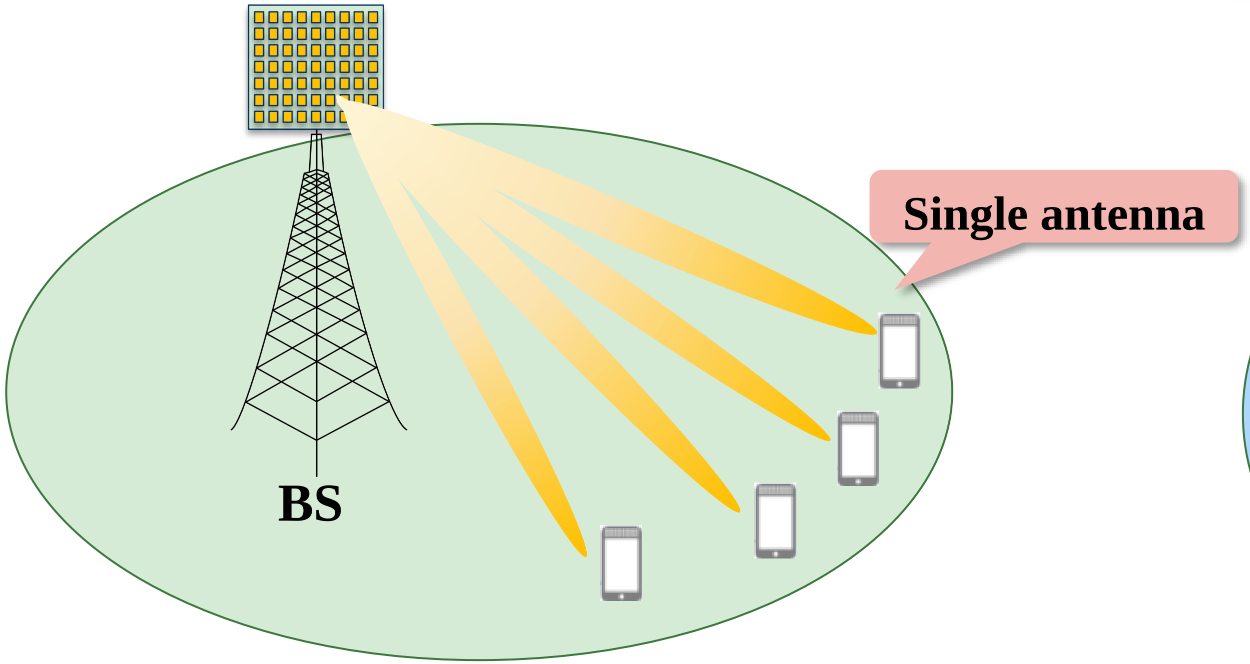

MISO

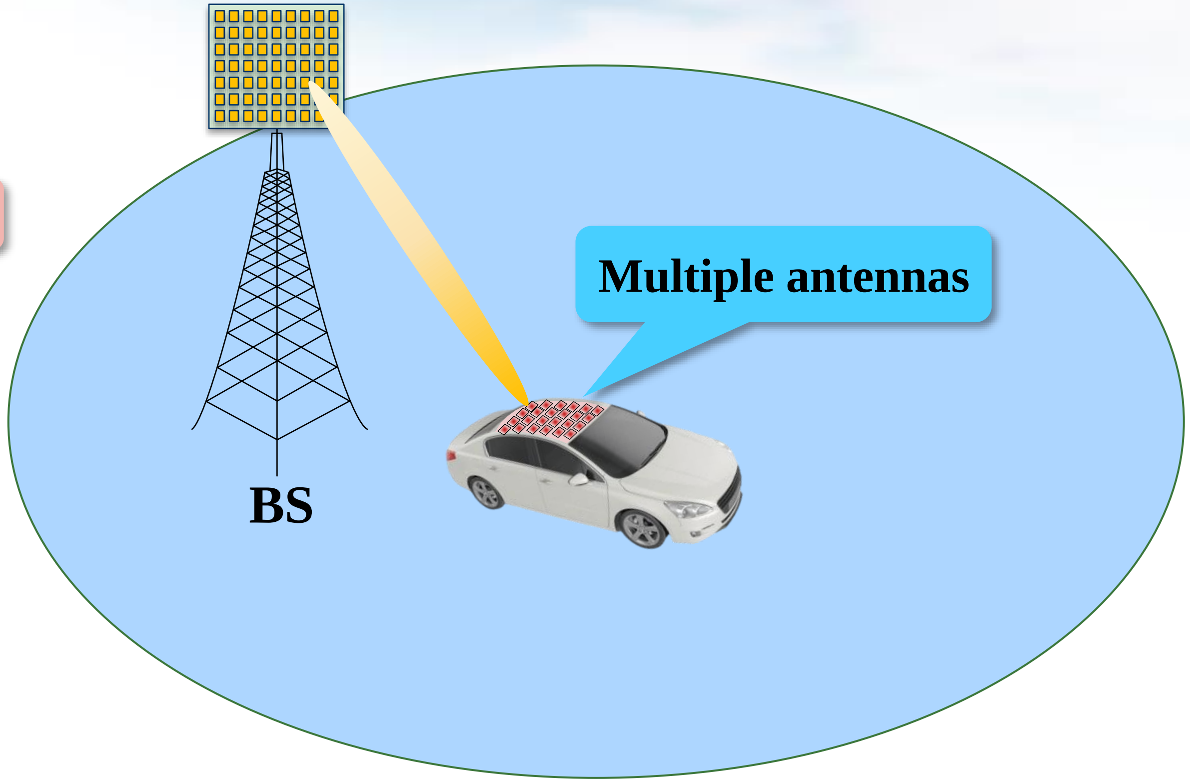

MIMO

Near-Field MIMO Channel Model

- **Similar to far-field MIMO channel model, the existing near-field MIMO channel model is based on the near-field steering vector**

$$\mathbf{H}_{\text{near-field}} = \sqrt{\frac{N_1 N_2}{L}} \sum_{l=1}^{L} g_l \mathbf{a}(\theta_r^l, d_r^l)\, \mathbf{b}^H(\theta_t^l, d_t^l)$$

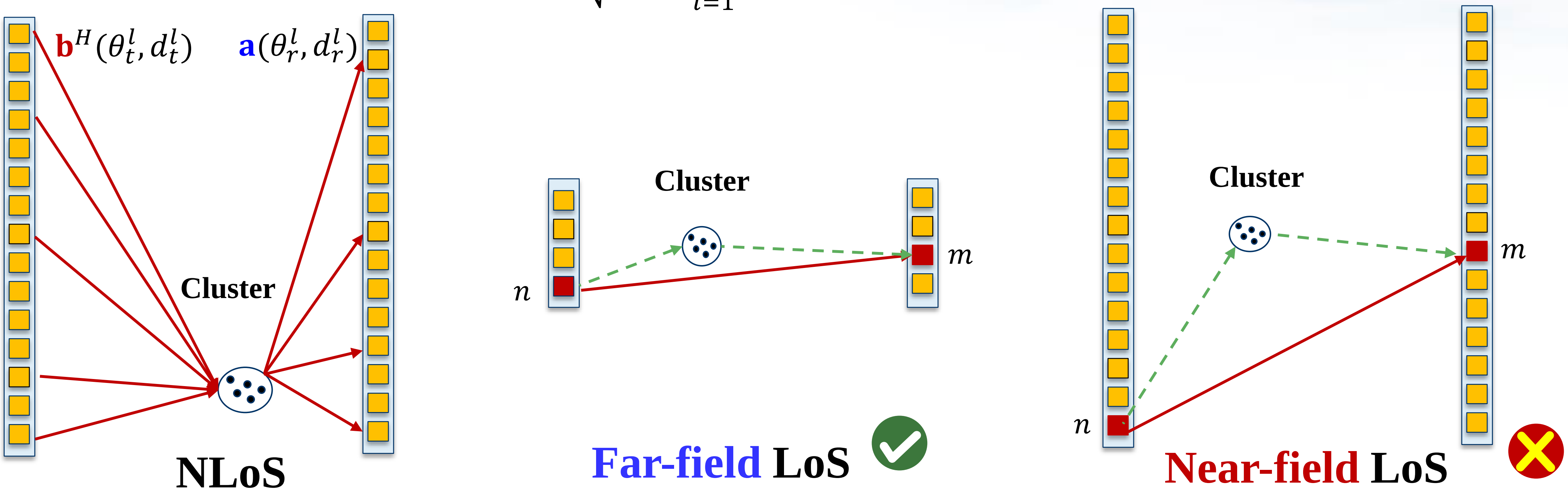

The existing model cannot accurately describe the characteristic of near-field LoS path

Proposed Near-Field MIMO Channel Model

- **The LoS and NLoS paths are modeled separately**

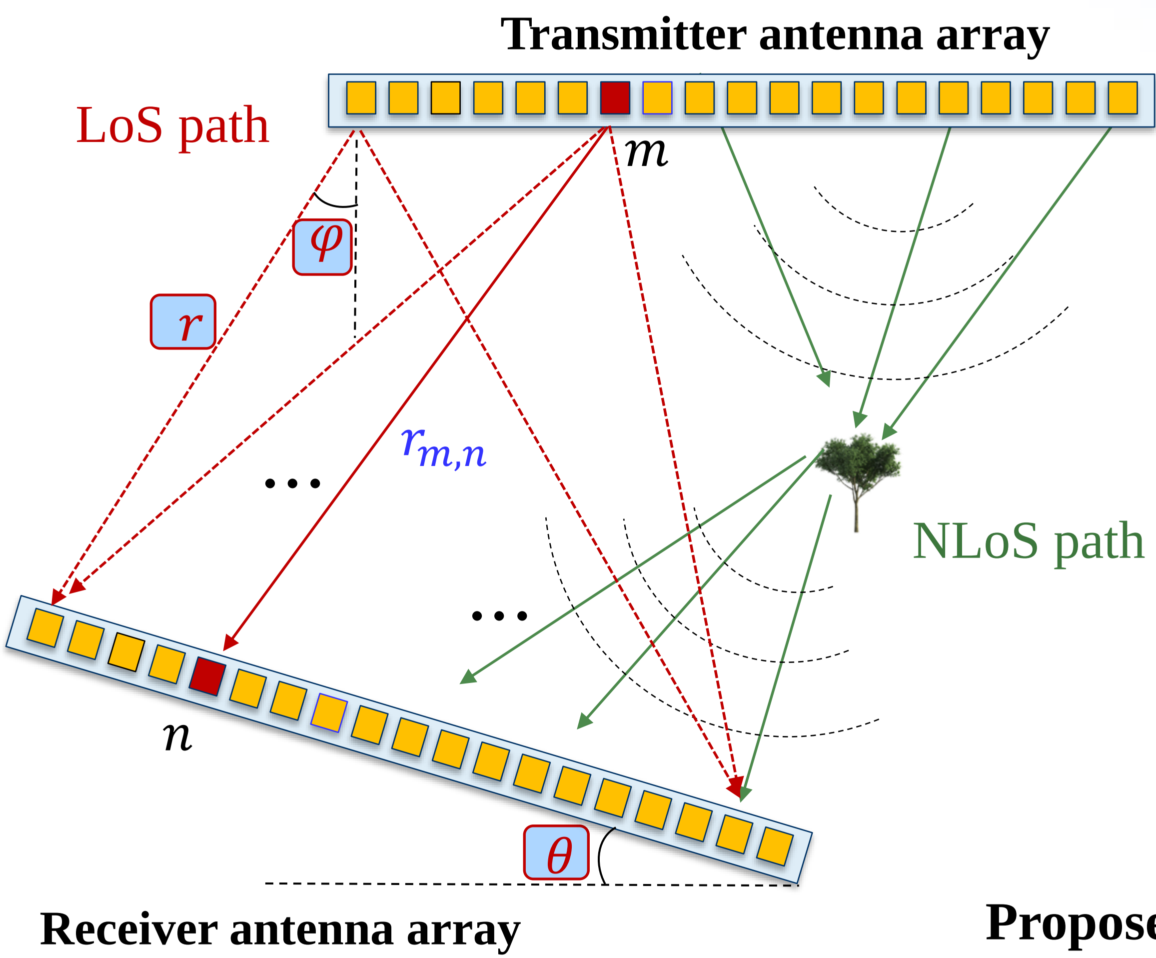

LoS: Free-space propagation

$$\mathbf{H}_{\mathrm{LoS},(m,n)} = \frac{e^{-j2\pi r_{m,n}/\lambda}}{r_{m,n}}$$

$$r_{m,n} = \sqrt{r^2 + (md)^2 + (nd)^2 - 2rmd\cos(\theta+\varphi) + 2rnd\cos(\theta) - 2mnr^2\cos(\varphi)}$$

$$\mathbf{H}_{\mathrm{LoS}}(r,\theta,\varphi) = \begin{bmatrix} \frac{e^{-j2\pi r_{1,1}/\lambda}}{r_{1,1}} & \cdots & \frac{e^{-j2\pi r_{1,N}/\lambda}}{r_{1,N}} \\ \vdots & \ddots & \vdots \\ \frac{e^{-j2\pi r_{M,1}/\lambda}}{r_{M,1}} & \cdots & \frac{e^{-j2\pi r_{M,N}/\lambda}}{r_{M,N}} \end{bmatrix}$$

NLoS: Based on near-field steering vector

$$\mathbf{H}_{\mathrm{NLoS}} = \sum_{l=1}^{L} g_l \boldsymbol{a}(\theta_r^l, r_r^l)\, \mathbf{b}^H(\theta_t^l, r_t^l)$$

Proposed near-field MIMO channel model: $\mathbf{H} = \mathbf{H}_{\mathrm{LoS}} + \mathbf{H}_{\mathrm{NLoS}}$

Y. Lu and L. Dai, "Near-field channel estimation in mixed LoS/NLoS environments for extremely large-scale MIMO systems," *IEEE Trans. Commun.*, vol. 71, no. 11, pp. 7748-7760, Jun. 2023.

Near-Field MIMO Rayleigh Distance

- **Rayleigh distance: The transceiver distance when the maximum phase discrepancy between spherical wave and plane wave is $\pi/8$**
  - **Classical MISO Rayleigh Distance:** $R_1 = 2D^2/\lambda$
  - **Proposed MIMO Rayleigh Distance:** $R_2 = 2(D_1 + D_2)^2/\lambda$

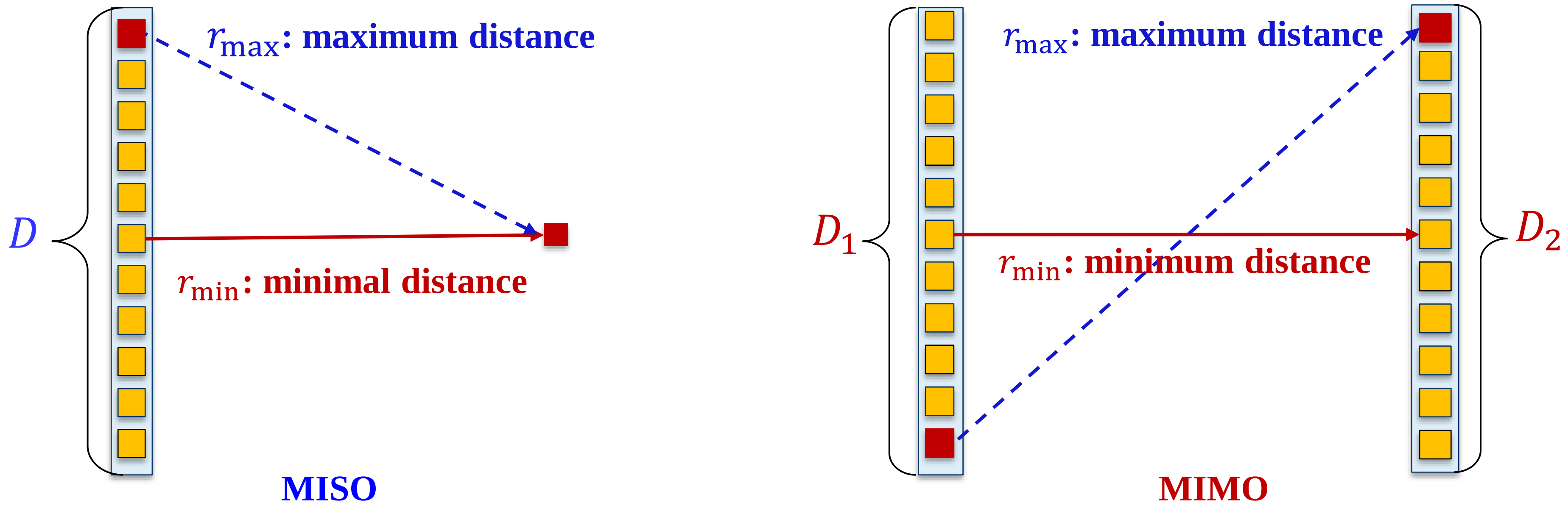

Y. Lu and L. Dai, "Near-field channel estimation in mixed LoS/NLoS environments for extremely large-scale MIMO systems," *IEEE Trans. Commun.*, vol. 71, no. 11, pp. 7748-7760, Jun. 2023.

Simulation Results

- **The proposed scheme can accurately estimate the near-field MIMO channel**

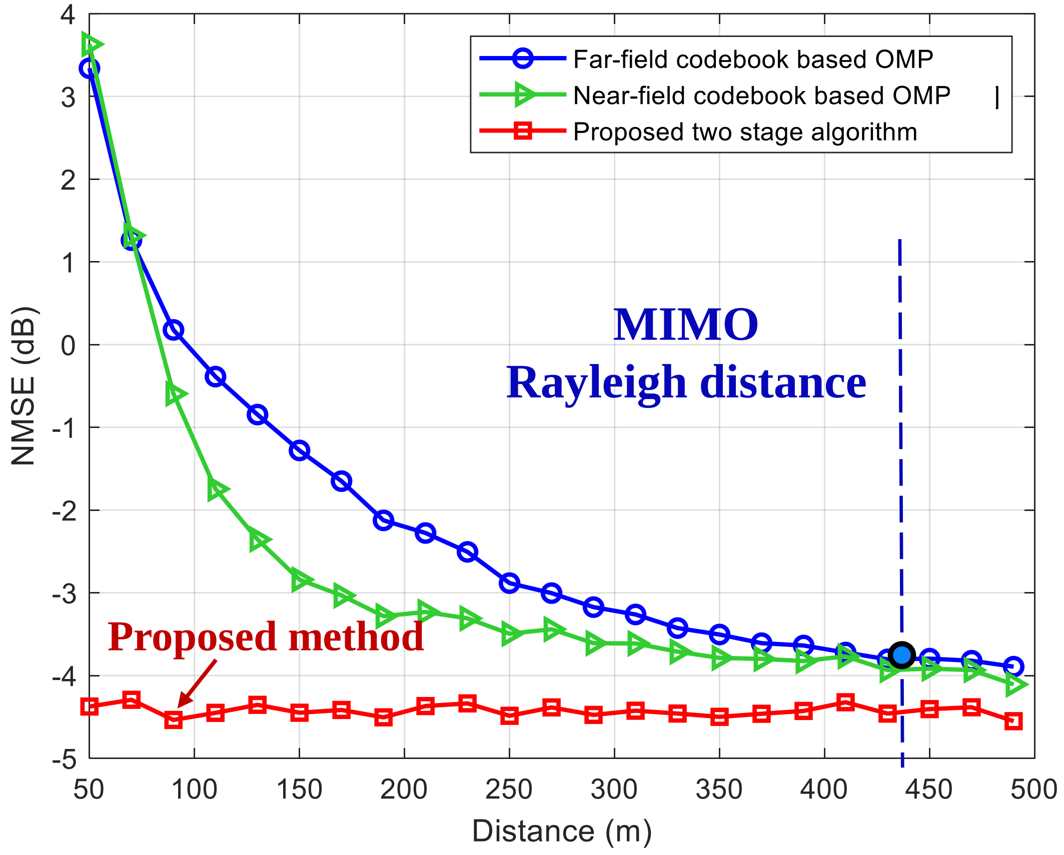

Parameters	Value
Carrier	50 GHz
Element number of transmit antenna array	256
Element number of transmit antenna array	128
Number of NLoS Paths	5
SNR	5 dB
Pilot compression ratio	0.5

Y. Lu and L. Dai, "Near-field channel estimation in mixed LoS/NLoS environments for extremely large-scale MIMO systems," *IEEE Trans. Commun.*, vol. 71, no. 11, pp. 7748-7760, Jun. 2023.

Outline of Part 4

- **Near-Field Channel State Information Acquisition**
  - Near-field MISO channel estimation
  - Near-field MIMO channel estimation
  - Near-field EM-based channel model
  - Near-field beam training
- **Near-Field Beam Split**
  - Phase-delay beam focusing
  - Near-field rainbow-based beam training
  - Distance-dependent beam split based beam training

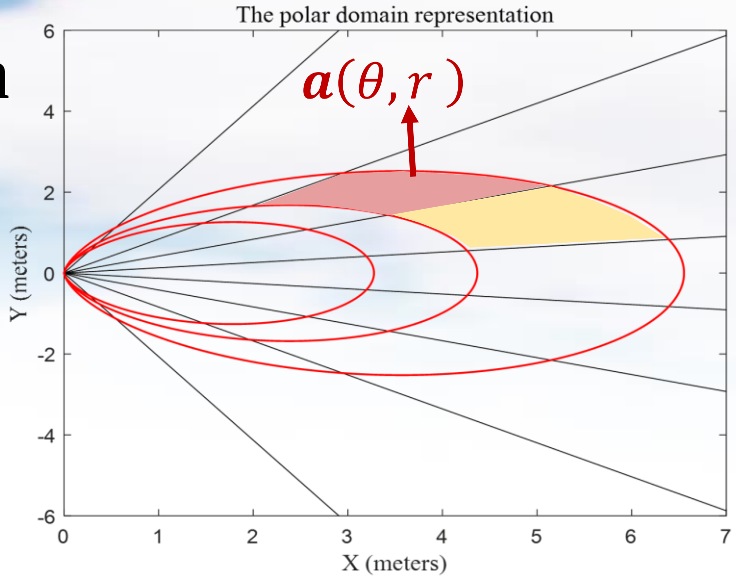

Challenge of Existing Near-Field Channel Model

- **Widely adopted schemes in wireless communication view scatterer as point: simple but inaccurate**
- **Schemes like full-wave simulation based on electromagnetism: accurate but complex, without analytical expression for theoretical analysis**

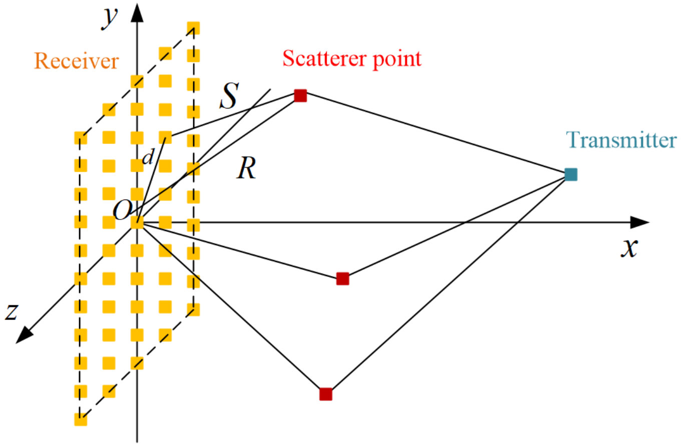

Single point assumption

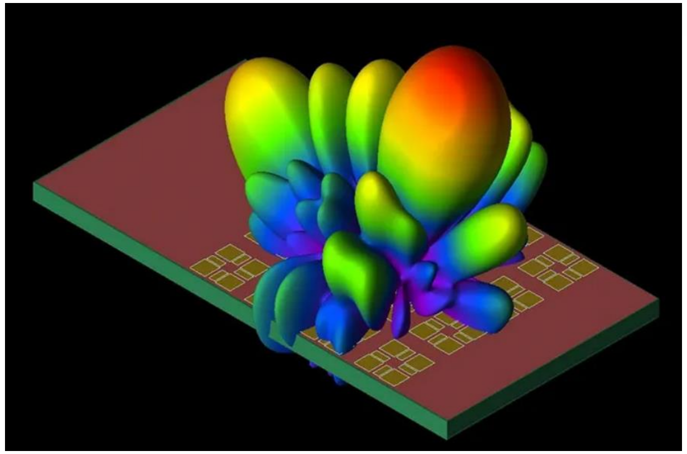

Full-wave simulation

How to construct a simple analytical channel model with enough accuracy

Electromagnetism-Based Channel Model (1)

- Unlike point assumption of scatterers, we view the scatterers as **inhomogeneous media** in the electromagnetic equations

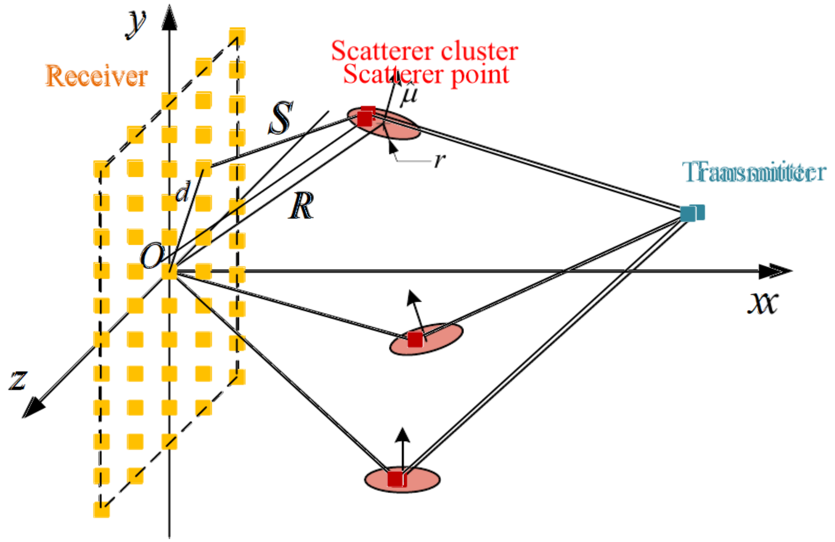

Maxwell's equation in inhomogeneous space

$$\nabla \times \mathbf{E}(\mathbf{r}) = \mathrm{j}\omega\mu(\mathbf{r})\mathbf{H}(\mathbf{r}), \quad (1a)$$

$$\nabla \times \mathbf{H}(\mathbf{r}) = -\mathrm{j}\omega\epsilon(\mathbf{r})\mathbf{E}(\mathbf{r}) + \mathbf{J}(\mathbf{r}), \quad (1b)$$

$$\nabla \cdot (\epsilon(\mathbf{r})\mathbf{E}(\mathbf{r})) = \rho(\mathbf{r}), \quad (1c)$$

$$\nabla \cdot (\mu(\mathbf{r})\mathbf{H}(\mathbf{r})) = 0 \quad (1d)$$

$$\mathbf{G}(\mathbf{r},\mathbf{r}') = \frac{1}{4\pi}\left(\mathbf{I} + \frac{\nabla_{\mathbf{r}}\nabla_{\mathbf{r}}^{\mathrm{H}}}{\kappa_0^2}\right)\frac{e^{\mathrm{j}\kappa_0\|\mathbf{r}-\mathbf{r}'\|}}{\|\mathbf{r}-\mathbf{r}'\|}$$

Direct link: simple

Scatterer field: complex

Source-destination relationship $\mathbf{E}(\mathbf{r}) = \mathrm{j}\omega\int_{\boxed{V_s}}\mathbf{G}(\mathbf{r},\mathbf{r}')\mu_0\mathbf{J}(\mathbf{r}')\mathrm{d}\mathbf{r}' + \int_{\boxed{V}}\mathbf{G}(\mathbf{r},\mathbf{r}')(k^2(\mathbf{r}') - k_0^2)\mathbf{E}(\mathbf{r}')\mathrm{d}\mathbf{r}'$

source **scatterer** $k(\mathbf{r}) = \omega\sqrt{\mu(\mathbf{r})\epsilon(\mathbf{r})}$

W. C. Chew, "Waves and fields in inhomogenous media," *John Wiley & Sons*, 1999, vol. 16.

Electromagnetism-Based Channel Model (2)

- Derive an **analytical model** based on the following parameter assumptions

$\int_V \mathbf{G}(\mathbf{r},\mathbf{r}')(k^2(\mathbf{r}')-k_0^2)\mathbf{E}(\mathbf{r}')\mathrm{d}\mathbf{r}'$

Complex scattering environment

Scattering region V	→	Solid circle	$\mathrm{d}\mathbf{r}=\rho\mathrm{d}\rho\mathrm{d}\theta \begin{cases} 0\leqslant\rho\leqslant r_0 \\ 0\leqslant\theta\leqslant 2\pi \end{cases}$
$k^2(\mathbf{r}')-k_0^2$	→	Scatterer inhomogeneity	$f(\mathbf{r})=\frac{a+1}{\pi r^{2a+2}}\rho(r^2-\rho^2)^a$
Electric field $\mathbf{E}(\mathbf{r}')$	→	Random field	$\mathbb{E}[E(\mathbf{r}_1')E(\mathbf{r}_2')^*]$

- Analytical expression of the **channel correlation**

Lemma 1 Assume a circle-shaped scatterer centered at R, its radius is r, its direction is μ, its concentration parameter is a. Assume that the radius r is **far smaller than the distance** R between the scatterer and the receiver, then the received electric field d_1 at position d_2 and has the following **channel correlation function**:

$$\tilde{R}_E(\mathbf{d}_1,\mathbf{d}_2)=\beta_0\frac{A(\mathbf{d}_0)}{\sqrt{A(\mathbf{d}_1)A(\mathbf{d}_2)}}e^{-\mathrm{j}\frac{2\pi}{\lambda}R\left(\sqrt{A(\mathbf{d}_1)}-\sqrt{A(\mathbf{d}_2)}\right)}2(a+1)2^a\Gamma(a+1)(\sqrt{C}r)^{-(a+1)}J_{a+1}(\sqrt{C}r)$$

- The channel can be generated by $\boxed{\mathbf{H}=\mathbf{L}\mathbf{N} \qquad \mathbf{R}=\mathbf{L}\mathbf{L}^{\mathrm{H}} \qquad \mathbf{N}\sim\mathcal{CN}(0,\mathbf{I})}$

Z. Wan, J. Zhu, and L. Dai, "Near-field channel modeling for electromagnetic information theory," submitted to *IEEE Trans. Wireless Commun*, Major revision, 2024.

Channel DoF

- **Channel DoF** is determined by the **eigenvalues** of the channel matrix $\mathbf{H}$
- **The slower the eigenvalue decays, the larger the channel DoF is**

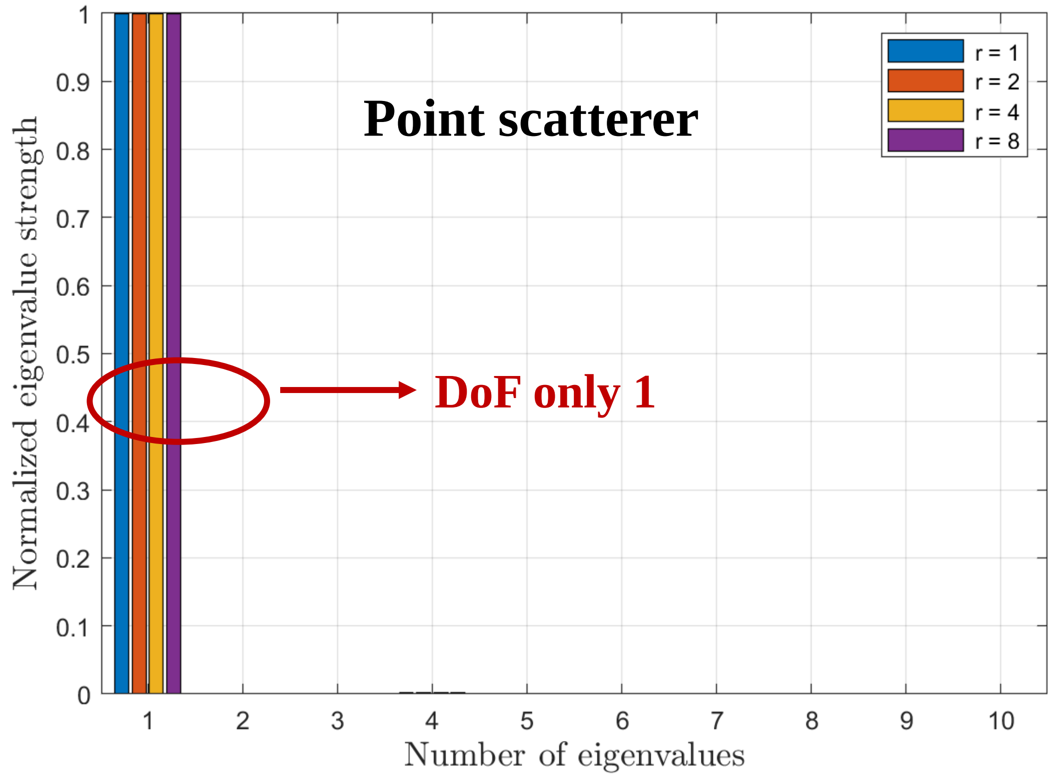

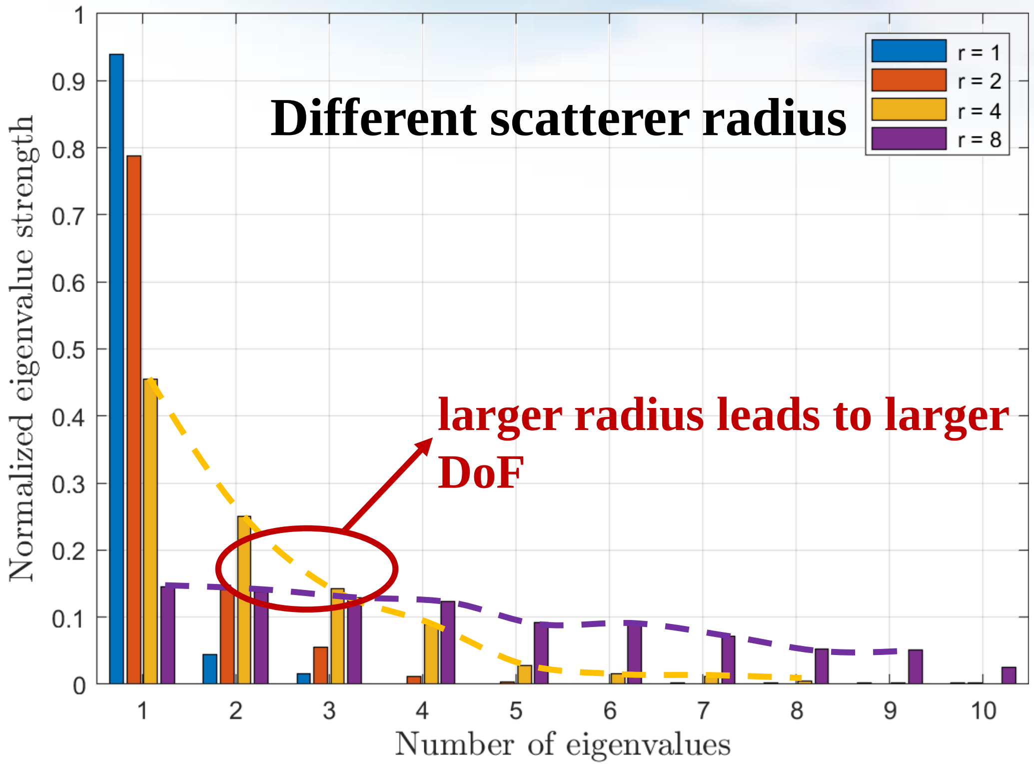

Proposed channel model can better capture the DoF of the channel

Channel estimation with EM prior information

- **The proposed channel model integrates electromagnetic prior information**
- **By utilizing the proposed model, channel estimation performance can be improved**

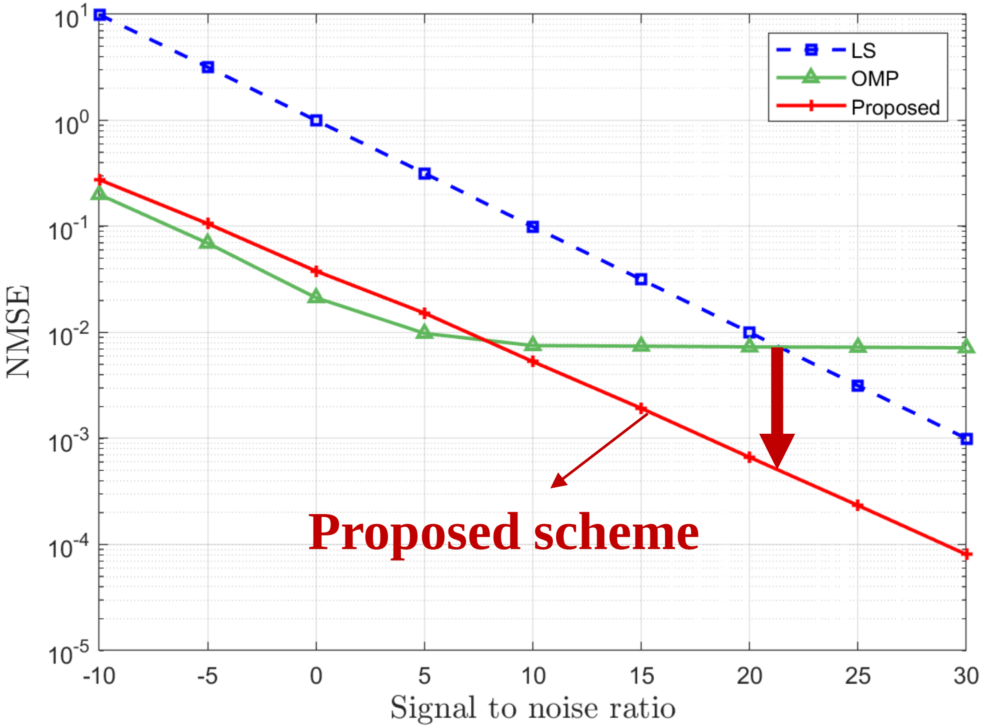

Simulation parameter	Setting
Channel model	CDL-D channel
Transmitter array size	81*81
Carrier	0.75 GHz
Antenna spacing	0.05 m
OMP support size	20

Proposed channel estimation scheme achieves performance gain compared to LS

Z. Wan, J. Zhu, and L. Dai, "Near-Field Channel Modeling for Electromagnetic Information Theory," submitted to *IEEE Trans. Wireless Commun*, Major revision, 2024.

Outline of Part 4

- **Near-Field Channel State Information Acquisition**
  - **Near-field MISO channel estimation**
  - **Near-field MIMO channel estimation**
  - **Near-field EM-based channel model**
  - **Near-field beam training**
- **Near-Field Beam Split**
  - **Phase-delay beam focusing**
  - **Near-field rainbow-based beam training**
  - **Distance-dependent beam split based beam training**

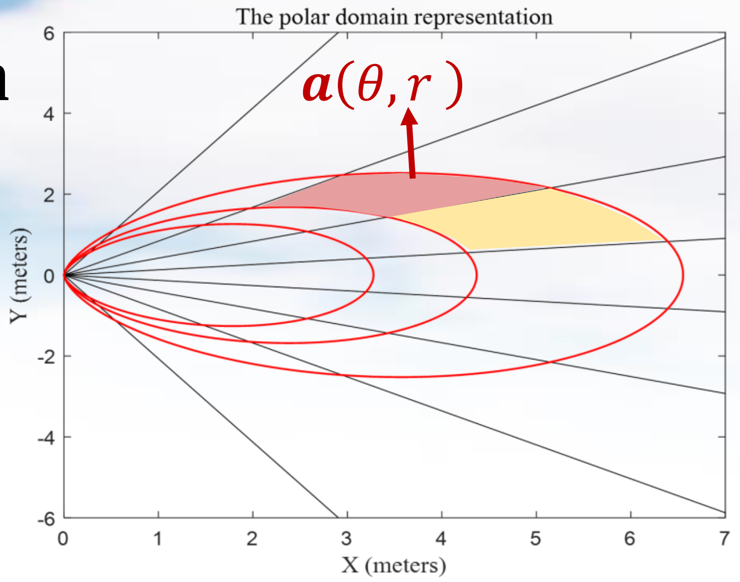

The Challenge of Near-Field Beam Training

- Beam training is an essential method is acquire the channel state information (CSI)
- However, since the near-field codebook requires extra grids on the distance domain, its codebook size is much larger than that of the far-field codebook

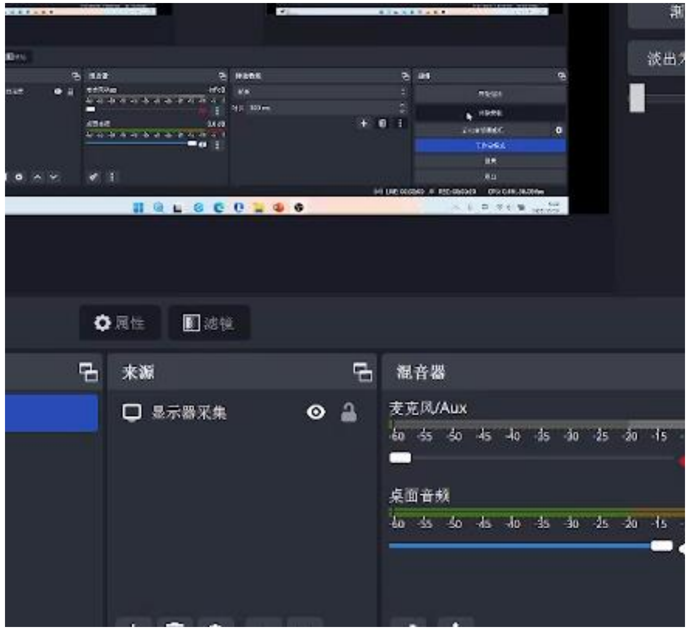

Exhaustive search

Parameters	Far-field codebook	Near-field codebook
Number of antennas	512	512
Carriers	100 GHz	100 GHz
Number of angle grids	512	512
Number of distance grids	1	20
Codebook size	512	10240

The overhead of near-field exhaustive beam training is unaffordable

Near-Field Hierarchical Beam Training

- **Low-resolution** beam covers a wider range of angle and distance, and each layer of codebook narrows the search range gradually
- Perform binary search on both angle and distance simultaneously

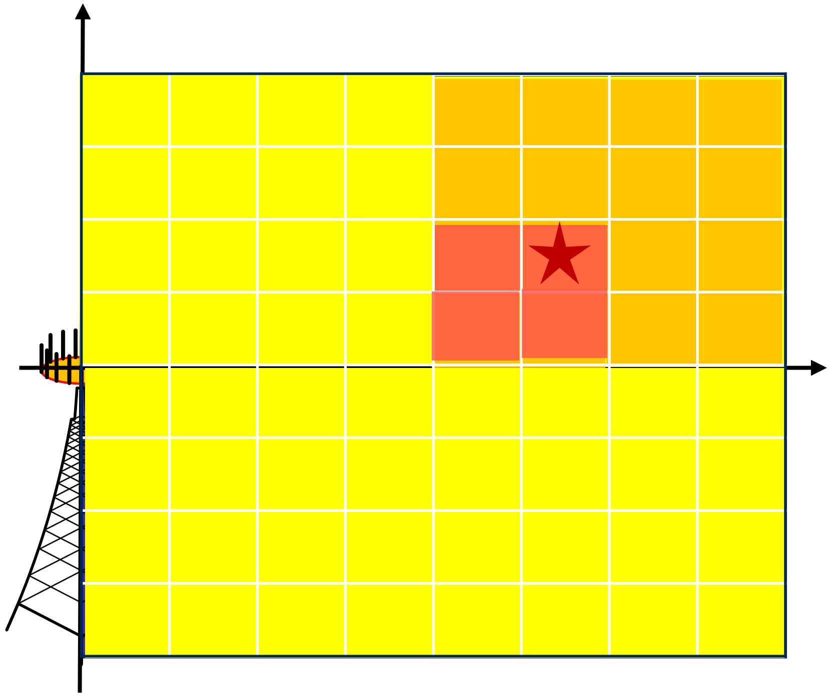

Near-Field Hierarchical Beam Training

N: number of angle grids
S: number of distance grids

Schemes	Complexity
far-field	$\mathcal{O}(NS)$
near-field	$\mathcal{O}(\log(N)+\log(S))$

Near-Field Multi-Resolution Codeword Design

- The aim to design a codeword $\mathbf{v}$ is to approach the ideal beam pattern after beamforming with $\mathbf{v}$

codeword needed to be designed

ideal beam pattern

$$\min_{\mathbf{v}, f(\theta,r)} \|\mathbf{A}^H \mathbf{v} - \mathbf{g}\|_2^2 \qquad \mathbf{A} \triangleq \sqrt{N}\left[\mathbf{a}(\theta_1, r_1), \cdots, \mathbf{a}\left(\theta_N, r_{S_N}\right)\right]$$

$$\text{s.t.} \quad \|\mathbf{v}\|_2 = 1;$$

$$[\mathbf{g}]_{\theta,r} = |G(\theta,r)|\, e^{jf(\theta,r)}$$

additional phase: increase design freedom

ideal beam pattern

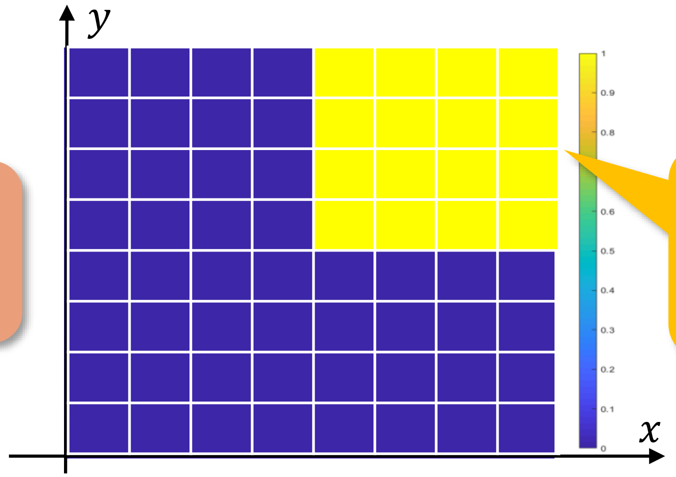

Target coverage $B_{\theta,r}$

$$|G(\theta,r)| = \begin{cases} \sqrt{C}, & (\theta,r) \in B_{\theta,r} \\ 0, & (\theta,r) \notin B_{\theta,r} \end{cases}$$

beamforming gains in target coverage are flattened

beamforming gains outside target coverage are zero

GS（Gerchberg-Saxton）Algorithm

- **Phase recovery in holographic imaging ≜ designing near-field multi-resolution codewords**

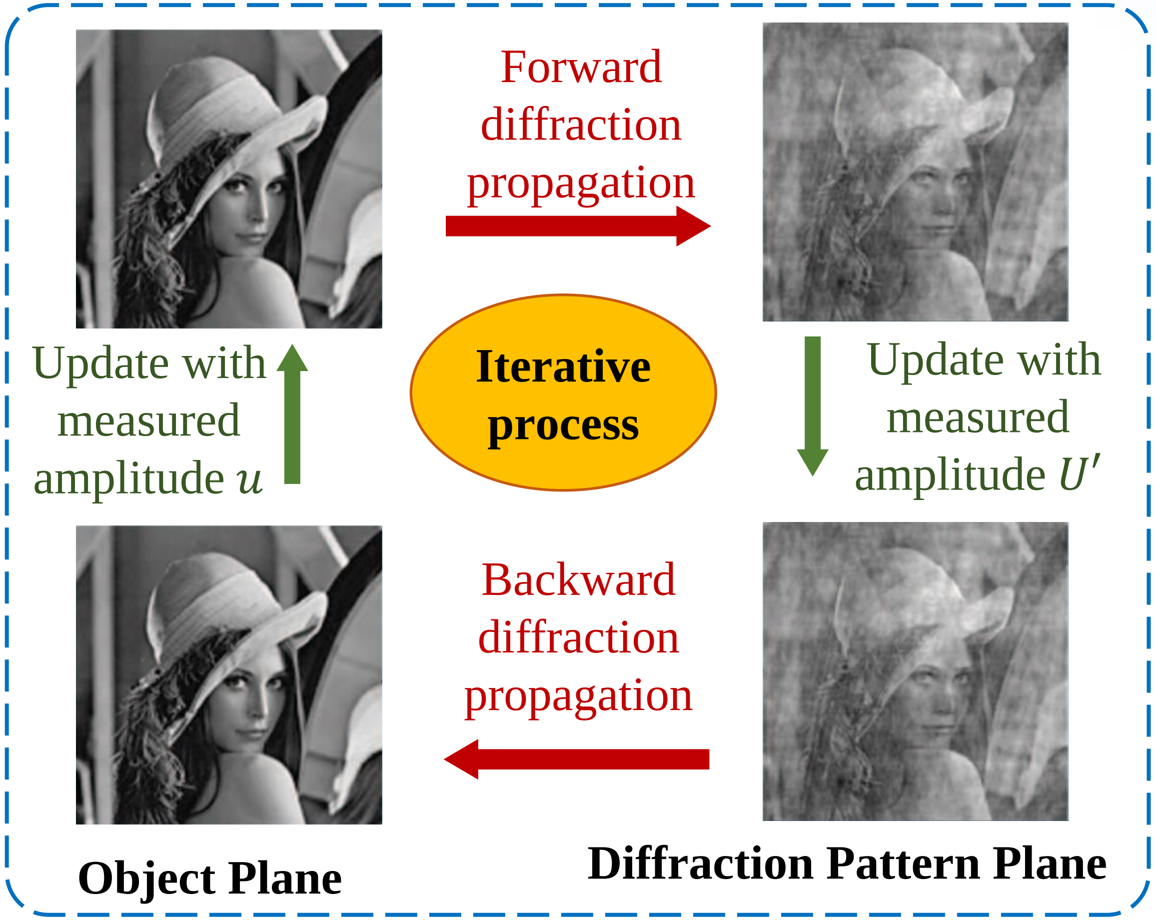

(a) GS algorithm in iterative phase retrieval problem.

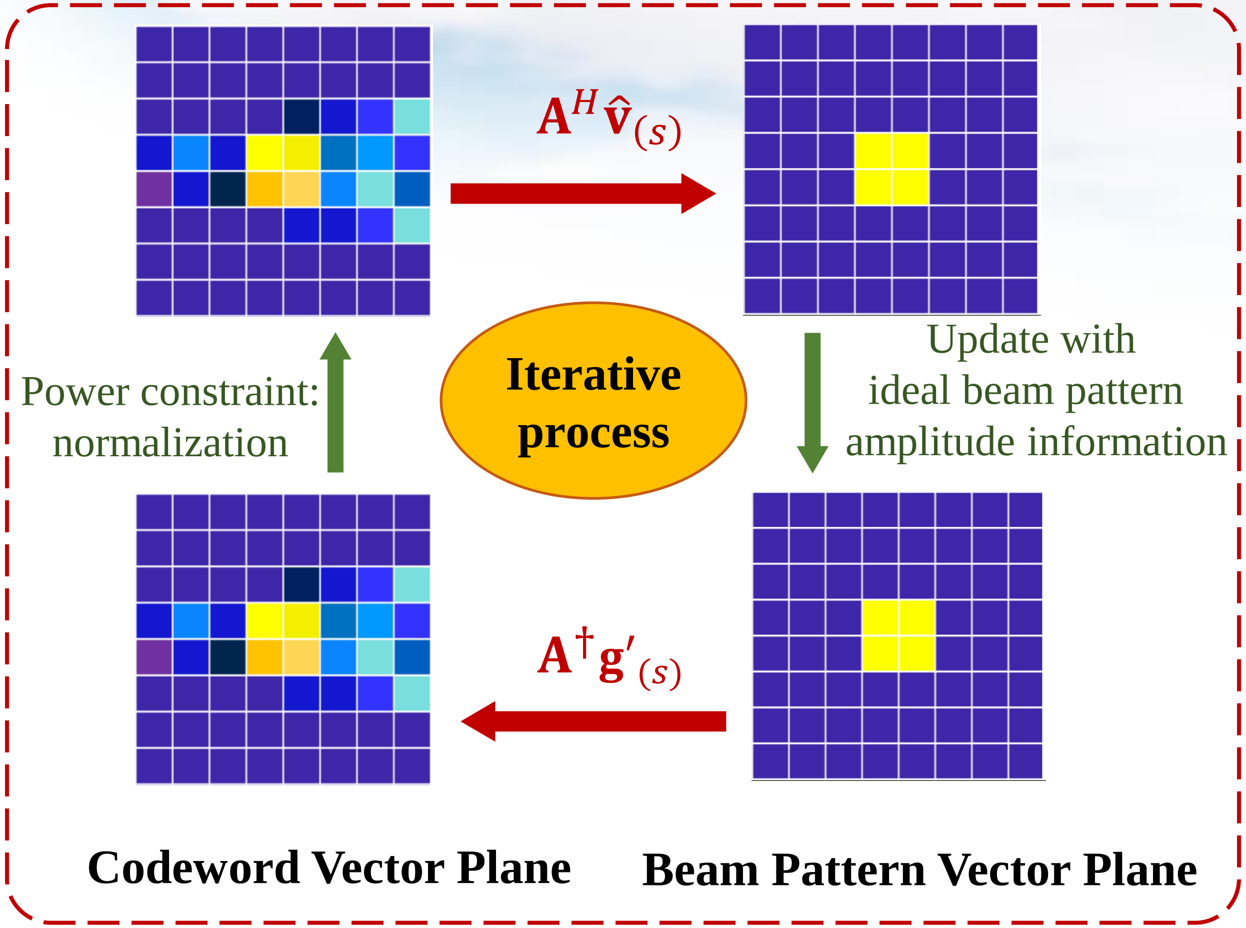

(b) GS algorithm in codeword design.

Simulation Results

- **The proposed scheme provides a tradeoff between the performance and overhead**

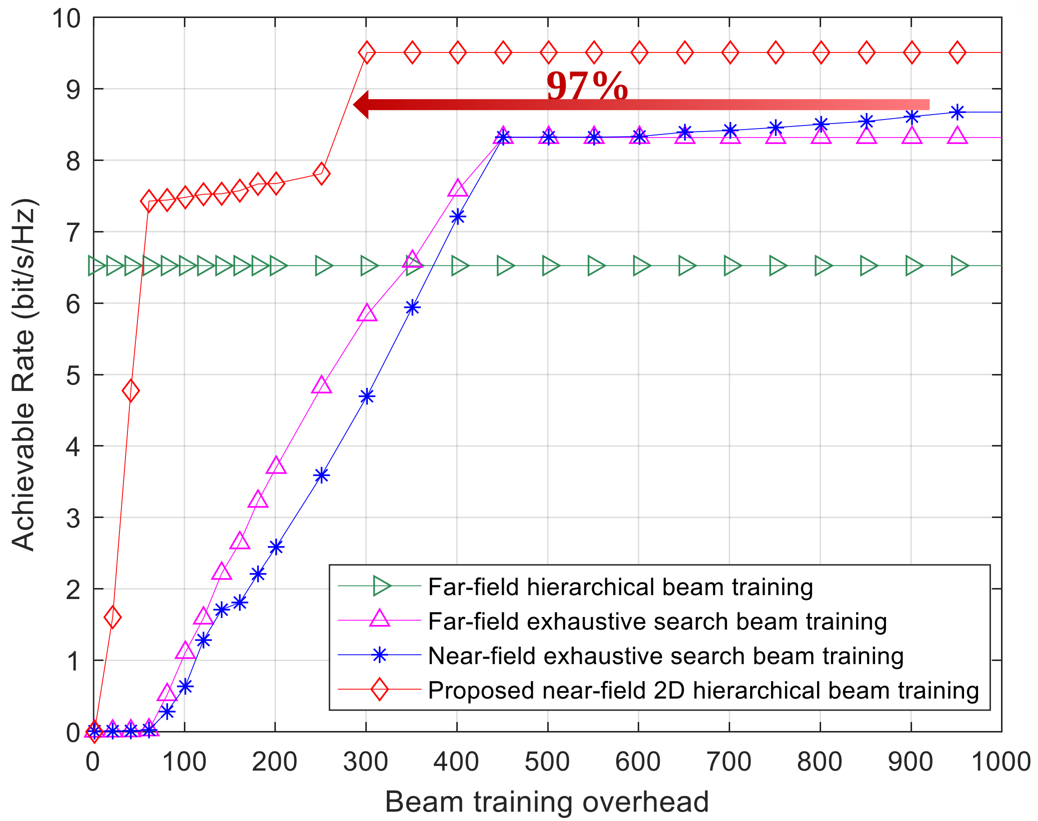

Scheme	Overhead
Near-field exhaustive search beam training	8192
Proposed near-field 2D hierarchical beam training	268

Parameters	Value
Number of antennas	512
Carrier	60GHz
Number of angle grids	512
Number of distance grids	16

Y. Lu and L. Dai, "Hierarchical beam training for extremely large-scale MIMO: from far-field to near-field ," *IEEE Trans. Commun.*, vol. 72, no. 5, pp. 3064-3078, May 2024.

Outline of Part 4

- **Near-Field Channel State Information Acquisition**
  - Near-field MISO channel estimation
  - Near-field MIMO channel estimation
  - Near-field EM-based channel model
  - Near-field beam training
- **Near-Field Beam Split**
  - Phase-delay beam focusing
  - Near-field rainbow-based beam training
  - Distance-dependent beam split based beam training

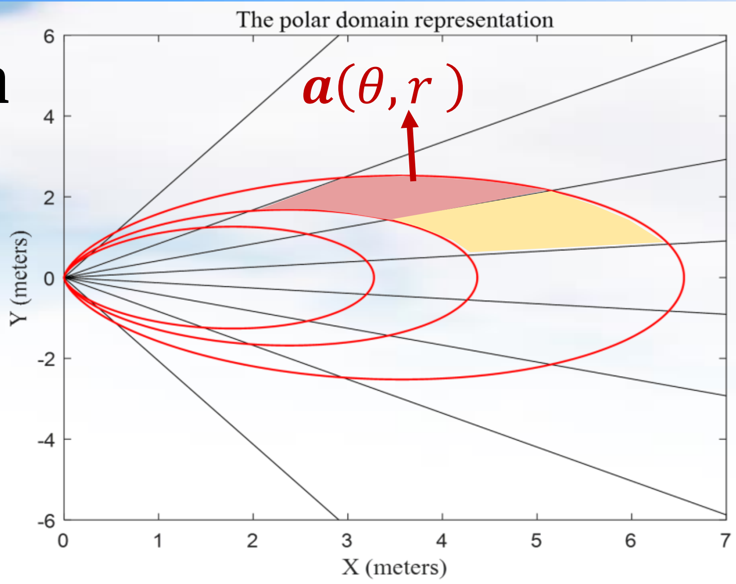

Far-Field Beam Split Effect

- **Beam split effect induced in wideband ELAA systems**
  - **For narrowband, beamforming is generally designed according to the central carrier f_c**
  - **In wideband systems, the beams at different frequencies will split towards different angles, where $f_c \sin\theta_0 = f \sin\theta$**

Prism

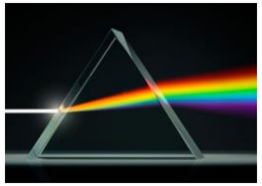

dispersion of light

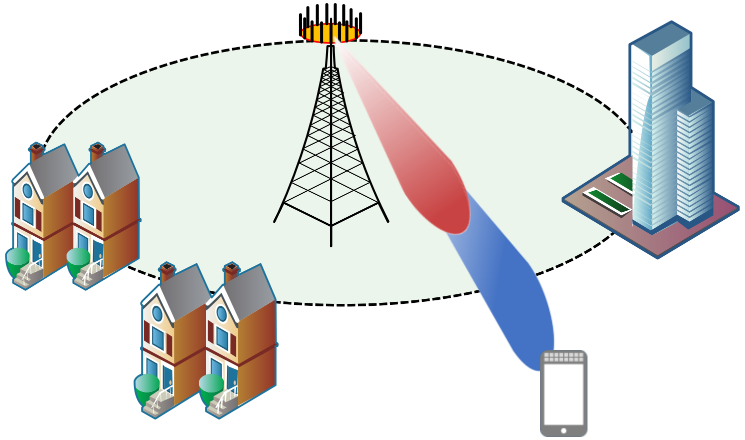

Beam squint[1] → Beam split[2]

System parameters	Beam width	Beam split	Relative split
Carrier 30 GHz, bandwidth 2 GHz, Antenna array 16×16	11.25°	3°	26%
Carrier 30 GHz, bandwidth 2 GHz, Antenna array 60×60	3°	3°	100%
Carrier 100 GHz, bandwidth 20 GHz, antenna array 16×16	11.25°	9°	80%
Carrier 100 GHz, bandwidth 20 GHz, antenna array 60×60	3°	9°	300%

ELAA introduces a severe beam split effect in far field

[1] X. Gao, L. Dai, S. Zhou, A. Sayeed, and L. Hanzo, "Beamspace channel estimation for wideband millimeter-wave MIMO with lens antenna array," in *Proc. IEEE Int. Conf. Commun. (IEEE ICC'18)*, Kansas, US, May 2018. (**IEEE ICC 2018 Best Paper Award**)

[2] L. Dai, J. Tan, Z. Chen, and H. Vincent Poor, "Delay-phase precoding for wideband THz massive MIMO," *IEEE Trans. Wireless Commun.* vol. 21, no. 9, pp. 7271-7286, Sep. 2022.

Near-Field Beam Split Effect

- **In the near-field region, the near-field beam split effect induces the beams at different frequencies will split towards different locations**

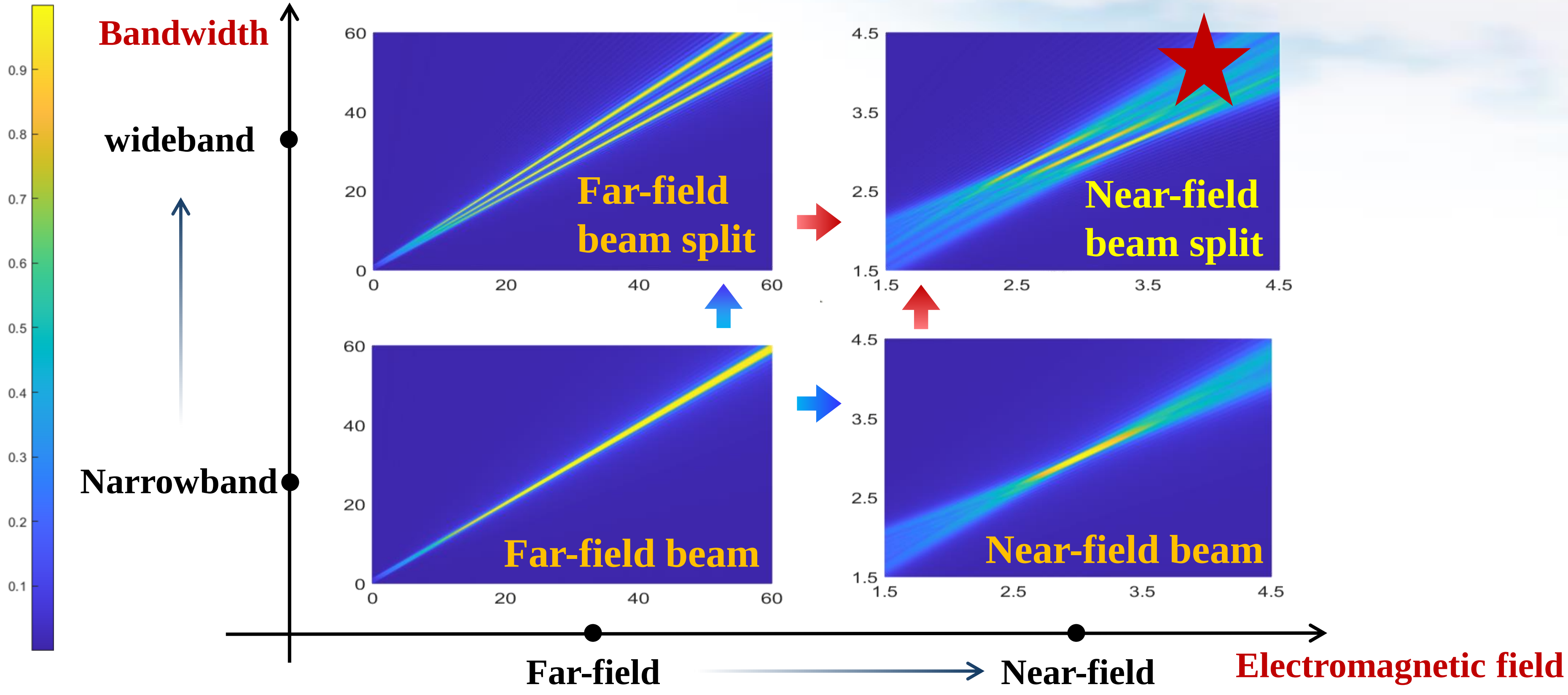

The near-field beam split effect has not been well studied

Challenge in Near-field Wideband Systems

- **Existing transmission technologies suffer from a severe performance loss in near-field wideband systems due to the near-field beam split effect**

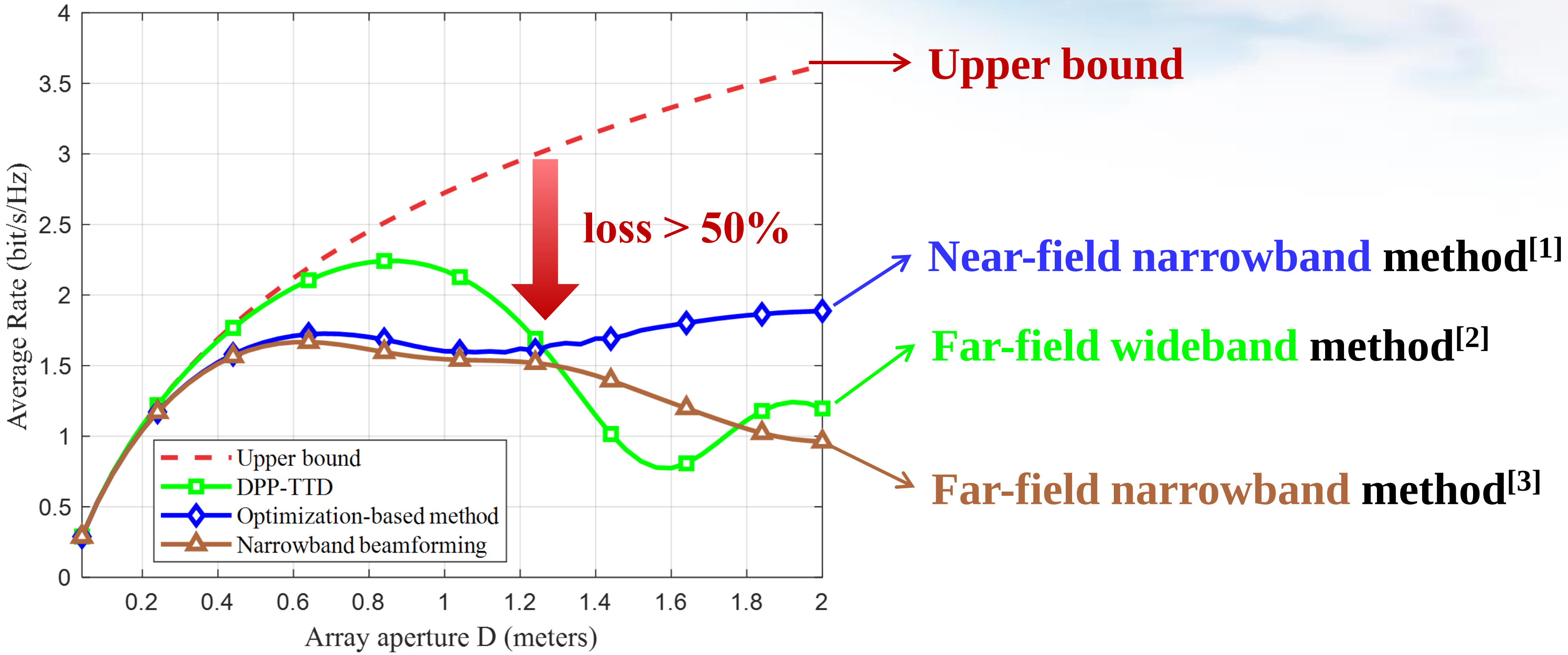

[1] N. J. Myers and R. W. Heath, "InFocus: A spatial coding technique to mitigate misfocus in near-field LoS beamforming," *IEEE Trans. Wireless Commun.*, vol. 21, no. 4, pp. 2193-2209, Apr, 2022.
[2] X. Yu, J. Shen, J. Zhang, and K. B. Letaief, "Alternating minimization algorithms for hybrid precoding in millimeter wave MIMO systems," *IEEE J. Sel. Topics Signal Process.*, vol. 10, no. 3, pp. 485-500, Mar. 2016.
[3] L. Dai, J. Tan, Z. Chen, and H. Vincent Poor, "Delay-phase precoding for wideband THz massive MIMO," *IEEE Trans. Wireless Commun.* vol. 21, no. 9, pp. 7271-7286, Sep. 2022.

Phase-Delay Focusing (PDF)

- **The partitioned-far-field approximation of the near-field channel**
  - **The entire large array is partitioned into Q small sub-arrays**

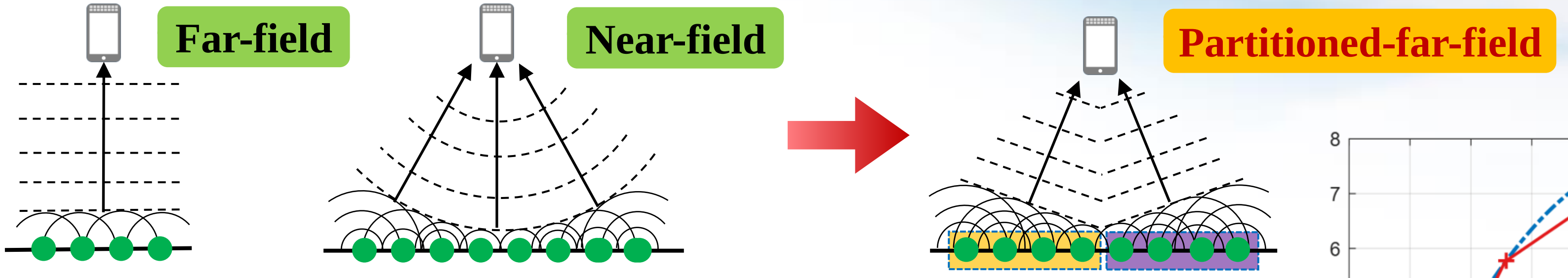

  - **The user is located in the far-field region of each small subarray**
    - **For the p-th antenna of the q-th subarray**

Distance: $r_q^{(p)} \approx r_q + pd\theta_q$

Phase: $\phi_q^{(p)} = \frac{2\pi}{\lambda} r_q^{(p)} = \boxed{\frac{2\pi}{\lambda} r_q} + \boxed{\frac{2\pi}{\lambda} pd\theta_q}$

Subarray-wise near-field phase | **Antenna-wise far-field phase**

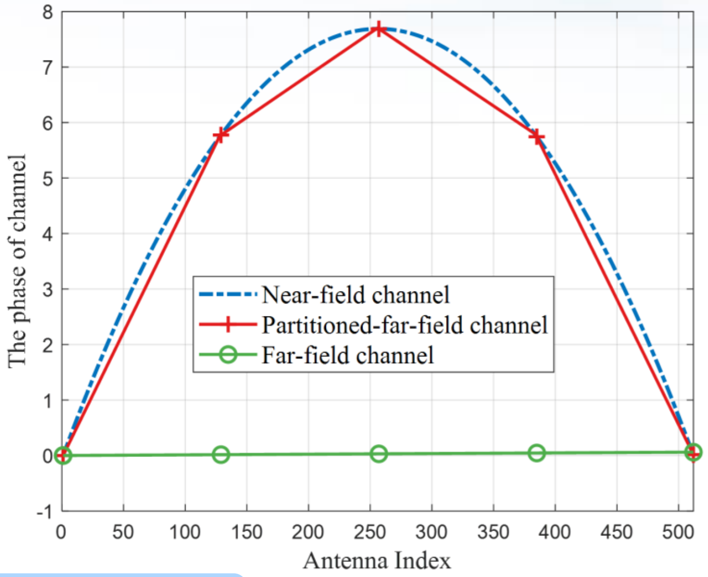

The complicated near-field channel is decoupled to multiple far-field channels across different subarrays

Phase-Delay Focusing (PDF)

- A very large phase-shift network to compensate the antenna-wise phase
- A small time-delay layer to compensate the subarray-wise phase

$$\phi_q^{(p)} = \boxed{\frac{2\pi}{\lambda} r_q} + \boxed{\frac{2\pi}{\lambda} p d \theta_q}$$

Subarray-wise phase variation → Compensated by **time-delay**

Antenna-wise phase variation → Compensated by **phase-shift**

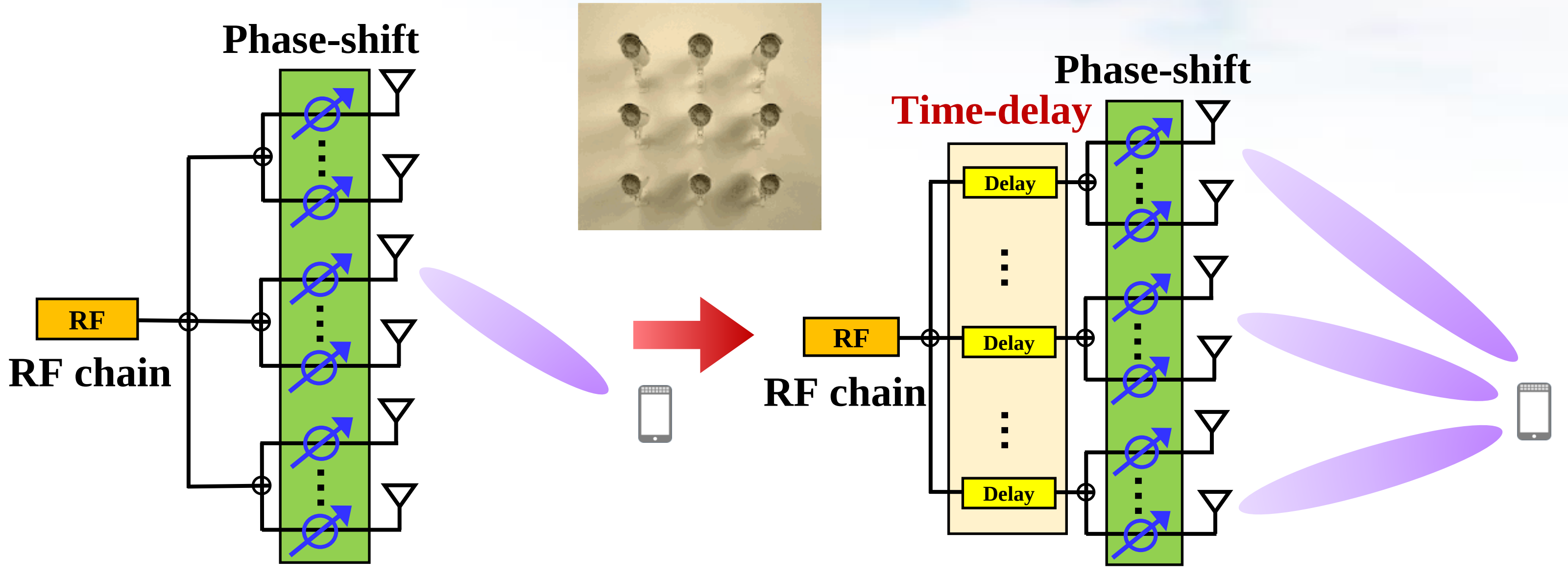

(a) Beamsteering (b) Phase-delay focusing

Overcome the near-field beam split effect with much reduced time-delay elements

Simulation Results (1)

- **Achievable average rate vs. distance**
  - ➢ **Near-optimal average rate is realized**

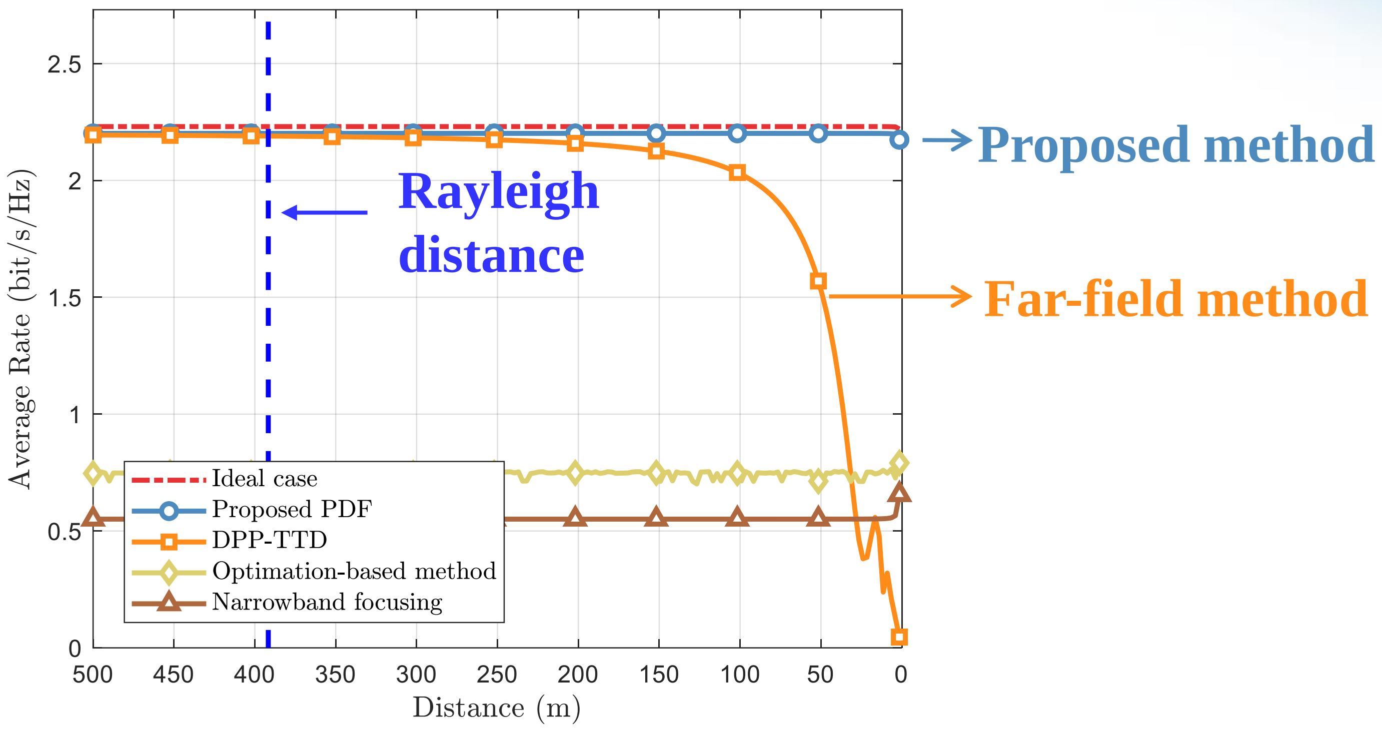

Parameters	Values
Carrier	100 GHz
Bandwidth	5 GHz
Number of subcarriers	1024
Number of antennas	512
Rayleigh distance	400 meters
SNR	20 dB

An unusual discovery: Rayleigh distance overestimates the near-field range

M. Cui and L. Dai, "Near-field wideband beamforming for extremely large antenna array," *IEEE Trans. Wireless Commun.*, 2024.

Outline of Part 4

- **Near-Field Channel State Information Acquisition**
  - Near-field MISO channel estimation
  - Near-field MIMO channel estimation
  - Near-field EM-based channel model
  - Near-field beam training
- **Near-Field Beam Split**
  - Phase-delay beam focusing
  - Near-field rainbow-based beam training
  - Distance-dependent beam split based beam training

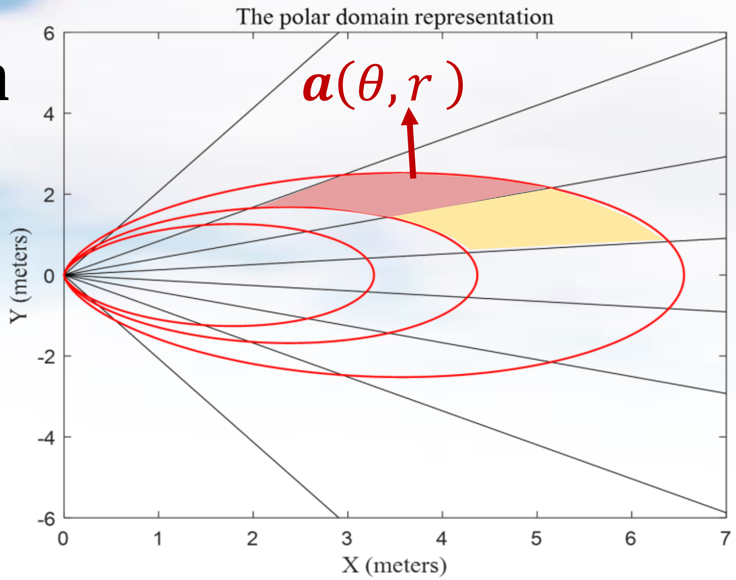

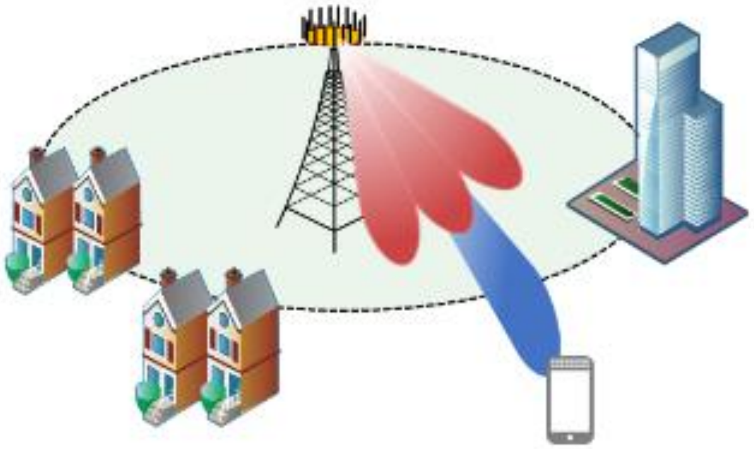

The Challenge of Near-Field Beam Training

- **Beam training is an essential method is acquire the channel state information (CSI)**
- **However, since the near-field codebook requires extra grids on the distance domain, its codebook size is much larger than that of the far-field codebook**

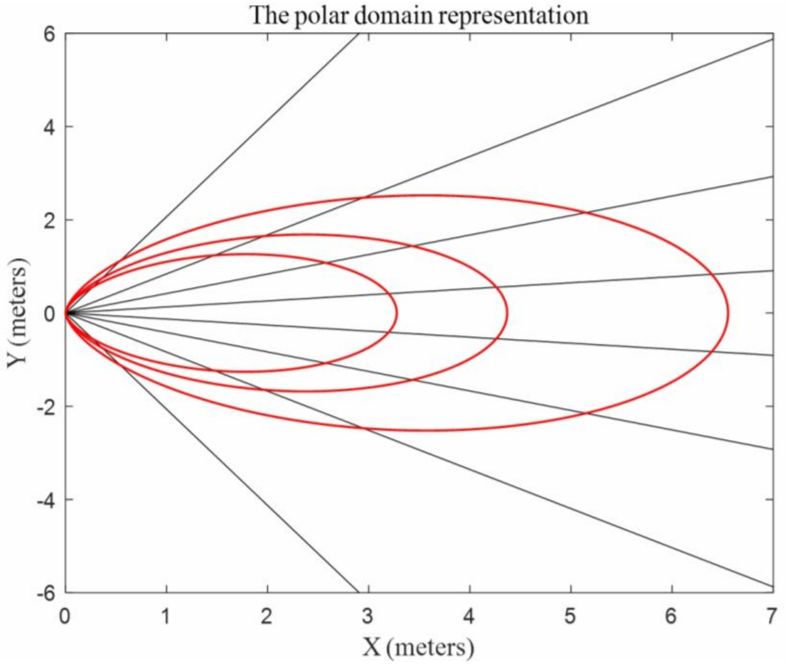

Exhaustive search

Parameters	Far-field codebook	Near-field codebook
Number of antennas	512	512
Carriers	100 GHz	100 GHz
Number of angle grids	512	512
Number of distance grids	1	20
Codebook size	512	10240

The overhead of near-field exhaustive beam training is unaffordable

Near-field Rainbow based Beam Training

- **Time-delay circuits are able to control the degree of the near-field beam split effect**
  - **The optimal distance is searched in a time division manner**
  - **The optimal angle is searched in a frequency division manner**

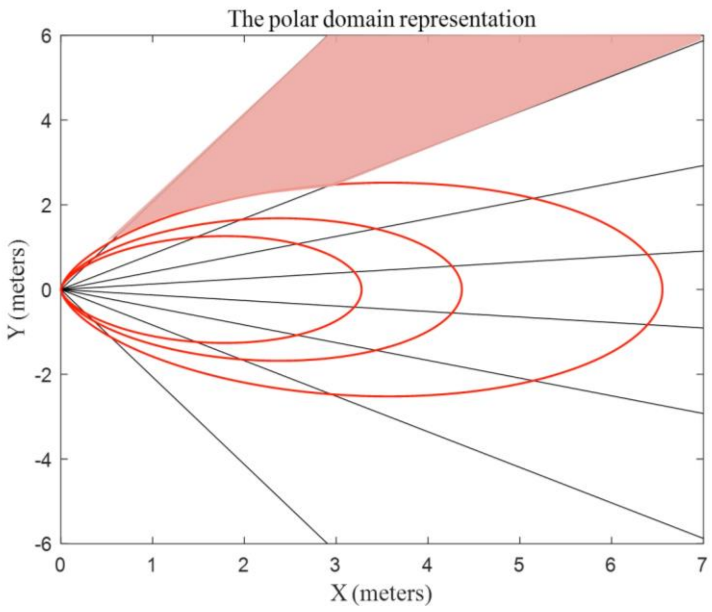

Exhaustive search

Prism

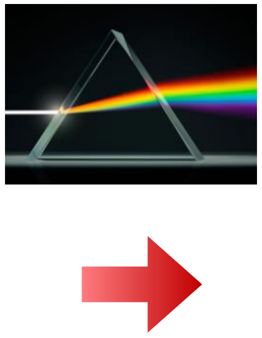

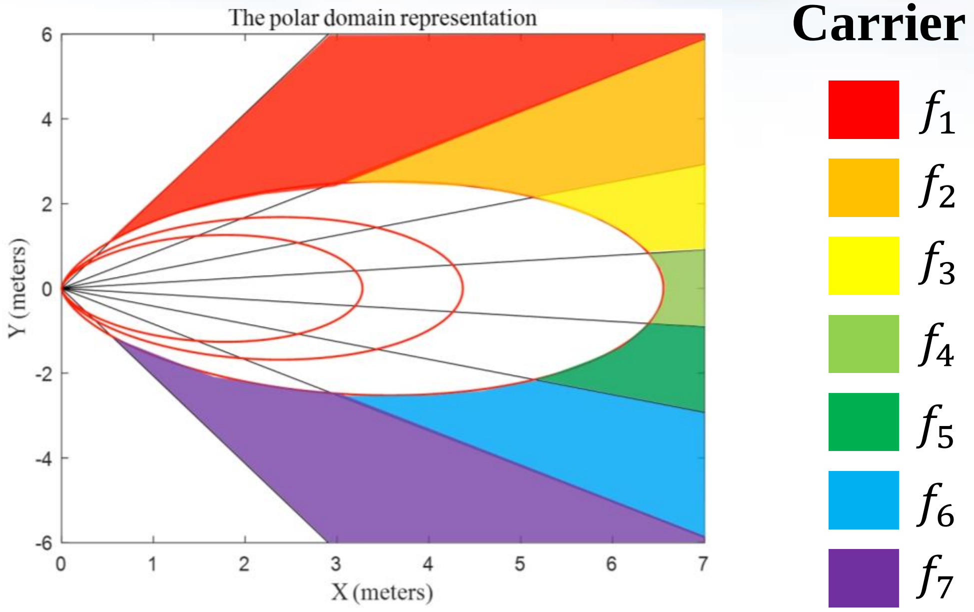

Near-field rainbow based search

The pilot overhead is determined by the search of distance

Simulation Results

- **The proposed scheme is able to achieve the near-optimal average rate performance with a very low training overhead**

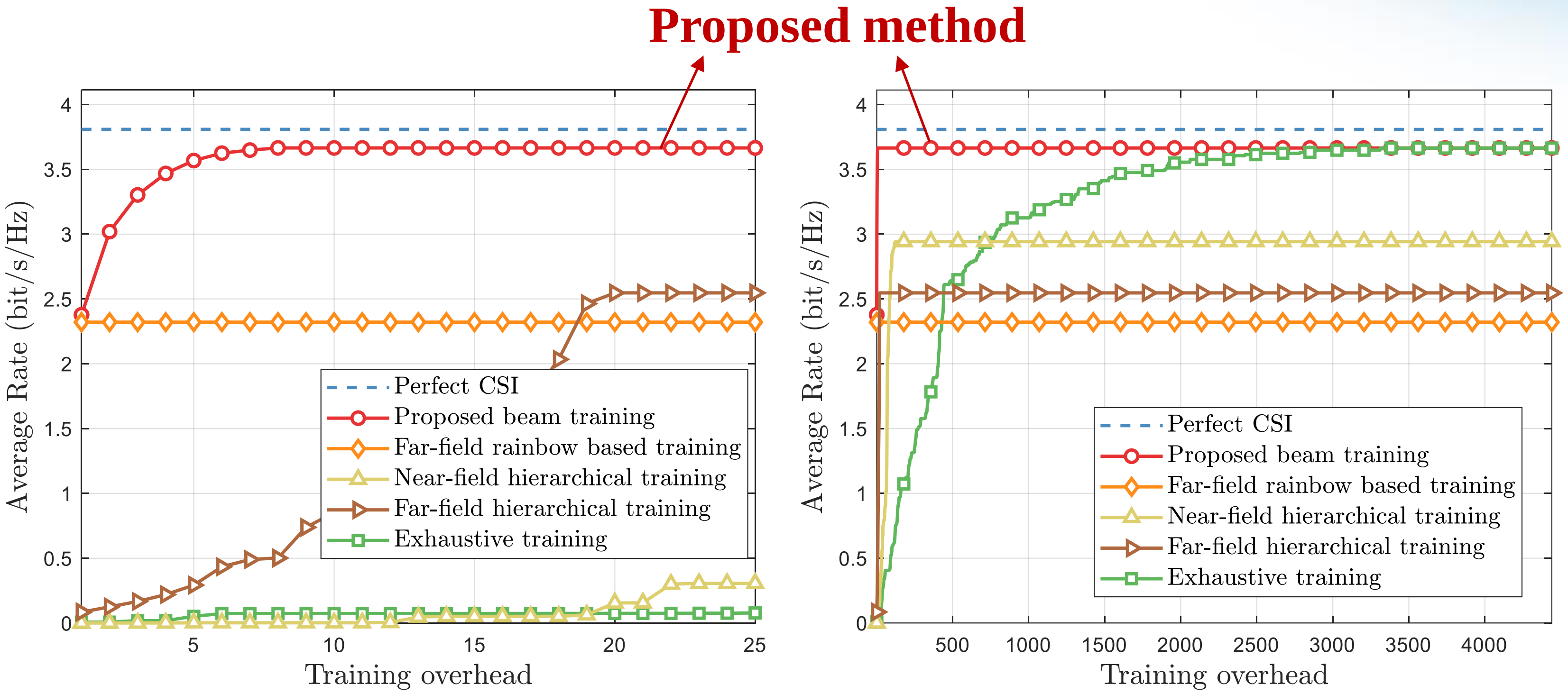

Parameter	Value
Carrier	60 GHz
Bandwidth	3 GHz
Subcarrier number	4096
Antenna number	256
SNR	20 dB
Distance	$U(3\ \text{m},\ 40\ \text{m})$
Angle	$U(-\sin\frac{\pi}{3}, \sin\frac{\pi}{3})$

M. Cui, L. Dai, Z. Wang, S. Zhou, and N. Ge, "Near-field rainbow: Wideband beam training for XL-MIMO," *IEEE Trans. Wireless Commun.*, vol. 22, no. 6, pp. 3899-3912, Jun. 2023.

Outline of Part 4

- **Near-Field Channel State Information Acquisition**
  - Near-field MISO channel estimation
  - Near-field MIMO channel estimation
  - Near-field EM-based channel model
  - Near-field beam training
- **Near-Field Beam Split**
  - Phase-delay beam focusing
  - Near-field rainbow-based beam training
  - Distance-dependent beam split based beam training

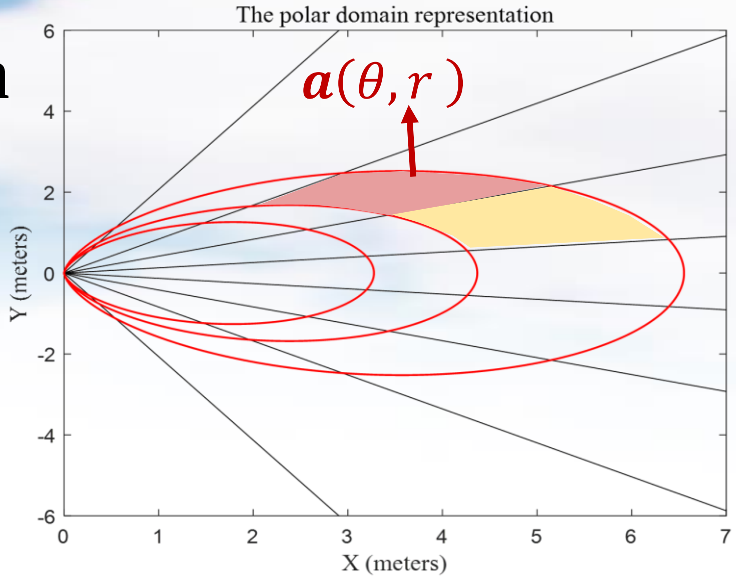

Limitations of Near-Field Rainbow

- **Beam split in near-field rainbow is essentially distance-independent beam split, which only involves beam split in angle domain**
- **The optimal distance is obtained by sequentially testing different distance rings**

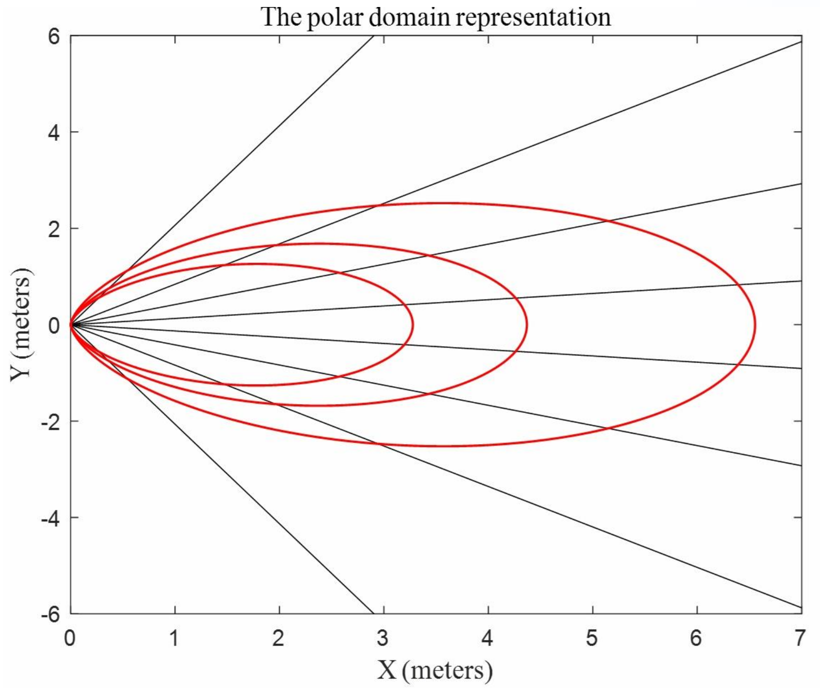

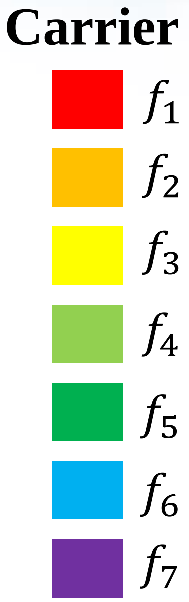

Can we design distance-dependent beam split to simultaneously search angles and distances

Distance-Dependent Beam Split Based Beam Training

- **Spread the focused points of beams on different angles of multi-distance-rings**
  - ➢ **The focused direction of the multi-frequency beams fluctuate periodically between the angular range while the focused distance ring increases monotonically with the frequency**
  - ➢ **Both different angles and distances can be search with a single pilot simultaneously in one time slot**

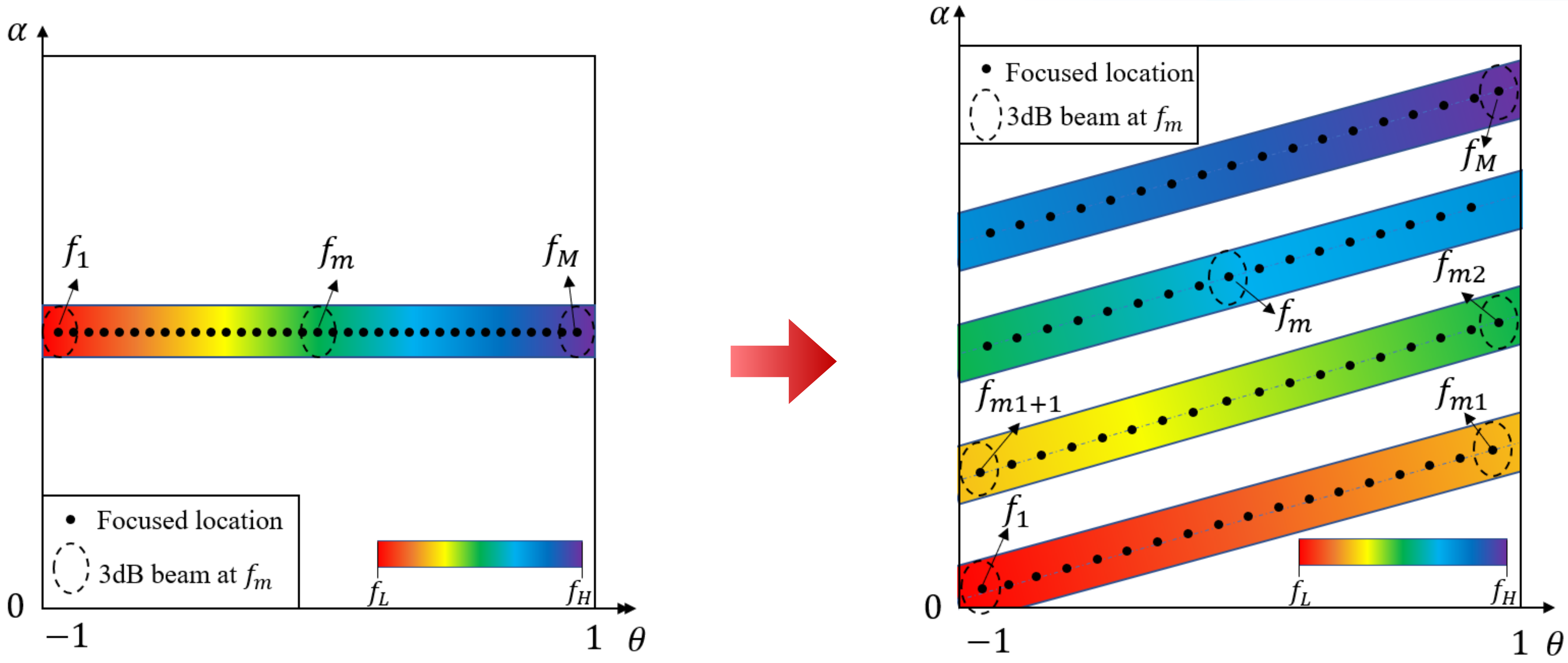

T. Zheng and L. Dai, "Near-field beam training based on distance-dependent beam split for XL-MIMO," submitted to *IEEE Trans. Wireless Commun.*, 2024.

Simulation Results

- The proposed scheme can achieve the near-optimal average rate performance with **extremely low training overhead (only 3 pilots)**

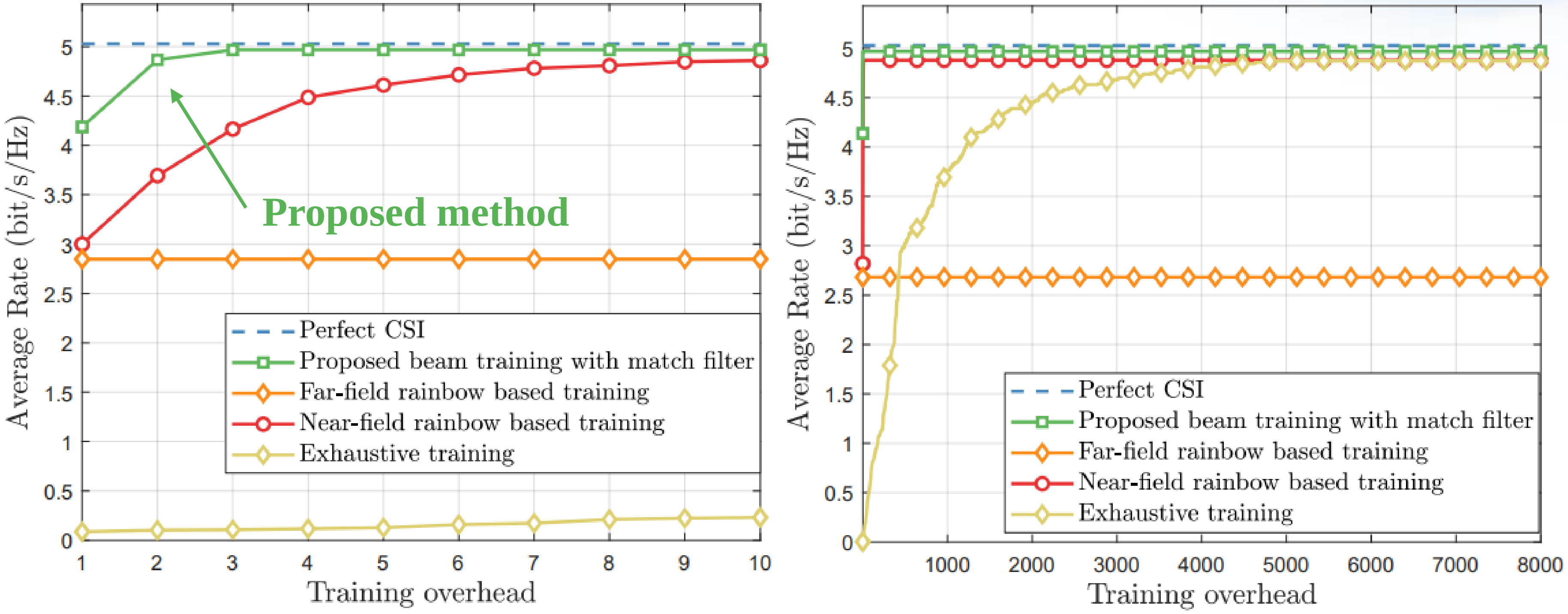

Parameter	Value
Carrier	30 GHz
Bandwidth	3 GHz
Subcarrier number	1024
Antenna number	256
Distance	[5m,200m]
Angle	$U(-\sin\frac{\pi}{3}, \sin\frac{\pi}{3})$
SNR	15 dB

T. Zheng and L. Dai, "Near-field beam training based on distance-dependent beam split for XL-MIMO," submitted to *IEEE Trans. Wireless Commun.*, 2024.

Part 5: Future Research Directions

1. Electromagnetic Information Theory (EIT)

- **Generalized near-field capacity analysis based on EIT**
  - **Existing near-field analysis on the DoFs assumes the uniform parallel array or LoS scenarios**
  - **DoFs analysis for generalized scenarios, such as RIS, cell-free, or NLoS scenarios, is required**

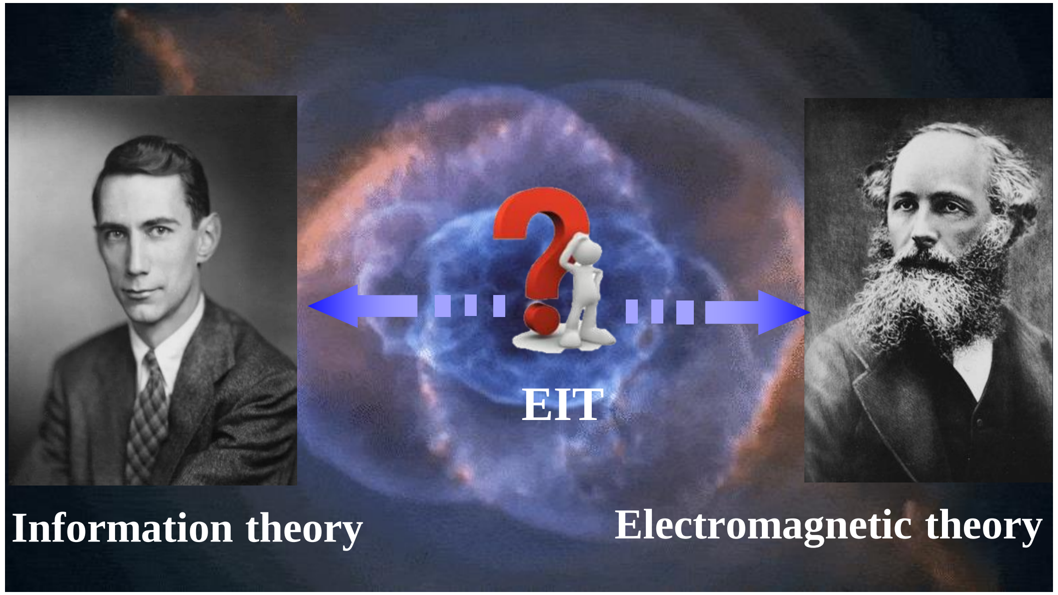

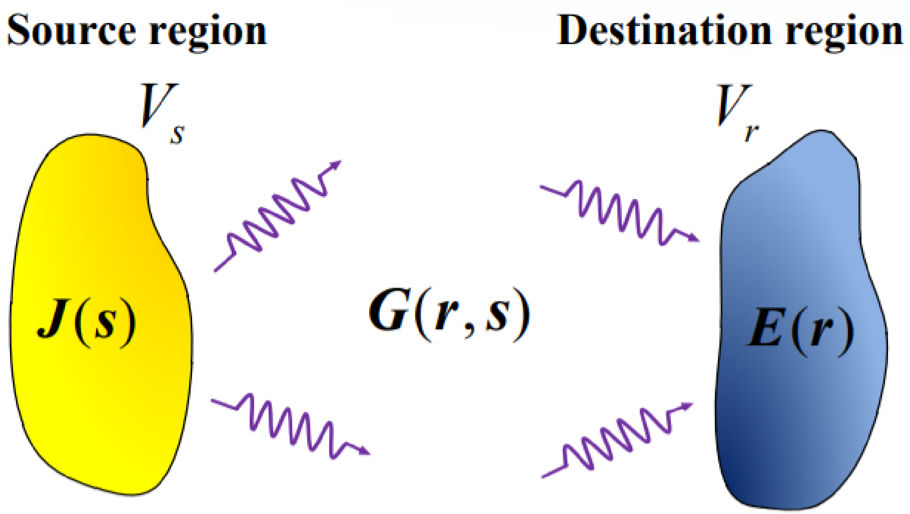

J. Zhu, Z. Wan, L. Dai, M. Debbah, and H. V. Poor, "Electromagnetic information theory: Fundamentals, modeling, applications, and open problems," *IEEE Wireless Commun.*, 2024.

2. Near-Field Chanel Modeling

- **Near-field channel modeling faces high complexity issues**
- **The problem of spatial non-stationary can affect near-field channel modeling**

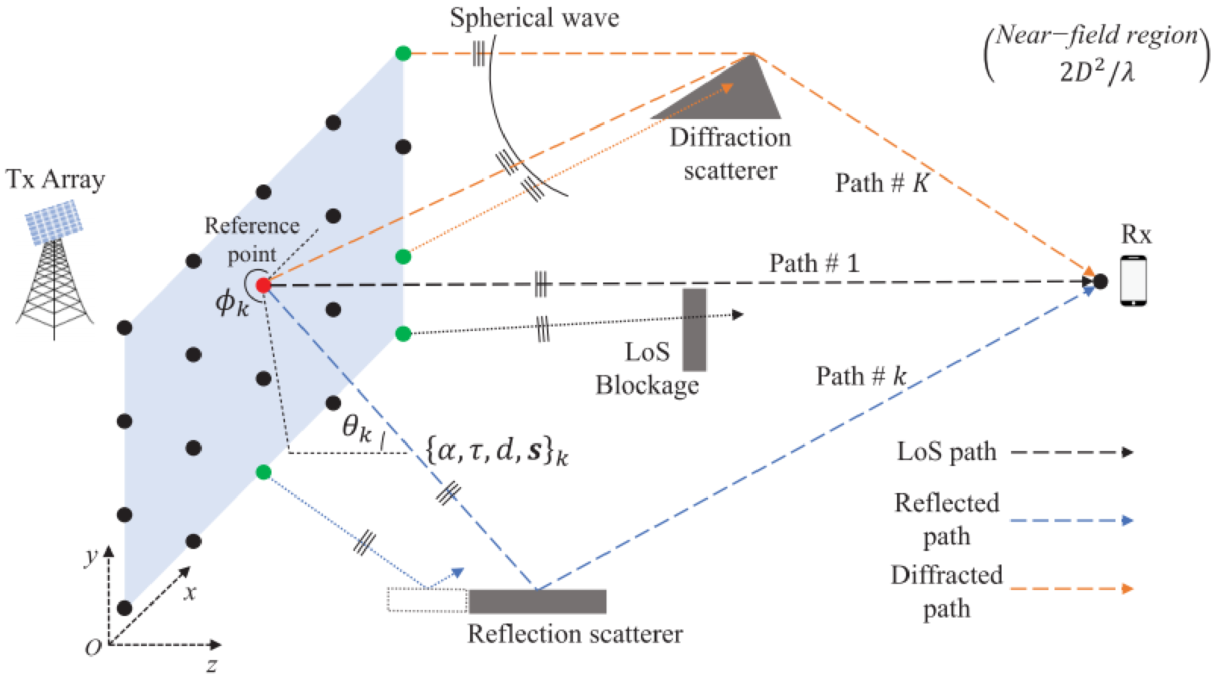

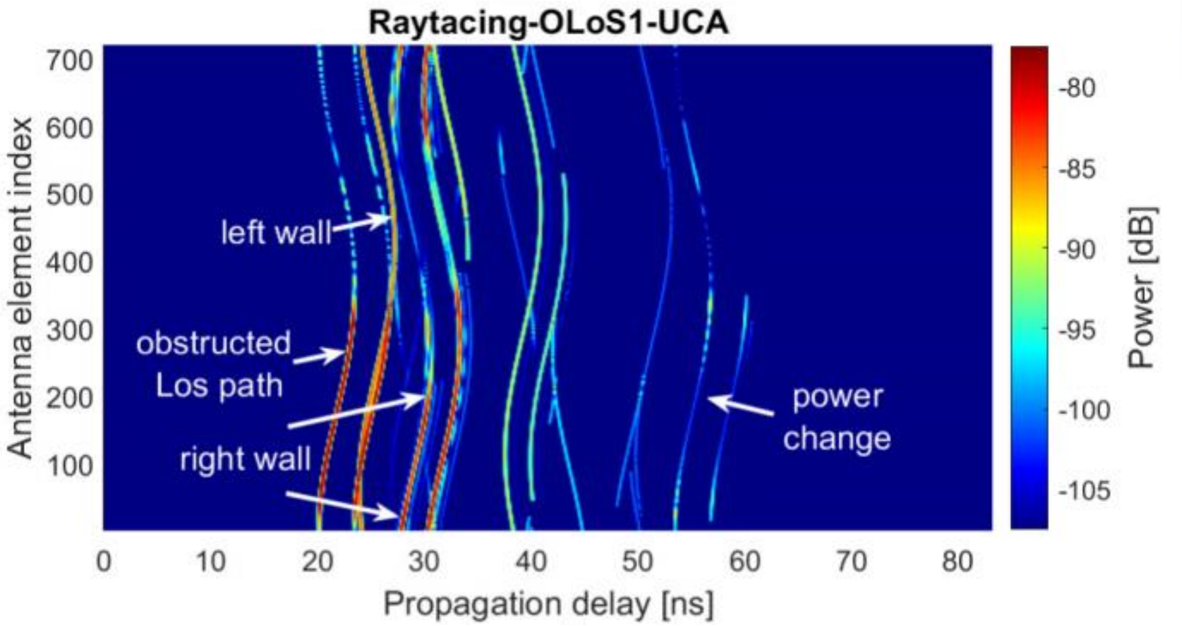

Z. Yuan, J. Zhang, Y. Ji, G. F. Pedersen and W. Fan, “Spatial non-stationary near-field channel modeling and validation for Massive MIMO systems,” *IEEE Trans. Antennas Propag.*, vol. 71, no. 1, pp. 921-933, Jan. 2023.

3. Near-Field Curved Beams

- **Realize THz near-field curved beams curving around obstacles**
- **New possibilities of wave front manipulation for mmWave/THz communications**

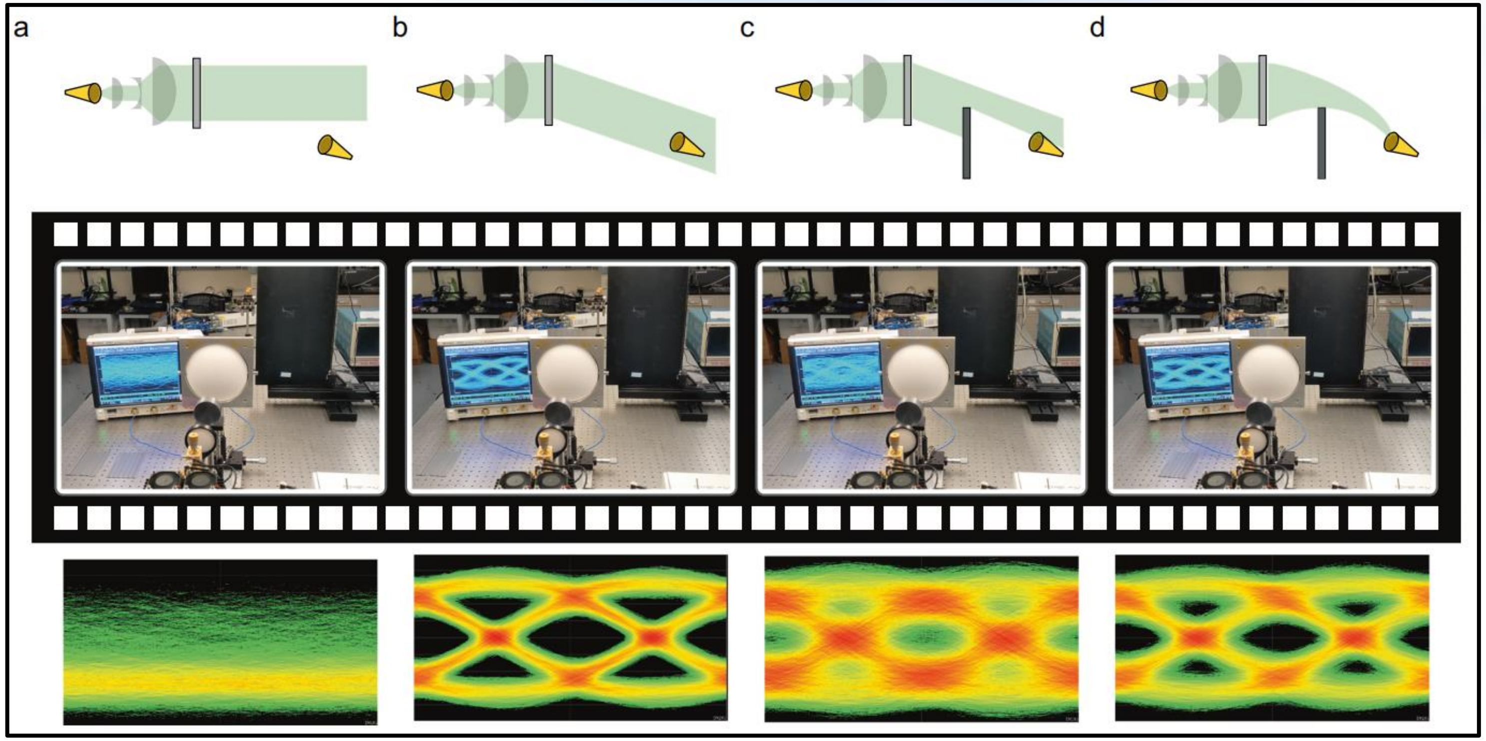

H. Guerboukha, B. Zhao, Z. Fang, Z. Fang, E. Knightly, and D. M. Mittleman, "Curving THz wireless data links around obstacles," *Commun. Eng.*, vol. 3, no. 1, pp. 1-8, Mar. 2024.

4. Near-Field Cell-Free MIMO

- **Cell-free MIMO with multiple BSs has larger virtual ELAA than cellular system**
  - **The near-field range will become larger in a cell-free MIMO systems**
  - **The near-field effect can improve the capacity of cell-free MIMO system**

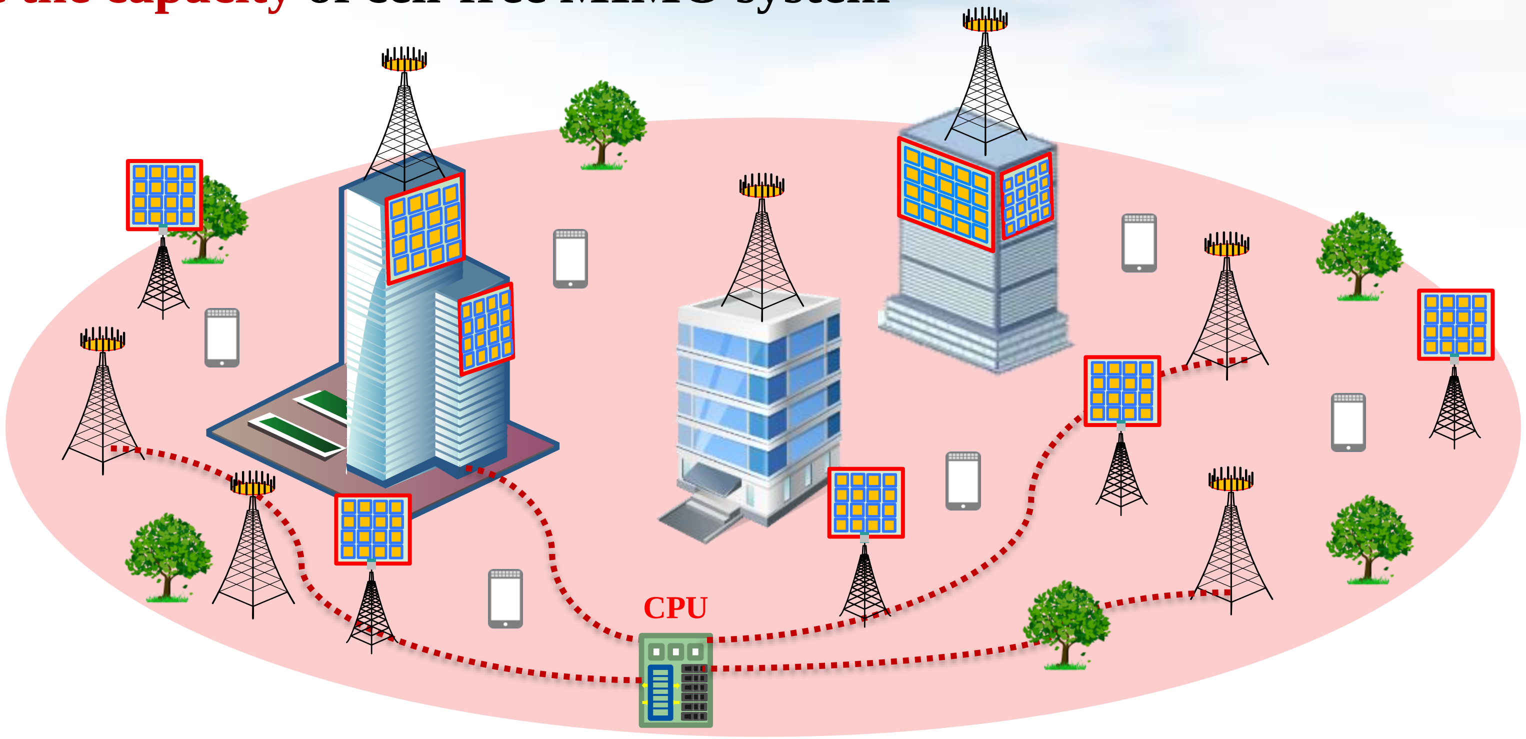

Q. Li, M. El-Hajjar, Y. Sun, and L. Hanzo, "Performance analysis of reconfigurable holographic surfaces in the near-field scenario of cell-free networks under hardware impairments," *IEEE Trans. Wireless Commun.*, early access, Apr. 2024.

5. RIS-Aided Near-Field Communications

- **Compared with MIMO, near-field becomes more dominant in RIS-aided systems**

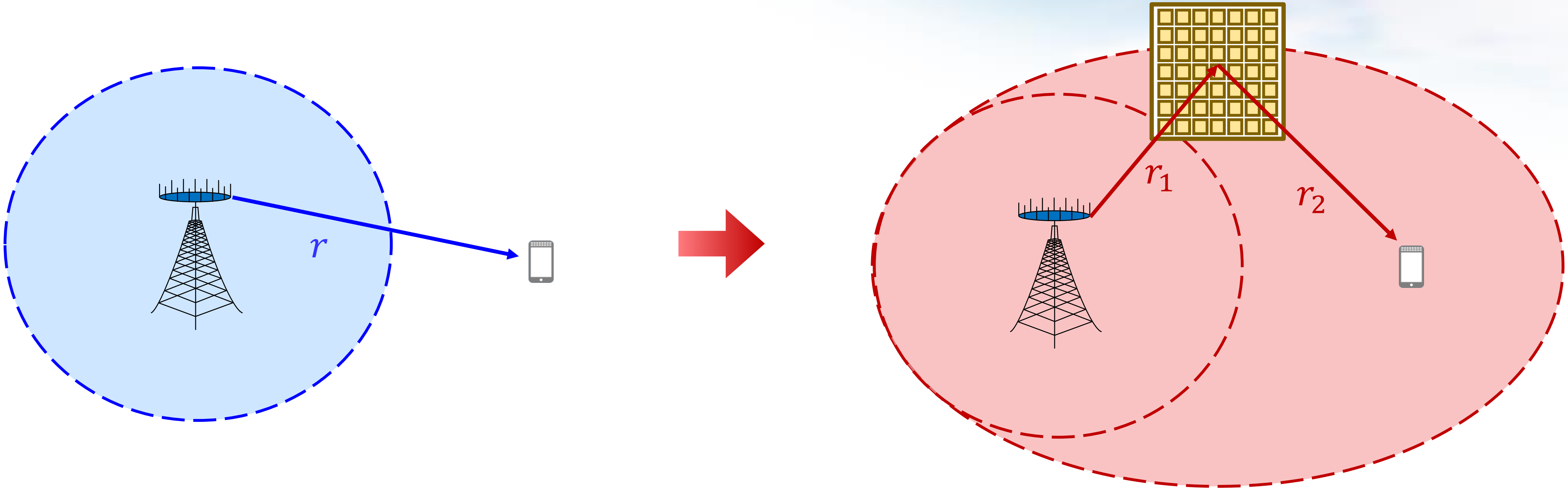

Near-field range for MIMO: $r < \frac{2D^2}{\lambda}$

Near-field range for RIS: $\frac{r_1 r_2}{r_1 + r_2} < \frac{2D^2}{\lambda}$

X. Wei, L. Dai, Y. Zhao, G. Yu, and X. Duan, "Codebook design and beam training for extremely large-scale RIS: Far-field or near-field?," *China Commun.*, vol. 19, no. 6, pp. 193-204, Jun. 2022. (**Invited Paper**)

6. AI-Aided Near-Field Transmission Techniques

- **The near-field channel model are much more complex**
  - **Non-linear channel phase in near-field compared to the linear channel phase in far-field**
  - **Much larger codebook size than the far-field codebook**

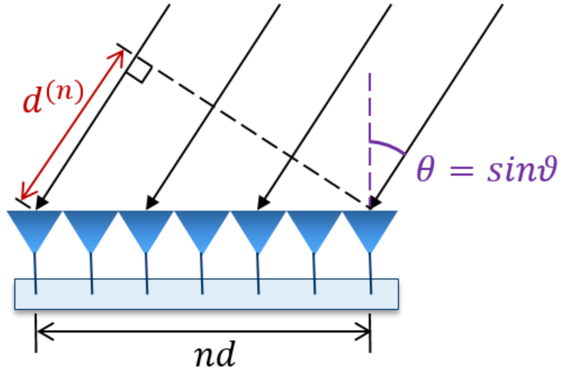

Far-field linear phase

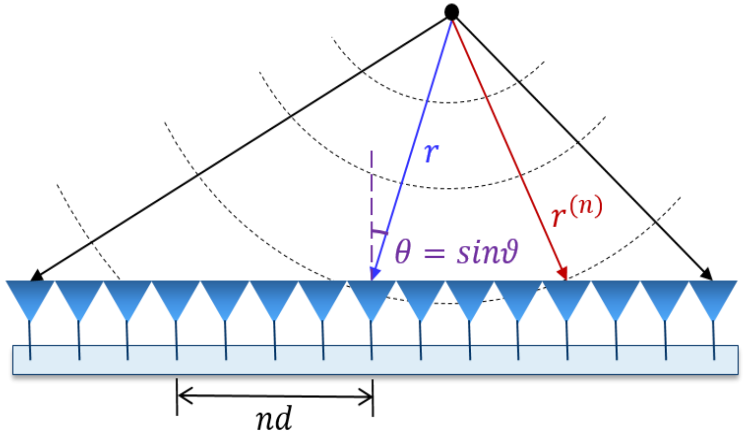

Near-field non-linear phase

Codebook size @ 100 GHz

Parameters	Far-field codebook	Near-field codebook
Number of antennas	512	512
Number of distance grids	1	20
Codebook size	512	10240

AI is promising to address this problem through non-linear neural networks

[1] X. Wei, C. Hu, and L. Dai, "Deep learning for beamspace channel estimation in millimeter-wave massive MIMO systems," *IEEE Trans. Commun.*, vol. 69, no. 1, pp. 182-193, Jan. 2021.
[2] Y. Chen, L. Yan, and C. Han, "Hybrid spherical- and planar-wave modeling and DCNN-powered estimation of Terahertz ultra-massive MIMO channels," *IEEE Trans. Commun.*, vol. 69, no. 10, pp. 7063-7076, Oct. 2021.

7. Near-Field Localization

- **Enhanced localization accuracy exploiting the distance-aware channels**
  - **The curvature of arrival (CoA) can be used to infer the source position**

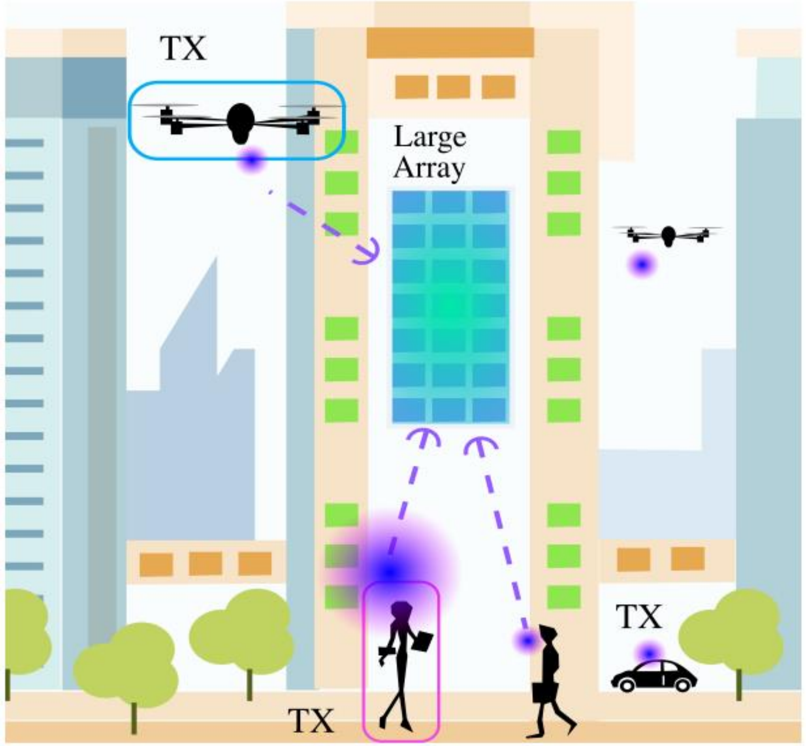

Localization scenario with ELAA

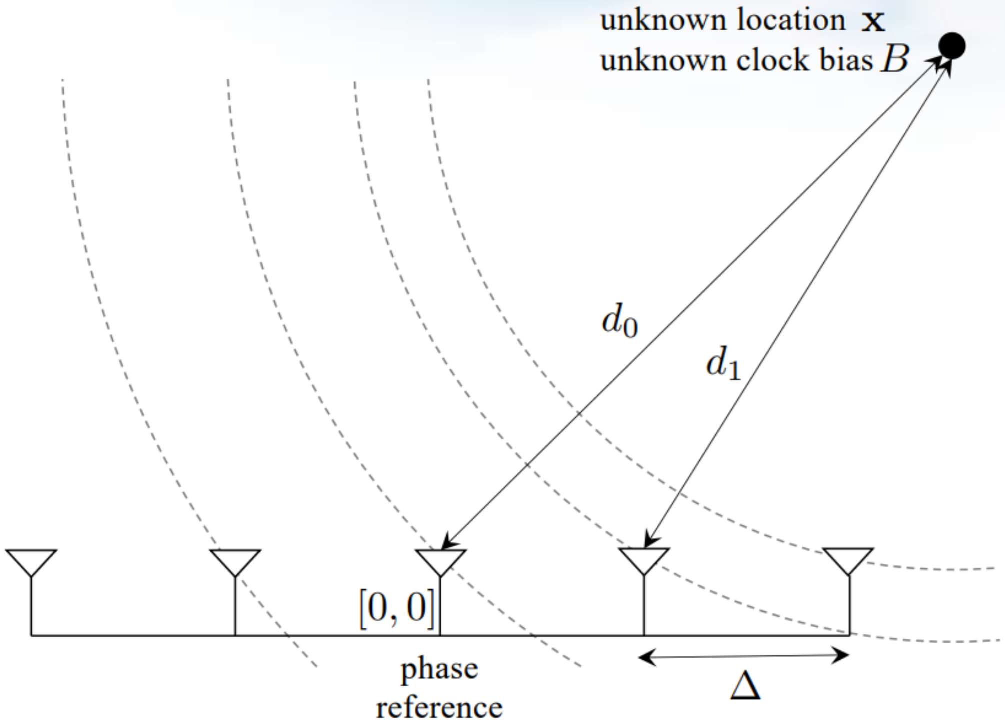

The curvature of spherical wavefront

A. Guerra, F. Guidi, D. Dardari, and P. M. Djurić, "Near-field tracking with large antenna arrays: Fundamental limits and practical algorithms," *IEEE Trans. Signal Process.*, vol. 69, pp. 5723-5738, 2021.

8. Near-Field ISAC

- Near-field spherical wave holds the **extra resolution** in the **distance** domain
- Near-field propagation can potentially provide **higher** localization and tracking accuracy for ISAC

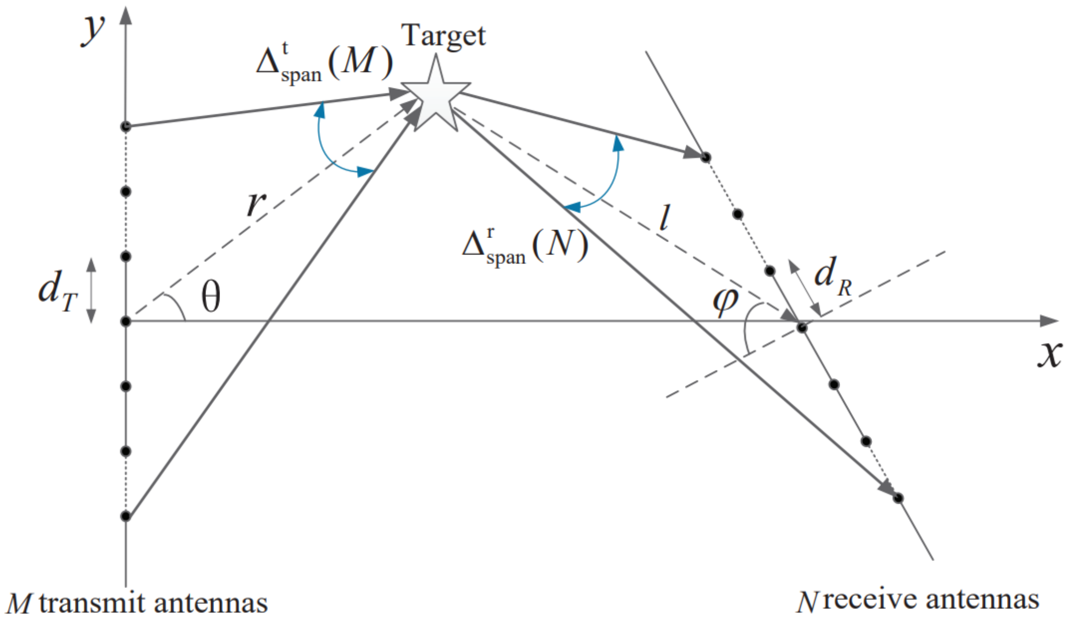

Radar sensing with extremely large-scale MIMO

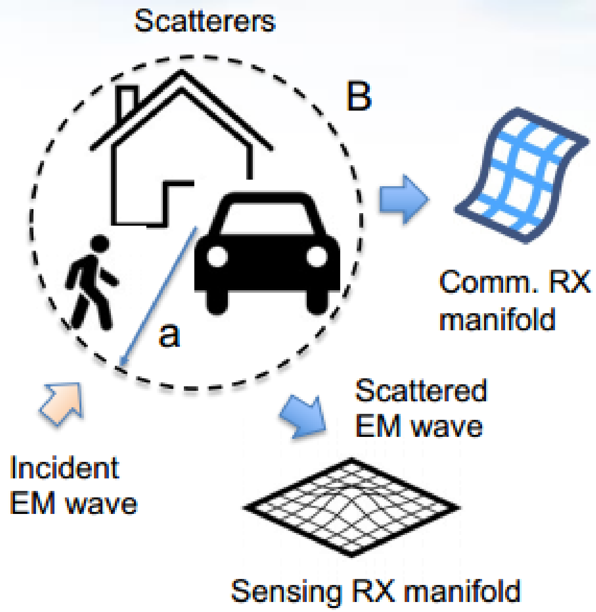

[1] A. M. Elbir, K. V. Mishra, S. Chatzinotas, and M. Bennis, "Terahertz-band integrated sensing and communications: Challenges and opportunities," *arXiv preprint arXiv:2208.01235*, Aug. 2022.
[2] H. Wang and Y. Zeng, "SNR scaling laws for radio sensing with extremely large-scale MIMO," in *Proc. 2022 IEEE International Conference on Communications Workshops (ICC Workshops)*, 2022, pp. 121-126.

9. Near-Field Holographic Imaging

- **Near-field holographic imaging with large-scale MIMO antennas**
  - **Near-field propagation would increase the number of exploitable degrees of freedom (DoF)**
  - **More informative measurements can be collected, thus leading to improved imaging capabilities**

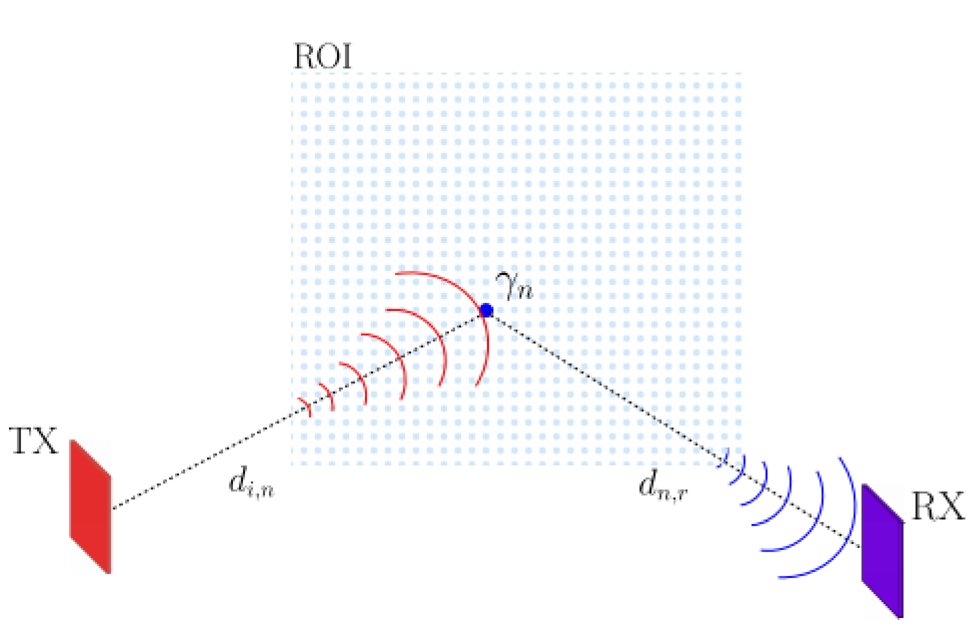

(a) LOS holographic imaging

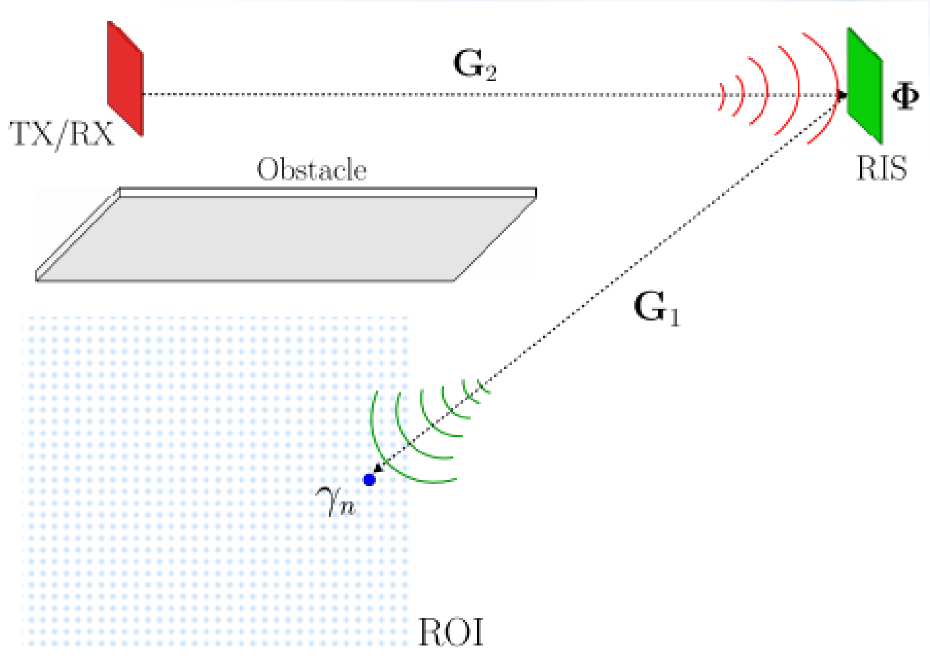

(b) NLOS holographic imaging

G. Torcolacci, A. Guerra, H. Zhang, F. Guidi, Q. Yang, Y. C. Eldar, and D. Dardari, "Holographic imaging with XL-MIMO and RIS: Illumination and reflection design," *IEEE JSTSP*, 2024.

10. Hybrid Far- and Near-Field Communications

- **Hybrid far- and near-field communications will be more practical**
  - **The environment coexists both far-field and near-field scatters**
  - **Channel modeling, channel estimation, hybrid precoding, localization, and so on**

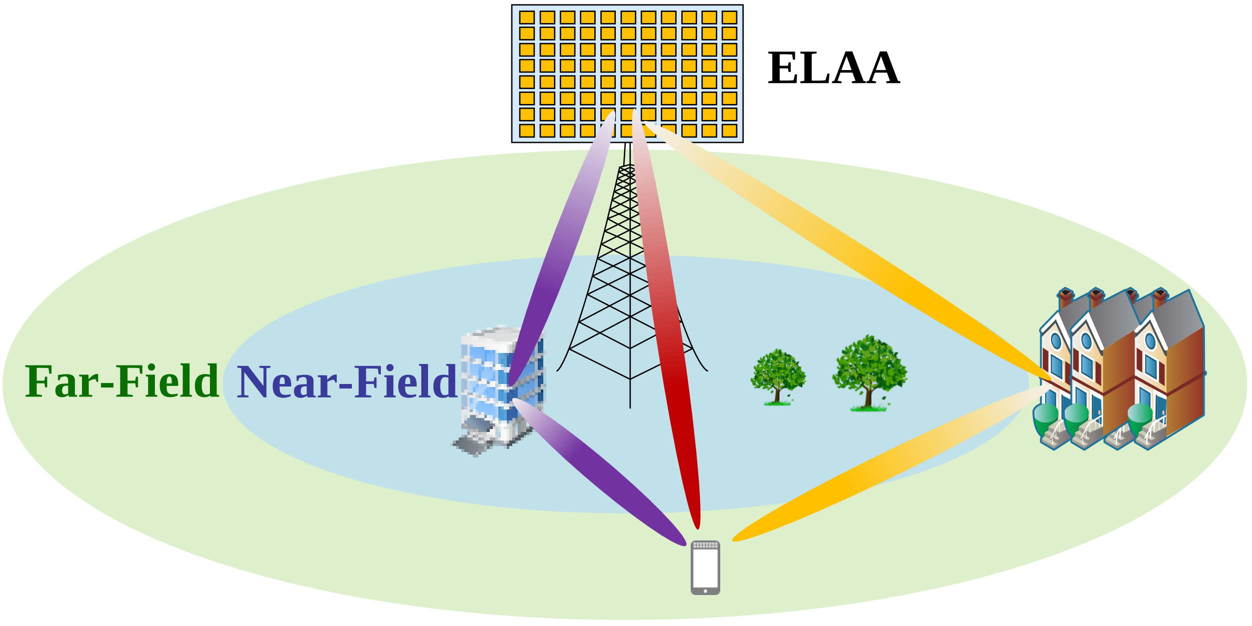

Hybrid-field communications[1]

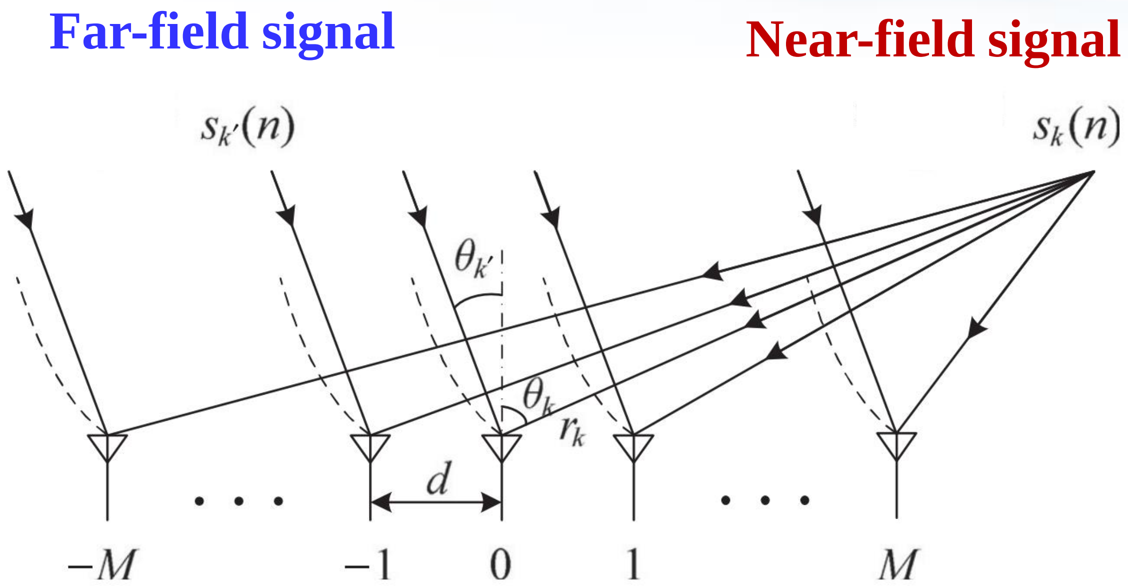

Hybrid-field localization[2]

[1] X. Wei and L. Dai, "Channel estimation for extremely large-scale massive MIMO: Far-field, near-field, or hybrid-field?," *IEEE Commun. Lett.*, vol. 26, no. 1, pp. 177-181, Jan. 2022.
[2] W. Zuo, J. Xin, N. Zheng, and A. Sano, "Subspace-based localization of far-field and near-field signals without eigendecomposition," *IEEE Trans. Signal Process.*, vol. 66, no. 17, pp. 4461-4476, Sep. 2018.

11. Hardware Verification

- **Extremely large antenna array prototypes**
  - **Tsinghua (2022): 2304-element ELAA, carrier 28 GHz, bandwidth 800 MHz, peak data rate 1.68 Gbps**
  - **Qualcomm (WMC 2024): 4096-element ELAA, 13 GHz, Rayleigh distance 95 m**

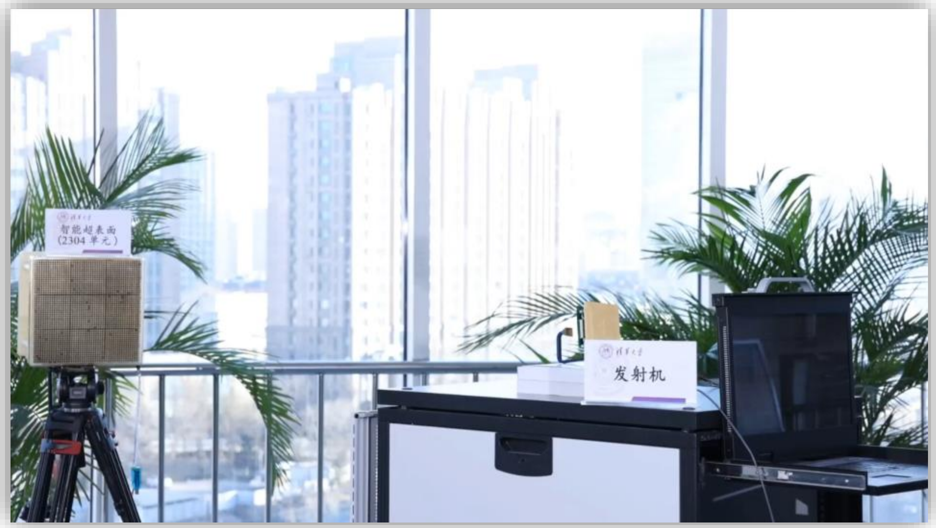

2304-element ELAA

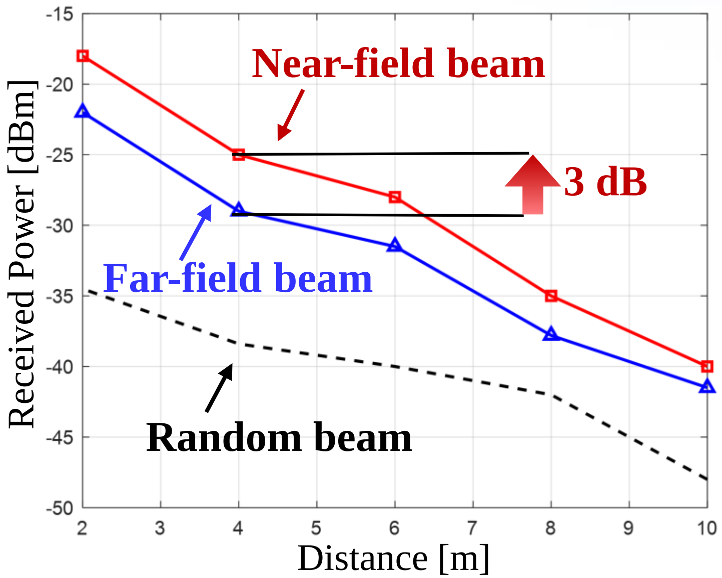

4096-element ELAA

M. Cui, Z. Wu, Y. Chen, S. Xu, F. Yang, and L. Dai, "Demo: Low-power communications based on RIS and AI for 6G," in *Proc. IEEE ICC 2022*, May 2022. (**IEEE ICC 2022 Outstanding Demo Award**)

Conclusions

Conclusions

- **Overview of near-field communications for 6G**
- **Fundamentals**
  - ➢ **Derivation of Rayleigh distance**
  - ➢ **Beamsteering vs. beamfocusing**
- **Potentials**
  - ➢ **Near-field capaticy enhancement**
  - ➢ **Near-field accessibility improvement**
  - ➢ **Near-field power transfer**
  - ➢ **Near-field channel localization**
  - ➢ **...**
- **Challenges**
  - ➢ **Near-field channel estimation**
  - ➢ **Near-field beam split**
- **Future directions**
  - ➢ **EIT, channel modeling, RIS, ISAC, prototypes, …**

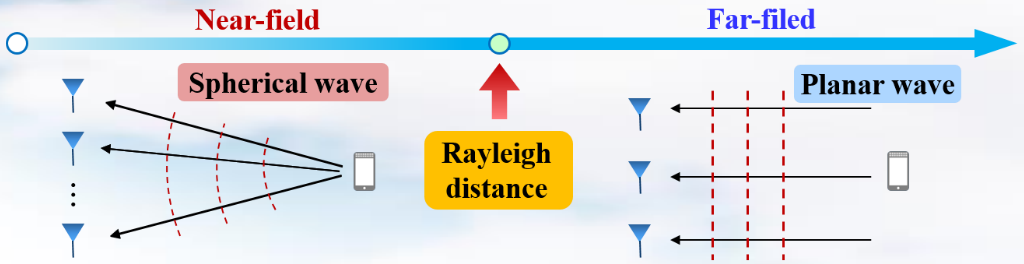

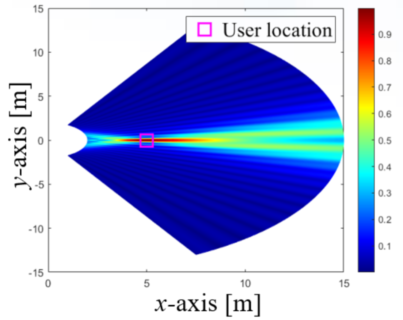

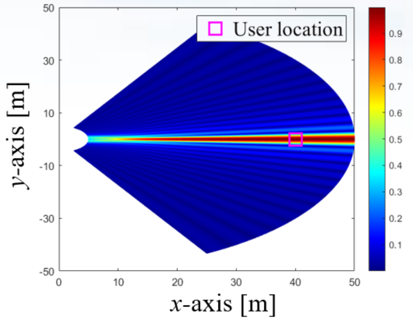

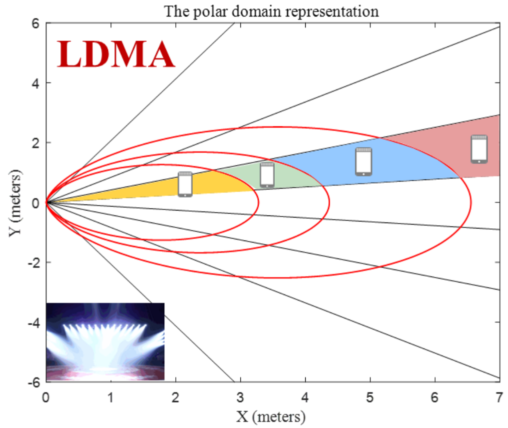

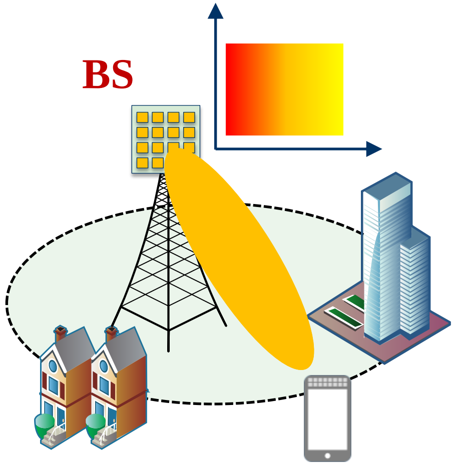

Near-Field Communication: A Double-Edged Sword

- Every coin has two sides
- Near-field communication is a double-edged sword for future 6G

Near-field communications

Potentials

- Near-field communication capacity enhancement
- Near-field sensing accuracy improvement

Challenges

- Near-field channel estimation
- Near-field beam split

Call for Papers: IEEE IoTJ Special Issue

- *IEEE Internet of Things Journal* (**IF: 10.6**) **Special Issue on Positioning and Sensing For Near-Field-Driven Internet-of-Everything**
- **Guest Editors**

Keshav Singh (Lead Guest Editor) National Sun Yat-sen University, Kaohsiung, Taiwan keshav.singh@mail.nsysu.edu.tw	**Cunhua Pan (Lead Guest Editor)** Southeast University, Nanjing, China cpan@seu.edu.cn
Linglong Dai Tsinghua University, Beijing, China daill@tsinghua.edu.cn	**Yuanwei Liu,** Queen Mary University of London, UK yuanwei.liu@qmul.ac.uk
Chongwen Huang Zhejiang University, China chongwenhuang@zju.edu.cn	**Octavia A. Dobre** Memorial University, Canada odobre@mun.ca
Robert Schober Friedrich-Alexander-University Erlangen-Nuremberg, Germany **robert.schober@fau.de**	**Sandeep Kumar Singh** Motilal Nehru National Institute of Technology Allahabad, India sksingh@mnnit.ac.in

- **Important Dates**
  - **Manuscript Submission Deadline: 31 December, 2024**
  - **Expected Publication Date: July, 2025**

IEEE
INTERNET OF THINGS JOURNAL
A JOINT PUBLICATION OF THE IEEE SENSORS COUNCIL
THE IEEE COMMUNICATIONS SOCIETY
THE IEEE COMPUTER SOCIETY
THE IEEE SIGNAL PROCESSING SOCIETY

Call for Papers: IEEE JSAIT Special Issue on EIT

- ***IEEE Journal on Selected Areas in Information Theory Special*** **Issue on Electromagnetic Information Theory (EIT)**
- **Guest Editors**

Prof. Massimo Franceschetti (Lead)
University of California San Diego
USA

Prof. Linglong Dai
Tsinghua University
China

Prof. Marco D. Migliore
University of Cassino
Italy

Prof. Thomas Marzetta
New York University
USA

- **Important Dates**
  - ➢ **Manuscript Submission Deadline: 15 August, 2024**
  - ➢ **Expected Publication Date: April, 2025**

https://www.itsoc.org/jsait/calls-for-papers

IEEE JOURNAL ON
SELECTED AREAS IN INFORMATION THEORY

Call for Contributions: White Paper on NFC

- The **first white paper** on near-field technologies released at **Global 6G Conference 2024**
- Contributed by **200+** people from **40+** global entities of **12** countries

The first white paper

Released at the Global 6G Conference, 2024

Consultants

Tiejun Cui (tjcui@seu.edu.cn), Southeast University

Ping Zhang (pzhang@bupt.edu.cn), Beijing University of Posts and Telecommunications

Xiaohu You (xhyu@seu.edu.cn), Southeast University

Yonina Eldar (yonina.eldar@weizmann.ac.il), Weizmann Institute of Science

Editors in Chief

Yajun Zhao (zhao.yajun1@zte.com.cn), ZTE Corporation

Linglong Dai (daill@tsinghua.edu.cn), Tsinghua University

Jianhua Zhang (jhzhang@bupt.edu.cn), Beijing University of Posts and Telecommunications

QR code for download

Y. Zhao, L. Dai, J. Zhang, *et al*. "6G near-field technologies white paper," FuTURE Forum, Nanjing, China, Apr. 2024.

If you have any questions, please contact:

- **Linglong Dai,** daill@tsinghua.edu.cn
- **Haiyang Zhang,** haiyang.zhang@njupt.edu.cn
- **Yonina C. Eldar,** yonina.eldar@weizmann.ac.il